Enclosure 9 to E-53166

CoC 1042 Amendment 1, Revision 3
UFSAR Changed Pages
(Public Version)

1.4 NUHOMS® EOS System Contents

1.4.1 EOS-37PTH DSC Contents

The EOS-37PTH DSC is designed to store up to 37 intact PWR FAs with or without CCs. *Up to eight damaged FAs, or up to four compartments with failed fuel may be stored in lieu of intact fuel as shown in Figures 1F and 1H of the Technical Specifications [1-7].*

The EOS-37PTH DSC is qualified for storage of Babcock and Wilcox (B&W) 15 x 15 class, Combustion Engineering (CE) 14 x 14 class, CE 15 x 15 class, CE 16 x 16 class, Westinghouse (WE) 14 x 14 class, WE 15 x 15 class, and WE 17x17 class PWR FA designs, as described in Chapter 2.

The EOS-37PTH DSC payload may include CCs that are contained within the FA, such as described in Chapter 2.

Reconstituted assemblies containing up to five replacement irradiated stainless steel rods per assembly or an unlimited number of low enriched or natural uranium fuel rods or *unirradiated* non-fuel rods are acceptable for storage in an EOS-37PTH DSC as intact FAs.

The EOS-37PTH DSC is also authorized to store FAs containing blended low enriched uranium (BLEU) fuel material.

The contents of the DSC are stored in an inert atmosphere of helium.

The maximum allowable planar average initial enrichment of the fuel to be stored is 5.00 wt. % U-235, and the maximum assembly average burnup is 62,000 MWd/MTU. The FAs (with or without CCs) must be cooled to meet the decay heat limits specified in *Figure 1A through 1I* of the Technical Specifications [1-7] prior to storage.

The criticality control features of the EOS-37PTH DSC are designed to maintain the neutron multiplication factor k-effective (including uncertainties and calculational bias) at less than 0.95 under normal, off-normal, and accident conditions.

The *gamma and neutron source terms* in the SFAs are described and tabulated in Chapter 6. Chapter 7 covers the criticality safety of the EOS-37PTH DSC and its parameters. These parameters include rod pitch, rod outside diameter, material densities, moderator ratios, soluble boron content and geometric configurations. The maximum pressure buildup in the EOS-37PTH DSC cavity is addressed in Chapter 4.

1.4.2 EOS-89BTH DSC Contents

The EOS-89BTH DSC is designed to store up to 89 intact BWR FAs with or without channels.

All Indicated Changes are in response to RAI 6-18

The EOS-89BTH DSC is qualified for storage of 7x7, 8x8, 9x9, and 10x10 class BWR FAs of initial design or equivalent reload FAs as described in Chapter 2.

Reconstituted assemblies containing up to five replacement irradiated stainless steel rods per assembly or an unlimited number of low enriched or natural uranium fuel rods or *unirradiated* non-fuel rods are acceptable for storage in an EOS-89BTH DSC as intact FAs.

The EOS-89BTH DSC is also authorized to store FAs containing BLEU fuel material.

The contents of the DSC are stored in an inert atmosphere of helium.

The maximum allowable lattice average initial enrichment of the fuel to be stored is 4.80 wt. % U-235 and the maximum assembly average burnup is 62,000 MWd/MTU. The FAs (with or without channels) must be cooled to meet the decay heat limits specified in Figure 2 of the Technical Specifications [1-7] prior to storage.

The criticality control features of the EOS-89BTH DSC are designed to maintain the neutron multiplication factor k-effective (including uncertainties and calculational bias) at less than 0.95 under normal, off-normal, and accident conditions.

The *gamma and neutron source terms* in the SFAs are described and tabulated in Chapter 6. Chapter 7 covers the criticality safety of the EOS-89BTH DSC and its parameters. These parameters include rod pitch, rod outside diameter, material densities, moderator ratios, and geometric configurations. The maximum pressure buildup in the EOS-89BTH DSC cavity is addressed in Chapter 4.

All Indicated Changes are in response to RAI 6-18

Table 1-2
System Configurations for the NUHOMS® EOS System and NUHOMS® MATRIX System

DSC	System Configuration	Basket Design	Basket Type	Emissivity/ Poison	Storage Module	Wind Deflector	HLZC	Intact	Damaged /Failed	Transfer Cask
EOS-37PTH	S1	Non-Staggered	1	High	EOS-HSM	Yes	1	Yes	No	EOS-TC125/135
	S2	Non-Staggered	2	High	EOS-HSM	No	2	Yes	No	EOS-TC108/125/135
		Non-Staggered	3	High	EOS-HSM	No	3	Yes	No	EOS-TC108/125/135
	S3	Staggered	4L	Low	EOS-HSM	Yes	4	Yes	No	EOS-TC125/135
		Staggered	4L	Low	EOS-HSM	Yes	5	Yes	No	EOS-TC125/135
		Staggered	4L	Low	EOS-HSM	Yes	6	Yes	Yes	EOS-TC125/135
	S4	Non-staggered	5	Low	EOS-HSM	Yes	4	Yes	No	EOS-TC125/135
		Non-staggered	5	Low	EOS-HSM	Yes	5	Yes	No	EOS-TC125/135
	S5	Staggered	4H	High	HSM-MX	N/A	7	Yes	No	EOS-TC125/135
	S6	Staggered	4L	Low	HSM-MX	N/A	8	Yes	Yes	EOS-TC125/135
		Staggered	4L.	Low	HSM-MX	N/A	9	Yes	No	EOS-TC125/135
	S7	Non-staggered	5	Low	HSM-MX	N/A	8	Yes	No	EOS-TC125/135
		Non-staggered	5	Low	HSM-MX	N/A	9	Yes	No	EOS-TC125/135
EOS-89BTH	S8	Non-Staggered	1	High	EOS-HSM	Yes	1	Yes	No	EOS-TC125
	S9	Non-Staggered	2	High	EOS-HSM	No	2	Yes	No	EOS-TC108/125
		Non-Staggered	3	High	EOS-HSM	No	3	Yes	No	EOS-TC108/125
	S10	Non-Staggered	3	High	HSM-MX	N/A	3	Yes	No	EOS-TC108/125

2.2 Spent Fuel to Be Stored

The NUHOMS® EOS System is designed to accommodate pressurized water reactor (PWR) (14x14, 15x15, 16x16 and 17x17 array designs) and boiling water reactor (BWR) (7x7, 8x8, 9x9 and 10x10 array designs) fuel types that are available for storage. As described in Chapter 1, there are two DSC designs for the NUHOMS® EOS System: the EOS-37PTH DSC for PWR fuel and EOS-89BTH DSC for BWR fuel. The EOS-37PTH DSC is designed to accommodate up to 37 intact PWR FAs with uranium dioxide (UO_2) fuel, zirconium-alloy cladding, and with or without control components. *The EOS-37PTH DSC is also designed to accommodate up to eight damaged FAs or up to four failed fuel canisters (FFCs), with the balance being intact FAs.* The EOS-89BTH DSC is designed to accommodate up to 89 intact BWR FAs with UO_2 fuel, zirconium-alloy cladding, and with or without fuel channels. *Specifications for the fuel to be stored in the NUHOMS® EOS System are provided in Technical Specifications (TS) Sections 2.1 and 2.2.*

The cavity length of the DSC is determined for a specific site to match the FA length used at that site, including control components (CCs), as applicable. Both DSCs store intact, including reconstituted and blended low enriched uranium (BLEU), FAs as specified in Table 2-2, Table 2-3 and Table 2-4. Any FA that has fuel characteristics within the range of Table 2-2, Table 2-3 and Table 2-4 and meets the other limits specified for initial enrichment, burnup and heat loads is acceptable for storage in the NUHOMS® EOS System. *Equivalent fuels manufactured by other vendors are also acceptable.*

Damaged and failed fuel from the FA classes detailed in Table 2-2 and PWR fuels in Table 2-4 are also acceptable for storage in the EOS-37PTH DSC in the appropriate compartments, as shown in Figures 1F and 1H of the Technical Specifications [2-18]. The potential for fuel reconfiguration for intact, damaged, and failed fuel under normal, off-normal, and accident conditions is summarized in Table 2-4a.

All fuel categorized as failed shall be placed in a failed fuel canister (FFC). Failed fuel may include FAs, fuel rods, segments of fuel rods, fuel pellets, and debris. FFCs are not required for damaged FAs, because damaged FAs maintain their geometry under normal and off-normal conditions.

The failed fuel content of each FFC is limited to the maximum metric tons of uranium (MTU) of an intact fuel assembly for each class. These limits are summarized in Table 2-4b.

Failed CCs may also be stored inside an FFC. The maximum Co-60 content for failed CCs is the same as intact CCs and is defined in Table 3 of the Technical Specifications [2-18].

All Indicated Changes are in response to RAI 6-2

The maximum allowable assembly average burnup is limited to 62 GWd/MTU and the minimum cooling time is *two* years. Dummy FAs *and* reconstituted FAs are also included in the EOS-37PTH DSC and EOS-89BTH DSC payloads. *L*ow enriched or natural uranium fuel rods or *unirradiated* non-fuel rods are acceptable for storage in an EOS-37PTH DSC and *EOS*-89BTH DSC as intact FAs.

Fuel assemblies that contain fixed integral non-fuel rods are also considered as intact FAs. These FAs are different than reconstituted assemblies because fuel rods are not "replaced" by non-fuel rods, rather the non-fuel rods are part of the initial fuel design. The non-fuel rods displace the same amount of moderator, with zirconium-alloy (or aluminum) cladding and typically contain burnable absorber (or other non-fuel) material. The radiation and thermal source terms for the non-fuel rods are significantly lower than those of the fuel rods since there is no significant radioactive decay source. The internal pressure of the non-fuel rods after irradiation is lower than those of the fuel rods since there is no fission gas generation. The reactivity of the fuel rods (from a criticality standpoint) is significantly higher than that of non-fuel rods. In summary, the mechanical, thermal, shielding, and criticality evaluations for these rods are bounded by those of the regular fuel rods. Therefore, no further evaluations are required for the qualification of these FAs.

RAI 6-13

Fuel assemblies are evaluated with five irradiated stainless steel rods *per assembly, 40 rods per EOS-37PTH DSC, and 100 rods per EOS-89BTH DSC.* The cooling time *is the same as unreconstituted FAs.* The reconstituted rods can be at any location in the FAs. *There is no limit on the number of reconstituted FAs per DSC; the FAs containing irradiated stainless steel reconstituted rods are modeled in the inner compartments as shown in Figure 6-1 for EOS-37PTH and Figure 6-2 for EOS-89BTH of Chapter 6.*

RAI 6-18

The EOS-37PTH DSC may contain less than 37 FAs and the EOS-89BTH DSC may contain less than 89 FAs. In both DSCs, the basket slots not loaded with FAs *may have empty slots or* be loaded with dummy FAs. The dummy FAs approximate the weight and center of gravity of an FA.

The NUHOMS® EOS-37PTH DSC can also accommodate up to eight damaged FAs placed in the DSC as shown in Figures 1F and 1H of the Technical Specifications [2-18]. Damaged PWR FAs are defined in Section 1.1 of the Technical Specifications [2-18].

The NUHOMS® EOS-37PTH DSCs can also accommodate up to a maximum of four FFCs, placed in cells located on the outer edge of the DSC as shown in Figures 1F and 1H of the Technical Specifications [2-18]. Failed fuel is defined in Section 1.1 of the Technical Specifications [2-18].

Damaged fuel containing control components may be stored in the designated damaged fuel compartments. Similarly, failed control component debris may be stored in the FFCs.

Control components not explicitly listed herein are also authorized within the DSC, as long as they meet the following criteria:

1. *External materials are limited to zirconium alloys, nickel alloys, and stainless steels,*
2. *Radiological limits listed in Table 3 and Figures 1A through 1I of the Technical Specifications are not exceeded, and*
3. *They fit within the weight limits and dimensional limits of the DSC.*

Figures 1*A through 1I* of the Technical Specifications [2-18] defines the maximum decay heat, *failed/damaged fuel locations,* and other parameters for PWR fuel assemblies, with or without CCs, authorized for storage. These tables are used to ensure that the decay heat load of the FA to be stored is less than that as specified in each table, and that the corresponding radiation source term is consistent with the shielding analysis presented in Chapter 6. The maximum weight of a FA plus CC, if applicable, is 1,900 lbs.

The heat loads listed in in Figures 1A through 1I of the Technical Specifications [2-18] are the maximum allowable heat loads for each FA and the maximum allowable heat load per DSC. These heat loads can be reduced to ensure adequate heat removal capability is maintained to accommodate site-specific conditions. Some examples of the site-specific conditions are a higher ambient temperature, different blocked vent duration, a requirement to use a different neutron absorber plate or a requirement for a specific coating on the basket steel plates. Each of these changes could result in a change to the inputs of the thermal evaluation utilized in the UFSAR. To ensure that adequate heat removal is maintained with these modified inputs, the bounding evaluations for storage and transfer operations should be re-evaluated. The maximum fuel cladding temperature based on the modified inputs shall be lower than the maximum fuel cladding temperatures listed in the Chapter 4 and Chapter A.4 for the same bounding evaluations.

As limited by their definition, damaged FAs maintain their geometric configuration for normal and off-normal conditions and are confined to their respective compartments by means of top and bottom end caps. Damaged FAs do not contain missing major sub-components like top and bottom nozzles that impact their ability to maintain their geometric configuration for normal and off-normal conditions during loading.

From the standpoint of NUREG-1536 Revision 1, the damaged FAs for the EOS System are more similar to the undamaged FAs, where their geometry is still in the form of intact bundles. For completeness, failed fuel for the EOS System is more similar to the damaged FAs per NUREG-1536 Revision 1 and will require FFCs.

All Indicated Changes are in response to RAI 8-1

Table 2-2
PWR Fuel Assembly Design Characteristics
3 Pages

Fuel Class	B&W 15x15				WE 17x17
Assembly Type	Mark B2 - B8	Mark B9	Mark B10	Mark B11	BW 17x17 Mark C
Fuel Parameters					
Number of Rods	208	208	208	208	264
Active Fuel Length (in.)	≤150	≤150	≤150	≤150	≤150
Pellet Diameter (in.)	0.3686	0.37	0.3735	0.3615	0.3232
Fuel Rod Pitch (in.)	0.568	0.568	0.568	0.568	0.502
Clad Outer Diameter (OD) (in.)	0.43	0.43	0.43	0.416	0.379
Clad Thickness (in.)	0.0265	0.0265	0.025	0.024	0.024
Guide and Instrument Tubes					
Number of Guide/Instrument Tubes	17	17	17	17	(25)
Guide/Instrument Tube Thickness (in.)	≥0.016	≥0.016	≥0.016	≥0.016	≥0.026

Fuel Class	WE 14 x 14			
Assembly Type	Std/LOPAR/ ZCA/ZCB	OFA	Exxon/ANF (ANP) WE	Exxon/ANF (ANP) Top rod
Fuel Parameters				
Number of Rods	179	179	179	179
Active Fuel Length (in.)	≤150	≤150	≤150	≤150
Pellet Diameter (in.)	(0.3565)	(0.3444)	0.3505	0.3505
Fuel Rod Pitch (in.)	0.556	0.556	0.556	0.556
Clad OD (in.)	0.422	0.400	0.424	0.417
Clad Thickness (in.)	0.0225-0.030	0.0243)	0.024-0.030	0.024-0.0295
Guide and Instrument Tubes				
Number of Guide/Instrument Tubes	17	17	17	17
Guide/Instrument Tube Thickness (in.)	≥0.015	≥0.015	≥0.016	≥0.019

Fuel Class	WE 17x17			
Assembly Type	LOPAR	OFA/ Van 5	Framatome 17x17 STD/Van 5H/RFA	Framatome 17x17 MK BW
Fuel Parameters				
Number of Rods	264	264	264	264
Active Fuel Length (in.)	≤150	≤150	≤150	≤150
Pellet Diameter (in.)	0.3225	0.3088	0.3225	0.3195
Fuel Rod Pitch (in.)	0.496	0.496	0.496	0.496
Clad OD (in.)	0.374	0.360	0.374	0.374
Clad Thickness (in.)	0.0225	0.0225	0.0225	0.0240
Guide and Instrument Tubes				
Number of Guide/Instrument Tubes	25	25	25	25
Guide/Instrument Tube Thickness (in.)	≥0.015	≥0.015	≥0.015	≥0.016

All Indicated Changes are in response to RAI 6-1

Table 2-2
PWR Fuel Assembly Design Characteristics
3 Pages

Fuel Class	CE 14 x 14		
Assembly Type	**Std/Gen/St. Lucie**	**Fort Calhoun**	**Framatome CE**
Fuel Parameters			
Number of Rods	176	(176)	176
Active Fuel Length (in.)	≤150	≤150	≤150
Pellet Diameter (in.)	0.370 – 0.3805	0.3765	0.3805
Fuel Rod Pitch (in.)	0.58	0.580	0.580
Clad OD (in.)	0.44	0.440	0.440
Clad Thickness (in.)	0.026 – 0.031	0.0280	0.0280
Guide and Instrument Tubes			
Number of Guide/Instrument Tubes	5	5	5
Guide/Instrument Tube Thickness (in.)	≥0.040	≥0.040	≥0.040

Fuel Class	WE 15 x 15			CE 15x15	
Assembly Type	**LOPAR/ OFA DRFA/ Van5**	**Std/ZC**	**Exxon ANF (ANP) WE**	**CE 15x15 Palisades**	**CE 15x15 Exxon/ ANF (ANP)**
Fuel Parameters					
Number of Rods	204	204	204	216	216
Active Fuel Length (in.)	≤150	≤150	≤150	≤150	≤150
Pellet Diameter (in.)	0.3659	0.3559	0.3565	0.3150 - 0.3600	0.3565
Fuel Rod Pitch (in.)	0.563	0.563	0.563	0.550	0.550
Clad OD (in.)	0.422	0.422	0.424	(0.4135- 0.4180	0.417
Clad Thickness (in.)	0.0280	0.0242	0.0300	0.024 – 0.0295	0.0300
Guide and Instrument Tubes					
Number of Guide/Instrument Tubes	21	21	21	(9)	Note 3
Guide/Instrument Tube Thickness (in.)	≥0.015	≥0.015	≥0.017	≥0.024	≥0.027

All Indicated Changes are in response to RAI 6-1

Table 2-2
PWR Fuel Assembly Design Characteristics
3 Pages

Fuel Class	CE 16x16			
Assembly Type	Standard	System 80	CE 16 x 16 SCE U2/3 Westinghouse Designs	CE 16 x 16 SCE U2/3 AREVA Designs
Fuel Parameters				
Number of Rods	236	236	236	236
Active Fuel Length (in.)	≤150	≤150	≤150	≤150
Pellet Diameter (in.)	(0.3250-0.3255)	(0.3250-0.3255)	(0.3245-0.3260)	(0.3250-0.3260)
Fuel Rod Pitch (in.)	0.506	0.506	0.506	0.506
Clad OD (in.)	0.382	0.382	0.382	(0.380-0.384)
Clad Thickness (in.)	0.025	0.023	0.025	(0.0246-0.0254)
Guide and Instrument Tubes				
Number of Guide/Instrument Tubes	5	5	5	5
Guide/Instrument Tube Thickness (in.)	≥0.041	≥0.041	≥0.040	≥0.040

Notes:

1. All dimensions shown are nominal.
2. Reload FAs from other manufacturers with these parameters are also acceptable.
3. One instrument tube and eight guide bars (solid Zr).

All Indicated Changes are in response to RAI 6-1

Table 2-3
BWR Fuel Assembly Design Characteristics
4 Pages

BWR Fuel ID/(Fuel Class)	GE-7-A (7 x 7)	GE-8-A (8 x 8)	GE-8-B (8 x 8)	GE-8-C (8 x 8)	GE-8-D (8 x 8)	GE-9-A (9 x 9)	GE-10-A (10 x 10)	GE-10-B (10 x 10)	ENC-7-B (7 x 7)
FA Design	**7 x 7-49/0**	**8 x 8-63/1**	**8 x 8-62/2**	**8 x 8-60/4**	**8 x 8-60/1**	**9 x 9-74/2**	**10x10-92/2**	**10x10**	**7 x 7-48(1)**
Reload Fuel Designation[1][2]	GE1 GE2 GE3	GE4	GE-5 GE-Pres GE-Barrier GE8 Type I	GE8 Type II	GE9 GE10	GE11 GE13	GE12 GE14	GNF2	ENC-III[6]
Rod Pitch (in.)	0.738	0.640	0.640	0.640	0.640	0.566	0.510	0.510	0.738
No of Fueled Rods	49	63	62	60	60	66 full 8 partial	78 full 14 partial	78 full 14 partial	48
Maximum Active Fuel Length (in.)	≤150	≤150	≤150	≤150	≤150	146" full 90" partial 108" partial GE13	150" full 93" partial 84" partial GE14	150.3" full 110.81" partial 59.4" partial	≤150
Fuel Rod OD (in.)	0.563	0.493	0.483	0.483	0.483	0.440	0.404	0.404	0.570
Clad Thickness (in.)	0.032 0.037	0.034	0.032	0.032	0.032	0.028	0.026	0.0236	≥0.0355
Fuel Pellet OD (in.)	0.491 0.477	0.416	0.410 0.411	0.410 0.411	0.411	0.376	0.345	0.350	0.468 - 0.491
No of Water Rods	0	1	2	4	1	2	2	2	1[3]
Water Rod OD (in.)	---	0.493	0.591	2 @ 0.591 2 @ 0.483	1.340	0.980	0.980	0.98	0.572[3]
Water Rod Inner Diameter ID (in.)	---	0.425	0.531	2 @ 0.531 2 @ 0.419	1.260	0.920	0.920	0.92	Note 3

All Indicated Changes are in response to RAI 6-1

Table 2-3
BWR Fuel Assembly Design Characteristics
4 Pages

BWR Fuel ID /(Fuel Class)	ABB-8-A (8 x 8)	ABB-8-B (8 x 8)	ABB-10-A (10 x 10)	ABB-10-A (10 x 10)	ABB-10-B (10 x 10)	ABB-10-B (10 x 10)	ABB-10-A (10 x 10)	ABB-10-B (10 x 10)
FA Design	**4x(4 x 4)**	**4x(4 x 4)**	**4x(5x5-2)**	**4x(5x5-2)**	**4x(5x5-1)**	**4x(5x5-1)**	**4x(5x5)**	**4x(5x5)**
Reload Fuel Designation[1][2]	SVEA-64[4]	SVEA-64[4]	SVEA-92[4]	SVEA-92[4]	SVEA-96[5][4]	SVEA-96[5][4]	SVEA-100[4]	SVEA-100[4]
Rod Pitch (in.)	0.610	0.622	0.500	0.500	0.496	0.488	0.500	0.496
No. of Fueled Rods	64	64	92	92	96	96	100	100
Maximum Active Fuel Length (in.)	150.59	150.59	150.59	150.59	150.59	150.59	151	151
Fuel Rod OD (in.)	0.461	0.483	0.387	0.378	0.387	0.378	0.443	0.387
Clad Thickness (in.)	0.027	0.031	0.0243	0.0243	0.0243	0.0243	0.028	0.0243
Fuel Pellet OD (in.)	0.3940	0.4110	0.3350	0.3224	0.3350	0.3224	0.3745	0.3350
No. of Water Rods	0	0	0	0	0	0	0	0
Water Rod OD (in.)	---	---	---	---	---	---	---	---
Water Rod ID (in.)	---	---	---	---	---	---	---	---

All Indicated Changes are in response to RAI 6-1

Table 2-3
BWR Fuel Assembly Design Characteristics
4 Pages

BWR Fuel ID /(Fuel Class)	ABB-10-A (10 x 10)	ABB-10-C (10 x 10)
FA Design	4x(5x5-3) 4x(5x5-1) Optima1	4x(5x5-4) 4x(5x5-2) 4x(5x5-1) Optima2
Reload Fuel Designation[1][2]	SVEA-96Opt[4][5]	SVEA-96Op2[4][5]
Rod Pitch (in.)	0.496 - 0.500	0.484 - 0.512
No of Fueled Rods	88, 96	84, 92, 96
Maximum Active Fuel Length (in.)	150.42	150.42
Fuel Rod OD (in.)	0.379-0.406	0.387
Clad Thickness (in.)	0.0248 -0.0268	0.0238
Fuel Pellet OD (in.)	0.323-0.346	0.334
No of Water Rods	0	0
Water Rod OD (in.)	---	---
Water Rod ID (in.)	---	---

Notes:

1. All dimensions shown are nominal.
2. Reload FAs from other manufacturers with these parameters are also acceptable.
3. Solid Zircaloy rod(s).
4. Fuel bundles designated as ABB or SVEA are typically assembled from four sub-assemblies. There is a cruciform internal water channel between the sub-assemblies. The thickness of the water channel is 0.8 mm, the inner width of the channel is 4 mm for most ABB or SVEA bundles, except 2.4 mm for SVEA-Optima 1 and SVEA-Optima 2.
5. There is one rod that occupies the four central fuel rod locations and four water bars/channels that divide the FA into four quadrants.
6. Includes ENC III-E and ENC III-F

All Indicated Changes are in response to RAI 6-1

Table 2-4
Additional PWR and BWR Fuel Assembly Design Characteristics
2 Pages

Fuel Class	**WE 14x14**	**WE17x17**	**WE17x17**	**WE15x15**	**WE17x17**	**WE17x17**
FA Design	**Doel 1&2 14x14**	**Doel 3 17x17**	**Doel 4 17x17**	**Tihange 1 15x15**	**Tihange 2 17x17**	**Tihange 3 17x17**
Fuel Parameters						
No. of Rods	179	264	264	204	264	264
Active Fuel Length (in.)	96	145	169	145	145	169
Pellet Diameter (in.)	0.368	0.322	0.323	0.368	0.323	0.323
Fuel Rod Pitch (in.)	0.556	0.496	0.496	0.563	0.496	0.496
Clad OD (in.)	0.424	0.376	0.376	0.426	0.376	0.376
Clad Thickness (in.)	0.0225	0.0225	0.0225	0.0242	0.0225	0.0225
Guide and Instrument Tubes						
No. of Guide/Instrument Tubes	17	25	25	21	25	25
Guide/Instrument Tube Thickness (in.)	≥0.015	≥0.015	≥0.015	≥0.015	≥0.015	≥0.015

Fuel Class	**WE 14x14**	**WE 15x15**	**WE 17x17**	**WE 17x17**	**WE 17x17**	**GE-8-C (8 x 8)**
FA Design [1] [2]	**Kansai 14x14 Step I Type A**	**Kansai 15x15 Step I Type A**	**Kansai 17x17 Step II**	***ENRESA ASCO* 17x17**	***AM1000* 17x17**	**8x8 Step II**
Fuel Parameters						
No. of Rods	179	204	264	264	264	60
Active Fuel Length (in.)	143	143	144	144	165	146
Pellet Diameter (in.)	0.366	0.366	0.317	0.322	0.322	0.409
Fuel Rod Pitch (in.)	0.555	0.563	0.496	0.496	0.496	0.642
Clad OD (in.)	0.422	0.422	0.374	*0.374*	0.372	0.484
Clad Thickness (in.)	0.0225	0.0242	0.0225	0.0225	0.0225	*0.032*
Guide and Instrument Tubes						
No. of Guide/Instrument Tubes	17	21	25	25	25	---
Guide/Instrument Tube Thickness (in.)	≥0.015	≥0.015	≥0.015	≥0.015	≥0.015	---
Number of Water Rods	---	---	---	---	---	*4*
Water Rod OD	---	---	---	---	---	*2 @ 0.591* *2 @ 0.483*
Water Rod ID	---	---	---	---	---	*2 @ 0.531* *2 @ 0.419*

All Indicated Changes are in response to RAI 6-1

Table 2-4
Additional PWR and BWR Fuel Assembly Design Characteristics
2 Pages

BWR Fuel ID/Fuel Class	GE-8-C (8 x 8)	GE-9-A (9 x 9)	GE-10-A (10 x 10)	ABB-8-A (8 x 8)	ABB-10-B (10 x 10)	ABB-10-A (10 x 10)	ABB-10-C (10 x 10)
	BWR 1/4	BWR 2/5/8	BWR 3/9/12/13	BWR 6	BWR 7/14	BWR 10/15	BWR 11/16
FA Design	KKL 8x8	KKL 9x9	KKL 10x10	KKL 4x4x4	KKL 4x(5x5-1)	KKL 4x(5x5-3)/ 4x(5x5-1)	KKL 4x(5x5-4)/ 4x(5x5-2)/ 4x(5x5-1)
Fuel Parameters							
Number of Rods	*60*	74	92	64	96	*88 96*	*84 92 96*
Active Fuel Length (in.)	150	146	148	151	151	151	151
Pellet Diameter (in.)	0.413	0.378	0.35	0.394	0.323	0.323 - 0.346	0.334 - 0.335
Fuel Rod Pitch (in.)	0.64	0.566	0.51	0.61	0.488	0.496 - 0.502	0.512
Clad OD (in.)	0.483	0.441	0.431	0.461	0.369 - 0.378	0.379 - 0.406	0.369 - 0.387
Clad Thickness (in.)	*0.032*	0.028	0.026	0.027	0.0228	0.023	0.024
Number of Water Rods	4	2	2	0	0	0	0
Water Rod OD	*2 @ 0.591* *2 @ 0.483*	0.98	0.98	---	---	---	---
Water Rod ID	*2 @ 0.531* *2 @ 0.419*	0.92	0.92	---	---	---	---

Notes:

1. All dimensions shown are nominal.
2. Reload fuel assemblies from other manufacturers with these parameters are also acceptable.
3. Solid Zirc rod(s).

All Indicated Changes are in response to RAI 6-1

3.9.2.3A.5 *Reconciliation*

The design change in the EOS-37PTH Type 4 Basket is a modification to stagger the alignment of the steel, aluminum, and poison basket plates. This change allows damaged, failed fuel or intact fuel assemblies to be loaded in an EOS-37PTH Type 4 Basket. Temperature distribution in the EOS-37PTH Type 4 Basket is bounded by the original analysis for Type 1 through 3. There are no changes to overall length, thickness or other structural dimensions of used in the structural evaluations. Therefore, no further analysis is required. The structural evaluation presented in Section 3.9.2.1 and Section 3.9.2.3 remains valid for EOS-37PTH Type 4 Basket.

3.9.2.3B *NUHOMS® EOS-37PTH Type 5 Basket Evaluation*

The NUHOMS® EOS-37PTH Type 5 basket is identical to the Type 1/2/3 basket, the only difference being the low emissivity coating steel plates and low conductivity poison plates. Only intact FAs can be stored in the Type 5 basket. The detailed description of the Type 5 basket is discussed in Chapter 1.

3.9.2.3B.1 *General Description*

The primary design change to the EOS-37PTH Type 5 basket is the low emissivity coating steel plates and low conductivity poison plates.

3.9.2.3B.2 *Dimensions and Materials*

The overall length, thickness, or dimensions used in the structural evaluations (Section 3.9.2.1 and Section 3.9.2.3) remain the same for the Type 5 basket. Similarly, the materials used in the Type 5 basket are consistent with those considered for the structural analysis in Section 3.9.2.1and Section 3.9.2.3. The key basket dimensions and materials are per Drawing EOS01-1010-SAR, as provided in Section 1.3.1.

3.9.2.3B.3 *Temperature*

The Type 5 basket accommodates only intact FAs, and the temperature distribution is bounded by the original analysis for Types 1 through 3.

3.9.2.3B.4 *Reconciliation*

The design change in the EOS-37PTH Type 5 basket only includes the low emissivity coating steel plates and low conductivity poison plates. Temperature distribution in the Type 5 basket is bounded by the original analysis for Type 1 through 3. There are no changes to overall length, thickness or other structural dimensions used in the structural evaluations. Therefore, no further analysis is required. The structural evaluation presented in Section 3.9.2.1 and Section 3.9.2.3 remains valid for EOS-37PTH Type 5 basket.

All Indicated Changes are in response to RAI 3-1

Proprietary Information on This Page
Withheld Pursuant to 10 CFR 2.390

Proprietary Information on This Page
Withheld Pursuant to 10 CFR 2.390

4.2 Material and Design Limits

To establish the heat removal capability, several thermal design criteria are established for the NUHOMS® EOS System. These are:

- Maximum temperatures of the containment structural components must not adversely affect the containment function.
- A maximum fuel cladding temperature limit of 400 °C (752 °F) has been established for normal conditions of storage and for short-term storage operations such as transfer and vacuum drying [4-1]. During off-normal storage and accident conditions, the fuel cladding temperature limit is 570 °C (1058 °F) [4-1].
- A maximum temperature limit of 327 °C (620 °F) is considered for the lead in the TC, corresponding to the melting point [4-2].
- A maximum temperature limit of 128 °C (262 °F) is considered for the bottom neutron shield (Borotron® HD050 *or equivalent*) in the TC, corresponding to the melting point [4-3]. 72.48
- The temperature of the water in the neutron shield is limited by the rating of the pressure relief valves (20 psig) on the neutron shield. The temperature of the water cannot rise above the equivalent steam saturation temperature at this pressure (i.e., approximately 259 °F) without risk of activating the relief valves and losing some of the water in the neutron shield.
- The ambient temperature ranges are -20 to 100 °F (-28.9 to 37.8 °C) for normal storage operations with heat load less than or equal to 41.8 kW for the EOS-37PTH DSC and 41.6 kW for the EOS-89BTH DSC. For normal storage operations with heat load greater than 41.8 kW for the EOS-37PTH DSC and 41.6 kW for the EOS-89BTH DSC, the minimum ambient temperature is -20 °F (-28.9 °C) and the maximum yearly average ambient temperature is 70 °F (21.1 °C). For off-normal storage operations, the ambient temperature range is -40 to 117 °F (-40 to 47.2 °C). The ambient temperature ranges are 0 to 100 °F (-17.8 to 37.8 °C) for normal transfer and 0 to 117 °F (-17.8 to 47.2 °C) for off-normal transfer operations. In general, all the thermal criteria are associated with maximum temperature limits and not minimum temperatures. All materials can be subjected to a minimum environment temperature of -40 °F (-40 °C) without adverse effects.
- The maximum DSC internal pressure during normal and off-normal conditions must be below the pressure of 20 psig used for structural evaluations. For hypothetical accident cases, the maximum DSC internal pressure must be lower than 130 psig. The evaluations of the maximum DSC internal pressure during normal, off-normal, and hypothetical accident conditions assume the rupture of 1%, 10 %, and 100% of the fuel rods, respectively.

All Indicated Changes are in response to RAI 8-3

Proprietary Information on This Page
Withheld Pursuant to 10 CFR 2.390

If the maximum temperatures from the above transient analyses and the accident evaluation are less than those previously approved for LC 1 with HLZC 1, the maximum temperatures for all other load cases (Load Cases 3, 6a, 6b and 7) evaluated for transfer operations of HLZC 1 in Table 4-23 will also remain bounded and no further evaluations are necessary for HLZCs 4, 5 and 6.

4.9.6.1.3.3 Ambient Operating Conditions

Ambient temperature for the EOS-37PTH DSC with HLZC 4, 5, and 6 are identical to those in Section 4.3.

In addition to the ambient temperature, normal thermal evaluation for EOS-HSM considers impact of wind on the maximum fuel cladding temperature. Based on the evaluations presented in Section 4.9.4, wind deflectors are implemented on top of the EOS-HSM and next to the outlet as shown in Figure 4.9.4-7.

For the EOS-37PTH DSC with HLZC 4, 5, and 6 during storage operations in an EOS-HSM, wind deflectors are implemented as follows:

- For HLZCs 4 and 6, wind deflectors shall be installed for storage operations with heat load greater than 41.8 kW per DSC similar to HLZC 1.
- For HLZC 5, wind deflectors shall be installed for storage operations if the heat load of a FA is greater than 1.625 kW irrespective of the total heat load per DSC.

All Indicated Changes are in response to RAI 4-4

For the EOS-37PTH DSC with HLZCs 4, 5, and 6, the time limit for normal and off-normal transfer operations is reduced from 10 hours to 8 hours *based on the comparisons of temperatures for HLZCs 4, 5, and 6 to HLZC 1, as shown in Table 4.9.6-5*. This ensures that the maximum fuel cladding temperatures for HLZCs 4, 5, and 6 remain below the design basis temperatures determined in Section 4.5.4 for HLZC 1, *as shown in Table 4.9.6-5 and discussed in the following section*. The duration available to complete the recovery actions if transfer operations cannot be completed within the time limit remains unchanged at 5 hours.

Therefore, the total duration for transfer operations is 13 hours (8-hour transfer time limit + 5-hour recovery time) for the EOS-37PTH DSC with HLZCs 4, 5 and 6, compared to 15 hours for design basis evaluation with HLZC 1 in Section 4.5.4.

B. Component Temperatures

Table 4.9.6-5 presents the maximum temperatures of the fuel cladding and the various components within the EOS-37PTH DSC and the EOS-TC125 for the bounding normal conditions at 13 hours for HLZCs 4 and 5. As shown in Table 4.9.6-5, the maximum fuel cladding temperature at 13 hours is 729 °F and 717 °F for HLZC 4 and HLZC 5, respectively, remaining below the allowable temperature limit of 752 °F. Figure 4.9.6-4 and Figure 4.9.6-5 present the temperature profiles for HLZCs 4 and 5, respectively for normal conditions at 13 hours. The design basis evaluation for HLZC 1 is also included in Table 4.9.6-5 to provide a comparison with the design basis temperatures. As shown in Table 4.9.6-5, the maximum temperatures for normal and off-normal conditions remain bounded by the design basis evaluation with HLZC 1 in Section 4.5 for the EOS-37PTH DSC. Since these temperatures are lower compared to HLZC 1, the remaining time limits listed in Table 4-31 of Section 4.5 for insertion of DSC into the EOS-HSM or restarting of air circulation after its inactivation also remain applicable. The time limits for transfer operations of the EOS-37PTH DSC with HLZCs 4, 5, and 6 are listed in Table 4.9.6-7.

For accident conditions, as shown in Table 4.9.6-6, the maximum fuel cladding temperature is 949 °F with a 14 °F increase compared to the design basis evaluation with HLZC 1 in Section 4.5 for the EOS-37PTH DSC. However, this remains below the allowable temperature limit of 1058 °F for accident conditions. Therefore, there is no impact on the fuel cladding integrity. Figure 4.9.6-6 presents the temperature profiles for HLZC 4 during accident conditions.

All Indicated Changes are in response to RAI 4-4

In addition, the maximum heat load for HLZC 8 while loaded with damaged or *FFCs* is limited to 41.8 kW compared to 46.0 kW for HLZC 6. Therefore, the thermal evaluation presented for HLZC 6 in Section 4.9.6.1.5 with damaged FAs, and Section 4.9.6.1.6 with failed *fuel* remains bounding for HLZC 8.

Similarly, the maximum heat load per DSC for HLZC 9 is limited to 37.80 kW, which is lower compared to the maximum heat load of 41.0 kW for HLZC 5. In addition, the maximum heat load per FA within zone 3 of HLZC 9 is reduced to 2.0 kW compared to 2.4 kW in HLZC 5. Since the total heat load per DSC and the maximum heat load per FA are lower, the thermal evaluation of HLZC 5 in Section 4.9.6.1.4 for transfer operations is bounding for HLZC 9, including the transfer time limits while loaded with intact FAs.

Time limits for transfer operations of the EOS-37PTH DSC with HLZCs 7, 8, and 9 are listed in *Table 4.9.6-11*.

All Indicated Changes are in response to the Thermal Editorial RAI

6. SHIELDING EVALUATION

RAI 6-3

The EOS system is designed to store intact, *damaged, or failed* pressurized water reactor (PWR) and *intact* boiling water reactor (BWR) fuel assemblies (FAs) within the EOS-37PTH dry shielded canister (DSC) and EOS-89BTH DSC, respectively. *Failed PWR fuel shall be stored in a failed fuel canister (FFC).* The transfer casks (TCs) EOS-TC108 and EOS-TC125/135 are used to transfer the EOS-DSC to the EOS horizontal storage module (EOS-HSM). Normal and off-normal condition, near-field dose rates are presented in this chapter for the EOS-TC and EOS-HSM. Detailed three-dimensional dose rate calculations are performed to determine the dose rate fields around the EOS-TCs during loading, decontamination, welding, drying, and transfer operations. Detailed three-dimensional dose rate calculations are also performed to determine the dose rate fields around an EOS-HSM. These near-field dose rates are used as input to the dose assessment documented in Chapter 11, Radiation Protection.

RAI 6-6

The methodology, source terms, and dose rates presented in this chapter are developed to be reasonably bounding for general licensee implementation of the EOS System. *Justification of the reasonably bounding source term methodology is provided in Section 6.2.8.* These results may be used in lieu of near-field calculations by the general licensee, although the inputs utilized in this chapter should be evaluated for applicability by each site. Site-specific EOS-TC and EOS-HSM near-field calculations may be performed by the general licensee to modify key input parameters.

Compliance with 10 CFR 72.106 is demonstrated in this chapter for a loss of neutron shield accident for a single EOS-TC. Further, site dose calculations for an array of EOS-HSMs under normal, off-normal, and accident conditions are documented in Chapter 11, based on the near-field EOS-HSM results presented in this chapter. Because the number and arrangement of EOS-HSMs and the distance to the site boundary is site-specific, compliance with 10 CFR 72.104 and 10 CFR 72.106 for an array of EOS-HSMs can only be demonstrated using a site-specific calculation. Inputs for the site dose calculations developed in the current chapter may be directly used as input to a site-specific dose calculation by the general licensee.

The shielding evaluation for the NUHOMS®MATRIX is documented in Appendix A.6.

6.1 Discussions and Results

The following is a summary of the methodology and results of the shielding analysis of the EOS system. More detailed information is presented in the body of the chapter.

The EOS-37PTH DSC stores up to 37 PWR FAs, while the EOS-89BTH stores up to 89 BWR FAs. Each EOS-DSC is configured into heat load zones in order to optimize the system performance for both thermal and shielding considerations. *Nine heat load zoning configurations (HLZCs) are available for the EOS-37PTH DSC, and three HLZCs are available for the EOS-89BTH DSC. The HLZCs are defined in the Technical Specifications (TS), Figure 1A through Figure 2 [6-11].* Fuel to be stored is limited by the decay heat and minimum cooling times *defined in the Technical Specifications.*

The EOS-37PTH DSC is authorized to store up to eight damaged FAs or four FFCs using HLZC 6 or HLZC 8. Damaged and failed fuel shall not be present in the same DSC.

Source Terms

The ORIGEN-ARP module of the Oak Ridge National Laboratory (ORNL) SCALE6.0 code package [6-1] is used to develop reasonably bounding gamma and neutron source terms. [

]

Control components (CCs) are allowed to be stored within a PWR FA. Examples of CCs include burnable poison rod assemblies (BPRAs) and thimble plug assemblies. Control components typically have a Co-60 source because of its light element activation, which contributes substantially to the dose rates. The CC source term *used in the analysis* is provided in Table 6-37. *Different CC source terms are used in the inner and peripheral zones. The inner and peripheral zones are defined in Figure 6-1 and are applicable to all PWR HLZCs. Co-60 equivalent activity limits per zone are provided in TS Table 3 [6-11].*

BWR fuel does not include CCs other than the fuel channel, which is conservatively included in the source term. The BWR fuel channel is fabricated from zirconium alloy and does not require a Co-60 limit because the contribution to the source term from the fuel channel is negligible.

[

]

Dose Rates

The Monte Carlo transport code, MCNP5 [6-5], is used to compute dose fields around the EOS-TCs and EOS-HSM using detailed three-dimensional models for the following normal configurations:

- EOS-37PTH DSC inside the EOS-TC108
- EOS-37PTH DSC inside the EOS-TC125/135
- EOS-37PTH DSC inside the EOS-HSM-Short
- EOS-89BTH DSC inside the EOS-TC108
- EOS-89BTH DSC inside the EOS-TC125/135
- EOS-89BTH DSC inside the EOS-HSM-Medium

The EOS-TC125 and EOS-TC135 provide equivalent shielding but accommodate different DSC lengths. The EOS-TC135 is used only with the EOS-37PTH DSC. The EOS-TC125 and EOS-TC135 designs are bounded by the same Monte Carlo N-particle (MCNP) model and are referred to in this chapter as EOS-TC125/135. The EOS-TC108 offers less shielding than the EOS-TC125/135 and features a removable neutron shield. The neutron shield is removed for fuel loading and attached subsequent to fuel loading. The neutron shield for the EOS-TC125/135 is integral to the cask and cannot be removed.

The shielding effectiveness of the EOS-TC and EOS-HSM is not impacted by any off-normal events. Two accident events have been identified:

- Loss of neutron shielding for the EOS-TCs
- Loss of EOS-HSM outlet vent covers due to a tornado or missile event

[ ]

MCNP cases are developed for the EOS-HSM in which the vent covers are absent. The EOS-HSM accident increases the average dose rate on the roof of the module to 7400 mrem/hr. The fluxes and dose rates on the surface of the EOS-HSM in an accident condition are used as input to an accident site dose calculation documented in Chapter 11.

6.2.1 Computer Programs

Source terms are generated using the ORIGEN-ARP module of SCALE6.0. ORIGEN-ARP is a control module for the ORIGEN-S computer program. ORIGEN-ARP allows a simplified input description that can rapidly compute source terms and decay heat compared to a full two-dimensional SCALE6.0/TRITON calculation.

Prior to using ORIGEN-ARP, detailed two-dimensional models of the design basis PWR and BWR FAs are developed in TRITON using the FA design data in Chapter 2. *The ENDF/B-VII 238-group cross section library (v7-238) is utilized in the TRITON input files.* TRITON is used to generate ORIGEN-ARP data libraries as a function of burnup and enrichment. These libraries are used by ORIGEN-ARP to compute the source terms.

RAI 6-10

ORIGEN-ARP uses interpolated cross section libraries to generate source terms that are essentially equivalent to the detailed TRITON runs. TRITON has been benchmarked against experimentally measured isotopes and results in excellent agreement with the measured data in ORNL/TM-2010 SCALE 5.1 [6-2]. As part of the code validation, the TRITON benchmark cases from SCALE 5.1 are rerun using the ENDF/B-VII 238-group cross section library. The isotopes important for shielding for which benchmark data are available include Cs-137/Ba-137m, Cs-134, Eu-154, Ce-144/Pr-144, Ru-106/Rh-106, Sr-90/Y-90, and Cm-244. The average ratio of the measured to calculated concentration for these nuclides is close to unity, indicating that TRITON/ORIGEN-ARP is an acceptable program for source term generation.

6.2.2 PWR and BWR Source Terms

Sources are developed for a variety of different enrichments. For a particular U-235 enrichment, the uranium fuel loading is distributed according to the following relationship from the SCALE 6.0 manual:

- wt. % U-234 = 0.0089 * wt. % U-235
- wt. % U-236 = 0.0046 * wt. % U-235
- wt. % U-238 = 100 – wt. % U-234 – wt. % U-235 – wt. % U-236

The EOS-DSC baskets are zoned by heat load. Heat load zoning allows hotter FAs, which generally have larger neutron and gamma source terms, to be placed in the inner zones and be shielded by FAs in the outer zone. The EOS-TC108 and EOS-TC125/135 have different heat load zone configurations because the EOS-TC125/135 is more heavily shielded than the EOS-TC108 and can therefore be loaded with stronger sources.

Nine HLZCs are available for the EOS-37PTH DSC and three HLZCs are available for the EOS-89BTH DSC. These HLZCs are defined in TS Figure 1A through Figure 2 [6-11]. All HLZCs may be transferred in the EOS-TC125/135, while the EOS-TC108 is limited to PWR HLZCs 2 and 3 and BWR HLZCs 2 and 3. The EOS-HSM may store PWR HLZCs 1 through 6 and all BWR HLZCs.

The bounding HLZCs are used for dose rate analysis. For each zone within a DSC, higher heat loads result in stronger source terms and larger dose rates if the minimum cooling time is the same. When the EOS-89BTH DSC is used with the EOS-TC125, the minimum cooling time is three years in all zones. The EOS-89BTH DSC HLZC 1 and 2 are identical except for Zone 2. The Zone 2 heat load is larger for HLZC 1 compared to HLZC 2. Therefore, HLZC 1 bounds HLZC 2. Also, every zone of HLZC 2 is hotter than the corresponding zone of HLZC 3. Therefore, HLZC 2 bounds HLZC 3. Because HLZC 1 > HLZC 2 > HLZC 3, EOS-89BTH DSC HLZC 1 is bounding for the EOS-TC125 analysis.

RAI 6-16

The EOS-89BTH DSC HLZC 1 is not allowed in the EOS-TC108. As discussed in the previous paragraph, HLZC 2 has larger heat loads in each zone compared to HLZC 3. When HLZC 2 or 3 is used with the EOS-TC108, the minimum cooling time in zone 3 is 9.7 years and 9.0 years, respectively. While the EOS-89BTH DSC HLZC 2 zone 3 has a slightly longer minimum cooling time than HLZC 3 zone 3, the minimum cooling time difference (0.7 years) is small compared to the large difference in decay heat (0.1 kW/FA). Therefore, EOS-89BTH DSC HLZC 2 is bounding for EOS-TC108 analysis.

Likewise, for the EOS-TC108, the EOS-37PTH DSC HLZC 2 has a larger heat load in each zone compared to HLZC 3. Also, the minimum cooling time is lower in HLZC 2 Zone 3 (five to eight years) compared to HLZC 3 (nine years). Therefore, EOS-37PTH DSC HLZC 2 bounds HLZC 3 for EOS-TC108 analysis.

For PWR fuel in the EOS-TC125/135, the bounding HLZC cannot readily be determined by inspection, although the nine HLZCs may be reduced to three candidates based on head load considerations. HLZC 4 has the largest total heat load in the peripheral zone, HLZC 1 has a large heat load in an inner zone, and HLZC 5 has the largest heat load per fuel assembly. Therefore, each of these HLZCs is examined explicitly.

Based on MCNP calculations, HLZC 4 bounds HLZC 1, and HLZC 4 and HLZC 5 result in similar peak dose rates for the EOS-TC125/135 and EOS-HSM. However, HLZC 4 results in larger average dose rates on the EOS-TC125/135 side surface compared to HLZC 5 because HLZC 4 has the largest heat load in the peripheral zone. The exposure analysis provided in Chapter 11 is based upon average EOS-TC dose rates because operations are performed at various locations around the EOS-TC. Therefore, HLZC 4 is used in design basis PWR calculations for the EOS-TC125/135 and EOS-HSM. Source terms for HLZC 4 are derived for 1.0 kW/FA in Zone 1 and 1.625 kW/FA in Zones 2 and 3 for a total DSC heat load of 52.0 kW. This bounds the maximum DSC heat load of 50.0 kW.

RAI 6-8

While HLZC 4 is the design basis PWR HLZC, explicit source terms are also developed for HLZC 5 for use in supplemental calculations. HLZC 5 source terms are developed for 0.7 kW/FA in Zone 1, 0.5 kW/FA in Zone 2, 2.4 kW/FA in Zone 3, and 0.85 kW/FA in Zone 4.

Note that up to eight damaged PWR fuel assemblies or up to four FFCs are authorized for HLZC 6 and HLZC 8. Source terms are also developed for a damaged/failed fuel HLZC that bounds both HLZC 6 and 8. These source terms are derived for 1.0 kW/FA in Zone 1, 1.5 kW/FA in Zone 2, 1.5 kW/FA for intact fuel in Zone 3, and 0.85 kW/FA for failed fuel in Zone 3. The ORIGEN-ARP methodology for developing damaged/failed fuel source terms is the same as used for developing intact fuel source terms. Reconfiguration of damaged/failed fuel source terms is addressed in Section 6.3.2.

Because the FAs are zoned by heat load, it is necessary to develop source terms for each zone. Candidate sources are developed for high burnup (62 GWd/MTU), medium burnup (50 GWd/MTU) and lower burnup (40 GWd/MTU) fuel. Cooling time is selected so that the decay heat meets or exceeds the heat load limit for each zone. Because the cooling time required at these burnups is generally much larger than the minimum allowed cooling time for each zone, the burnup that results in a cooling time that matches the minimum cooling time for each zone is also determined. From these four candidate burnup/cooling time combinations, a bounding source for each zone is selected.

[

]

All Indicated Changes are in response to RAI 6-12

During an EOS-TC accident, it is postulated that the water in the neutron shield is lost. In this scenario, there is no hydrogenous neutron shield and the neutron dose rate dominates the primary gamma dose rate. Therefore, the *burnup/enrichment/cooling time combination that results in the maximum neutron source* is used in accident calculations with no neutron shield. In many cases, the normal condition and accident condition sources are the same.

PWR source terms are reported in the following tables:

- PWR sources terms for EOS-TC108 *(HLZC 2)*:
  Table 6-10 through Table 6-13
- *PWR source terms for EOS-TC125/135*
  Intact fuel (HLZC 4): Table 6-14 through Table 6-16
  Damaged/failed fuel (HLZC 6/8): Table 6-14, Table 6-16a through Table 6-16c
  Intact fuel (HLZC 5): Table 6-16d through 6-16g
- PWR source terms for EOS-HSM:
  HLZC 4: Table 6-17 through Table 6-19
  HLZC 5: Table 6-19a through Table 6-19d

BWR source terms are reported in the following tables:

- BWR sources terms for EOS-TC108 *(HLZC 2)*:
  Table 6-20 through Table 6-22
- BWR source terms for EOS-TC125/135 *(HLZC 1)*:
  Table 6-23 through Table 6-26
- BWR source terms for EOS-HSM *(HLZC 1)*:
  Table 6-27 through Table 6-29

In these tables, the "raw" neutron source computed by ORIGEN-ARP is provided, as well as neutron sources that include neutron peaking factors and subcritical neutron multiplication. These factors are derived in Section 6.2.3. The scaled neutron sources are used in the detailed MCNP dose rate calculations. Only the total neutron source magnitude is reported because the Cm-244 spectrum is used in all dose rate calculations for simplicity because the neutron source is almost entirely due to Cm-244 decay. For example, for the 62 GWd/MTU, 10.25 year cooled PWR source, 95% of the neutron source is due to spontaneous fission of Cm-244. Cm-244 is also the dominant neutron source for shorter cooling times. For instance, for a 36.178 GWd/MTU, three-year cooled PWR source, Cm-244 represents 97% of the total neutron source. The effect on the neutron spectrum of neutron source isotopes with shorter half-lives, such as Cm-242 and Cf-252, is negligible.

All Indicated Changes are in response to RAI 6-8

To account for the reduced flux in the plenum and top regions, the BPRA input masses are scaled by the appropriate flux scaling factor. The ORIGEN-ARP inputs for the three BPRA regions are summarized in Table 6-35.

The methodology for TPAs is slightly different than for BPRAs. The reason is that a TPA may reside in several host FAs for a total host fuel assembly burnup of 300 GWd/MTU. ORIGEN-ARP cannot burn a single FA to such a high burnup. Therefore, rather than apply the flux scaling factors to the input masses, the true masses are input and the flux scaling factors are applied to the FA burnup. The TPA input masses are summarized in Table 6-33. These masses do not include flux scaling factors and are therefore larger than the BPRA input masses.

For the TPA plenum, the effective burnup is 300*0.2 = 60 GWd/MTU, while for the TPA top the effective burnup is 300*0.1 = 30 GWd/MTU. This reduces the cumulative burnup in each region to a value within the bounds of a typical ORIGEN-ARP model.

The TPA irradiation time is input to match the true irradiation time to properly credit Co-60 decay during the irradiation. Assuming a reactor assembly power of 19.68 MW and fuel loading of 0.492 MTU, the irradiation time to achieve a cumulative fuel assembly burnup of 300,000 GWd/MTU is 7,500 days. Because the irradiation time is fixed at 7,500 days, the FA power is selected to give the desired effective burnup in the plenum and top regions. For the top, the assembly power is 1.968 MW to achieve an effective burnup of 30 GWd/MTU. For the plenum, the assembly power is 3.936 MW to achieve an effective burnup of 60 GWd/MTU.

For simplicity of input preparation in the TPA calculation, no credit is taken for down time between cycles (typically assumed to be 30 days). Using approximately 12 cycles to achieve a burnup of 300 GWd/MTU, the conservatism of this assumption is 11*30 = 330 days of uncredited decay time.

Results for Co-60 activity and decay heat for both the BPRA and TPA are summarized in Table 6-36 for a cooling time of 10 years. It is observed that the BPRA source may be used in the active fuel region, as the TPA does not extend into this region. However, the TPA has a larger source than the BPRA in the plenum and top regions due to the high TPA burnup. Decay heat for both is small compared to SFA but must be accounted for during loading. The CC source used in the detailed PWR dose rate calculations is a hybrid CC source that combines the active fuel source of the BPRA with the top/plenum source of the TPA in *the inner zones (HLZC 4 Zones 1 and 2)*, but limits *the peripheral zone (HLZC 4 Zone 3)* to the lower BPRA source. This source is provided in Table 6-37. The CC source significantly impacts the peak dose rates on the side of the EOS-TC, due to the reduced lead thickness near the top nozzle.

While the specific CC source term presented in Table 6-37 is computed for a decay time of 10 years, this is not a minimum decay time requirement for licensing purposes. The actual CC to be loaded may have a shorter decay time as long as the as-loaded Co-60 activity is less than the limits provided *in TS Table 3 [6-11]*, and the total EOS-DSC decay heat remains below the applicable limit.

Encl. 4, B.1

6.2.5 Blended Low Enriched Uranium Fuel

[

]

6.2.6 Reconstituted Fuel

[

]

Proprietary Information on Pages 6-19 through 6-21
Withheld Pursuant to 10 CFR 2.390.

[

]

6.2.7 Irradiation Gases

During irradiation in a reactor, a FA will generate gases due to fission, alpha decay, and light element activation. The moles of gas generated are needed for subsequent pressure calculations documented in Chapter 4, Section 4.7, and are computed using ORIGEN-ARP. The noble gases (He, Ne, Ar, Kr, Xe, and Rn) are of primary interest as these gases do not react with other elements. The elements H, N, F, and Cl are conservatively assumed to be present in a gaseous state, although these elements may have formed solid compounds and may not be present as a gas. Bromine and iodine are also assumed to be present as a gas because the boiling points of these elements are low. Oxygen is not treated as a gas because it is present primarily in the compound UO_2.

The quantities of irradiation gases increase with burnup. Therefore, the quantity of gas is maximized for a burnup of 62 GWd/MTU. Most of the gases generated are stable isotopes. However, due to alpha decay of actinides present in spent fuel, the quantity of helium slowly increases with time. To obtain a bounding value for helium buildup due to alpha decay, 100 years of decay is assumed.

Integral fuel burnable absorber rods (IFBA) are used in some Westinghouse PWR designs. IFBA contains B-10, which results in helium gas generation due to the reaction B-10 + n → Li-7 + He-4. While the design basis B&W 15x15 FA does not contain IFBA, the effect of an IFBA FA is conservatively included by adding 450 g boron to the PWR input file.

Control components also may result in helium gas generation, primarily due to B-10 activation. No actinides or fission products are present in the CCs, so the quantity of gas is smaller than spent fuel. Because the BPRA contains boron while the TPA does not, the BPRA bounds the TPA for gas generation. BPRA data is summarized in Table 6-32. The B&W 15x15 BPRA contains poison in the form B_4C-Al_2O_3, typically up to 5% B_4C, while the WE 17x17 Pyrex design utilizes Pyrex poison. To conservatively bound these designs and potentially other designs, the boron mass is input as 450 g.

6.2.8 *Justification for the Reasonably Bounding Source Term Methodology*

Proprietary Information on Pages 6-25 through 6-26
Withheld Pursuant to 10 CFR 2.390.

- Downending/Transfer. The TC is fully assembled for the transfer operation. The OTCP and top cover plate (lid) are installed. The neutron shield is filled with water and all TC cavities are dry. The EOS-TC108 is modeled with the intermediate aluminum lid rather than the final steel lid.

These three configurations are also summarized in Table 6-49.

The EOS-TC108 has a removable neutron shield. The shield is formed of three panels that are connected with hinges on two joints and latches on the third joint. The interface joint between the three panels features 1.5 inches of aluminum, which allows limited neutron streaming through these three joints along the length of the EOS-TC108. The EOS-TC108 models do not include this streaming path, i.e., the neutron shield is modeled as continuous around the circumference. However, the neutron shield joints are modeled explicitly in a supplementary model, and the dose rates in the vicinity of the joints do not exceed the reported peak dose rates. In addition, the dose rates used in the dose assessment are essentially unchanged when the neutron shield joints are modeled. Therefore, it is acceptable to model the EOS-TC108 neutron shield as continuous around the circumference.

No temporary shielding is modeled, which would be used in practice to shield penetrations or localized areas of high dose rate. Therefore, the computed dose rates are larger than the dose rates that would be observed in actual practice.

The source terms used in the EOS-37PTH DSC models are the combined fuel and CC source terms. The CC source term from Table 6-37 is simply added to the *applicable* *PWR* fuel source term from *Section 6.2.2*. The CC source is added to every FA in the EOS-37PTH DSC. The EOS-89BTH DSC source terms are provided in Table 6-20 through Table 6-26. Note that the source term tables provide dry and wet neutron sources. Wet neutron sources are used only in the loading/decontamination models, while dry neutron sources are used in all other models. For the active fuel regions, an axial source distribution is applied per Table 6-30 and Table 6-31 for PWR and BWR fuel, respectively. For the top nozzle, plenum, and bottom nozzle regions, the source is evenly distributed throughout the region.

For each TC/DSC combination, dose rates are calculated on the surface, 30 cm, and 100 cm from the surfaces of the EOS-TC. Dose rates are also computed 300 cm from the side surface. All side dose rates are computed in 18 axial bins. The general tally locations are shown in Figure 6-7. In addition, for the final transfer configuration, dose rates are computed on the bottom and top surface in six radial segments (see Figure 6-8 and Figure 6-9) and on the side surface in 18 radial segments and 24 angular segments (see Figure 6-10).

All Indicated Changes are in response to RAI 6-8

Damaged or Failed Fuel, Normal and Off-Normal Conditions

Damaged or failed fuel may be tranferred in the EOS-37PTH DSC and EOS-TC125/135 using HLZC 6 or 8. Up to eight damaged fuel assemblies may be loaded in Zone 2, or up to four failed fuel canisters (FFCs)in Zone 3. Damaged and failed fuel may not be present in the same DSC. Damaged or failed fuel is not authorized for storage in the EOS-89BTH DSC or transfer in the EOS-TC108.

Proprietary Information on This Page
Withheld Pursuant to 10 CFR 2.390

All Indicated Changes are in response to RAI 6-14

[

]

Accident Conditions

Accident models are also developed for the four transfer configurations. In the accident models, the water neutron shield, neutron shield panel, and borated polyethylene bottom neutron shield are replaced with void, and the accident source terms are used. The dose rate is calculated at a distance of 100 m from the EOS-TC. Ground is modeled to account for ground scatter at large distances.

[

]

6.3.3 MCNP Model Geometry for the EOS-HSM

Detailed EOS-HSM MCNP models are developed for the following two configurations:

- EOS-HSM-Short with EOS-37PTH DSC
- EOS-HSM-Medium with EOS-89BTH DSC

The EOS-37PTH DSC and EOS-89BTH DSC models developed in Section 6.3.2 are used in the EOS-HSM models. Consistent with the EOS-DSC models, the Z-axis in the EOS-HSM models is along the length of the EOS-DSC. Because the DSC cavity has been reduced in length to match the length of the fuel, the EOS-37PTH DSC model is shorter than the EOS-89BTH DSC model. Short, medium, and long versions of the EOS-HSM may be used, depending on the length of EOS-DSC to be stored. The EOS-HSM modeled is the smallest EOS-HSM that fits the EOS-DSC. Therefore, the EOS-HSM-Short is modeled with the EOS-37PTH DSC and the EOS-HSM-Medium is modeled with the EOS-89BTH DSC.

The EOS-HSM features two DSC support structure designs. The original design utilizes I-beams, while an alternate design utilizes a flat plate system. These options do not affect the bulk shielding provided by the EOS-HSM, and the I-beam supports are represented in the MCNP models.

PWR source terms (without CCs) are provided in Table 6-17 through *Table 6-19d*, and the CC source provided in Table 6-37 is added to these PWR source terms for all FAs. BWR source terms are provided in Table 6-27 through Table 6-29. For the active fuel regions, an axial source distribution is applied per Table 6-30 and Table 6-31 for PWR and BWR fuel, respectively. For the top nozzle, plenum, and bottom nozzle regions, the source is evenly distributed throughout the region.

The EOS-HSMs are modeled explicitly, including the inlet (front) and outlet (roof) vents. Key dimensions used to develop the EOS-HSM models are summarized in Table 6-50, and figures illustrating the basic MCNP model are provided in Figure 6-11 through Figure 6-13. The figures illustrate the EOS-HSM-Medium with the EOS-89BTH DSC, although the geometry of the EOS-HSM-Short with the EOS-37PTH DSC is similar.

The EOS-HSM design consists of a base module that includes the door and 1-foot thick shield walls on the sides and rear. A 3-foot-8-inch thick roof block that matches the length and width of the base rests on the base module. The modules may be positioned either side-by-side in a single row or back-to-back in a double row. When positioned in a single row the rear of the base module is shielded by a 3-foot thick rear shield wall. An end (side) shield wall, which is also 3 feet thick, is placed beside the last module in the row. The end shield wall is comprised of two pieces mated with a Z-joint to prevent direct streaming through the joint. A corner shield wall is placed at the interface of the rear and end shield walls. When the modules are positioned back-to-back, no rear or corner shield walls are used.

Air inlet vents are located on the front and air outlet vents are located on the roof. Because little radiation directly penetrates the thick concrete shielding, essentially all of the dose rate is due to gamma radiation streaming from the vents. Radiation streaming through the outlet vents is mitigated by the use of vent covers. The vent covers feature a 1-inch thick steel plate and approximately 11 inches of concrete. The vent covers are 4 feet wide and are placed between adjacent EOS-HSMs or between an EOS-HSM and the end shield wall. Under normal and off-normal conditions the vent covers are always in place.

[

]

All Indicated Changes are in response to RAI 6-8

Proprietary Information on Pages 6-38 through 6-40
Withheld Pursuant to 10 CFR 2.390.

6.5 Supplemental Information

6.5.1 References

6-1 Oak Ridge National Laboratory, "A Modular Code System for Performing Standardized Computer Analyses for Licensing Evaluation," ORNL/TM-2005/39, Version 6, SCALE, January 2009.

6-2 Oak Ridge National Laboratory, "Predictions of PWR Spent Nuclear Fuel Isotopic Compositions," ORNL/TM-2010/44, SCALE 5.1, March 2010.

6-3 Oak Ridge National Laboratory, "Standard- and Extended-Burnup PWR and BWR Reactor Models for the ORIGEN2 Code," ORNL/TM-11018, December 1989.

6-4 Pacific Northwest Laboratory, "Spent Fuel Assembly Hardware: Characterization and 10 CFR 61 Classification for Waste Disposal, Volume 1 – Activation Measurements and Comparison with Calculations for Spent Fuel Assembly Hardware," PNL-6906, Vol. 1, June 1989.

6-5 Oak Ridge National Laboratory, "MCNP/MCNPX – Monte Carlo N-Particle Transport Code System Including MCNP5 1.40 and MCNPX 2.5.0 and Data Libraries," CCC-730, RSICC Computer Code Collection, January 2006.

6-6 NUREG/CR-6801, "Recommendations for Addressing Axial Burnup in PWR Burnup Credit Analyses," March 2003.

6-7 NUREG-1536, Rev. 1, "Standard Review Plan for Spent Fuel Dry Storage Systems at a General License Facility," July 2010.

6-8 Design Data Document DI-81001-02, NOK Document, "Technical Specification for the Supply of Transportable Casks for the Storage of Kernkraftwerk Leibstardt (KKL) Spent Fuel in ZWILAG," TS 07/01, Rev. 1.

6-9 Pacific Northwest National Laboratory, "Compendium of Material Composition Data for Radiation Transport Modeling," PNNL-15870, Rev. 1, March 2011.

6-10 ANSI/ANS-6.1.1-1977, "American National Standard Neutron and Gamma-Ray Flux-to-Dose-Rate Factors," American National Standards Institute, Inc., New York, New York.

6-11 CoC 1042 Appendix A, NUHOMS® EOS System Generic Technical Specifications, Amendment *1*.

(6-12) NUREG/CR-6999, "Technical Basis for a Proposed Expansion of Regulatory Guide 3.54 - Decay Heat Generation in an Independent Spent Fuel Storage Installation," February 2010.

(6-13) U.S. Energy Information Administration (EIA), Spent Nuclear Fuel GC-859 Database, Accessed January 20, 2019. URL: https://www.eia.gov/nuclear/spent_fuel/

RAI 6-11

RAI 6-6

Table 6-16d
PWR Source Term for the EOS-TC125/135, HLZC 5, Zone 1, 0.7 kW/FA
(Normal)

Burnup (GWd/MTU)			*24.54*	*50*	*24.54*	*24.54*
Enrichment (wt. % U-235)			*1.8*	*3.1*	*1.8*	*1.8*
Cooling Time (years)			*5.000*	*24.86*	*5.000*	*5.000*
Gamma Source Term, g/(sec*FA)						
E_{min}, MeV	***to***	***E_{max}, MeV***	***Bottom Nozzle***	***In-core***	***Plenum***	***Top Nozzle***
1.00E-02	*to*	*5.00E-02*	*1.745E+11*	*6.875E+14*	*1.169E+11*	*4.051E+10*
5.00E-02	*to*	*1.00E-01*	*1.408E+10*	*2.015E+14*	*8.930E+09*	*7.869E+09*
1.00E-01	*to*	*2.00E-01*	*1.292E+10*	*1.254E+14*	*8.335E+09*	*1.928E+09*
2.00E-01	*to*	*3.00E-01*	*8.456E+08*	*3.811E+13*	*5.500E+08*	*9.491E+07*
3.00E-01	*to*	*4.00E-01*	*2.480E+09*	*2.518E+13*	*1.612E+09*	*1.232E+08*
4.00E-01	*to*	*6.00E-01*	*5.093E+10*	*2.093E+13*	*3.315E+10*	*8.717E+06*
6.00E-01	*to*	*8.00E-01*	*2.742E+10*	*1.327E+15*	*2.163E+10*	*7.238E+08*
8.00E-01	*to*	*1.00E+00*	*9.757E+10*	*1.365E+13*	*2.063E+10*	*5.572E+10*
1.00E+00	*to*	*1.33E+00*	*3.903E+12*	*2.149E+13*	*2.470E+12*	*2.280E+12*
1.33E+00	*to*	*1.66E+00*	*1.102E+12*	*2.208E+12*	*6.975E+11*	*6.438E+11*
1.66E+00	*to*	*2.00E+00*	*6.486E+02*	*6.470E+10*	*1.274E+03*	*3.779E+02*
2.00E+00	*to*	*2.50E+00*	*2.637E+07*	*3.335E+09*	*1.669E+07*	*1.540E+07*
2.50E+00	*to*	*3.00E+00*	*2.253E+04*	*5.679E+08*	*1.426E+04*	*1.316E+04*
3.00E+00	*to*	*4.00E+00*	*5.139E-06*	*4.256E+07*	*2.552E-05*	*4.232E-06*
4.00E+00	*to*	*5.00E+00*	*2.987E-29*	*1.436E+07*	*1.944E-29*	*0.000E+00*
5.00E+00	*to*	*6.50E+00*	*8.606E-30*	*5.763E+06*	*5.602E-30*	*0.000E+00*
6.50E+00	*to*	*8.00E+00*	*1.095E-30*	*1.130E+06*	*7.125E-31*	*0.000E+00*
8.00E+00	*to*	*1.00E+01*	*1.461E-31*	*2.400E+05*	*9.509E-32*	*0.000E+00*
*Total Gamma, g/(sec*FA)*			*5.386E+12*	*2.463E+15*	*3.379E+12*	*3.031E+12*
Total Neutron Source Term, n/(sec*FA)						
Raw ORIGEN-ARP source for uniform burnup						*4.170E+08*
Treated with peaking factor 1.215 and k-eff=0.4 (dry)						*8.444E+08*
Treated with peaking factor 1.215 and k-eff=0.65 (wet)						*1.448E+09*

All Indicated Changes are in response to RAI 6-8

Table 6-16e
PWR Source Term for the EOS-TC125/135, HLZC 5, Zone 2, 0.5 kW/FA (Normal)

Burnup (GWd/MTU)			*18.285*	*40*	*18.285*	*18.285*
Enrichment (wt. % U-235)			*1.8*	*2.5*	*1.8*	*1.8*
Cooling Time (yr)			*5.000*	*28.934*	*5.000*	*5.000*
Gamma Source Term, g/(sec*FA)						
E_{min}, MeV	***to***	***E_{max}, MeV***	***Bottom Nozzle***	***In-core***	***Plenum***	***Top Nozzle***
1.00E-02	*to*	*5.00E-02*	*1.356E+11*	*5.000E+14*	*9.010E+10*	*3.144E+10*
5.00E-02	*to*	*1.00E-01*	*1.095E+10*	*1.514E+14*	*6.829E+09*	*6.115E+09*
1.00E-01	*to*	*2.00E-01*	*9.930E+09*	*8.881E+13*	*6.380E+09*	*1.499E+09*
2.00E-01	*to*	*3.00E-01*	*6.494E+08*	*2.722E+13*	*4.210E+08*	*7.374E+07*
3.00E-01	*to*	*4.00E-01*	*1.903E+09*	*1.823E+13*	*1.235E+09*	*9.575E+07*
4.00E-01	*to*	*6.00E-01*	*3.899E+10*	*1.392E+13*	*2.538E+10*	*6.783E+06*
6.00E-01	*to*	*8.00E-01*	*2.097E+10*	*9.718E+14*	*1.646E+10*	*5.387E+08*
8.00E-01	*to*	*1.00E+00*	*8.011E+10*	*7.866E+12*	*1.662E+10*	*4.573E+10*
1.00E+00	*to*	*1.33E+00*	*3.036E+12*	*1.210E+13*	*1.889E+12*	*1.771E+12*
1.33E+00	*to*	*1.66E+00*	*8.574E+11*	*1.251E+12*	*5.334E+11*	*5.002E+11*
1.66E+00	*to*	*2.00E+00*	*5.999E+02*	*4.665E+10*	*1.217E+03*	*3.667E+02*
2.00E+00	*to*	*2.50E+00*	*2.051E+07*	*2.400E+09*	*1.276E+07*	*1.197E+07*
2.50E+00	*to*	*3.00E+00*	*1.753E+04*	*3.403E+08*	*1.090E+04*	*1.023E+04*
3.00E+00	*to*	*4.00E+00*	*3.127E-06*	*2.236E+07*	*1.553E-05*	*2.575E-06*
4.00E+00	*to*	*5.00E+00*	*3.270E-30*	*7.548E+06*	*2.129E-30*	*0.000E+00*
5.00E+00	*to*	*6.50E+00*	*9.423E-31*	*3.029E+06*	*6.134E-31*	*0.000E+00*
6.50E+00	*to*	*8.00E+00*	*1.198E-31*	*5.940E+05*	*7.801E-32*	*0.000E+00*
8.00E+00	*to*	*1.00E+01*	*1.599E-32*	*1.261E+05*	*1.041E-32*	*0.000E+00*
*Total Gamma, g/(sec*FA)*			*4.193E+12*	*1.793E+15*	*2.586E+12*	*2.357E+12*
Total Neutron Source Term, n/(sec*FA)						
Raw ORIGEN-ARP source for uniform burnup						*2.193E+08*
Treated with peaking factor 1.215 and k-eff=0.4 (dry)						*4.441E+08*
Treated with peaking factor 1.215 and k-eff=0.65 (wet)						*7.613E+08*

All Indicated Changes are in response to RAI 6-8

Table 6-16f
PWR Source Term for the EOS-TC125/135, HLZC 5, Zone 3, 2.4 kW/FA
(Normal)

Burnup (GWd/MTU)			*50*	*62*	*50*	*50*
Enrichment (wt. % U-235)			*3.1*	*3.8*	*3.1*	*3.1*
Cooling Time (yr)			*3.332*	*4.167*	*3.332*	*3.332*
Gamma Source Term, g/(sec*FA)						
E_{min}, MeV	***to***	***E_{max}, MeV***	***Bottom Nozzle***	***In-core***	***Plenum***	***Top Nozzle***
1.00E-02	*to*	*5.00E-02*	*4.336E+11*	*2.648E+15*	*2.933E+11*	*7.280E+10*
5.00E-02	*to*	*1.00E-01*	*2.565E+10*	*7.729E+14*	*1.719E+10*	*1.414E+10*
1.00E-01	*to*	*2.00E-01*	*2.940E+10*	*6.602E+14*	*1.923E+10*	*3.470E+09*
2.00E-01	*to*	*3.00E-01*	*1.971E+09*	*1.835E+14*	*1.293E+09*	*1.705E+08*
3.00E-01	*to*	*4.00E-01*	*6.254E+09*	*1.284E+14*	*4.080E+09*	*2.213E+08*
4.00E-01	*to*	*6.00E-01*	*1.244E+11*	*2.120E+15*	*8.098E+10*	*2.582E+07*
6.00E-01	*to*	*8.00E-01*	*6.652E+10*	*4.743E+15*	*5.000E+10*	*1.284E+09*
8.00E-01	*to*	*1.00E+00*	*4.949E+11*	*9.255E+14*	*9.115E+10*	*2.819E+11*
1.00E+00	*to*	*1.33E+00*	*6.982E+12*	*2.403E+14*	*4.686E+12*	*4.096E+12*
1.33E+00	*to*	*1.66E+00*	*1.972E+12*	*8.202E+13*	*1.323E+12*	*1.157E+12*
1.66E+00	*to*	*2.00E+00*	*2.421E+05*	*3.082E+12*	*5.204E+05*	*1.609E+05*
2.00E+00	*to*	*2.50E+00*	*4.718E+07*	*5.914E+12*	*3.166E+07*	*2.768E+07*
2.50E+00	*to*	*3.00E+00*	*4.031E+04*	*2.323E+11*	*2.705E+04*	*2.365E+04*
3.00E+00	*to*	*4.00E+00*	*1.331E-05*	*2.159E+10*	*6.607E-05*	*1.096E-05*
4.00E+00	*to*	*5.00E+00*	*2.027E-27*	*4.932E+07*	*1.319E-27*	*0.000E+00*
5.00E+00	*to*	*6.50E+00*	*5.840E-28*	*1.980E+07*	*3.801E-28*	*0.000E+00*
6.50E+00	*to*	*8.00E+00*	*7.427E-29*	*3.884E+06*	*4.834E-29*	*0.000E+00*
8.00E+00	*to*	*1.00E+01*	*9.912E-30*	*8.246E+05*	*6.452E-30*	*0.000E+00*
*Total Gamma, g/(sec*FA)*			*1.014E+13*	*1.251E+16*	*6.567E+12*	*5.626E+12*
Total Neutron Source Term, n/(sec*FA)						
Raw ORIGEN-ARP source for uniform burnup						*1.441E+09*
Treated with peaking factor 1.215 and k-eff=0.4 (dry)						*2.918E+09*
Treated with peaking factor 1.215 and k-eff=0.65 (wet)						*5.002E+09*

All Indicated Changes are in response to RAI 6-8

Table 6-16g
PWR Source Term for the EOS-TC125/135, HLZC 5, Zone 4, 0.85 kW/FA (Normal)

Burnup (GWd/MTU)			*28.71*	*8.298*	*28.71*	*28.71*
Enrichment (wt. % U-235)			*1.8*	*1.3*	*1.8*	*1.8*
Cooling Time (yr)			*5.000*	*2.000*	*5.000*	*5.000*
Gamma Source Term, g/(sec*FA)						
E_{min}, MeV	***to***	***E_{max}, MeV***	***Bottom Nozzle***	***In-core***	***Plenum***	***Top Nozzle***
1.00E-02	*to*	*5.00E-02*	*1.994E+11*	*1.916E+15*	*1.343E+11*	*4.636E+10*
5.00E-02	*to*	*1.00E-01*	*1.610E+10*	*6.245E+14*	*1.033E+10*	*9.001E+09*
1.00E-01	*to*	*2.00E-01*	*1.484E+10*	*6.301E+14*	*9.608E+09*	*2.205E+09*
2.00E-01	*to*	*3.00E-01*	*9.722E+08*	*1.570E+14*	*6.339E+08*	*1.086E+08*
3.00E-01	*to*	*4.00E-01*	*2.853E+09*	*1.237E+14*	*1.856E+09*	*1.410E+08*
4.00E-01	*to*	*6.00E-01*	*5.864E+10*	*4.554E+14*	*3.817E+10*	*9.964E+06*
6.00E-01	*to*	*8.00E-01*	*3.159E+10*	*7.470E+14*	*2.500E+10*	*8.492E+08*
8.00E-01	*to*	*1.00E+00*	*1.076E+11*	*1.011E+14*	*2.305E+10*	*6.149E+10*
1.00E+00	*to*	*1.33E+00*	*4.461E+12*	*5.810E+13*	*2.857E+12*	*2.608E+12*
1.33E+00	*to*	*1.66E+00*	*1.260E+12*	*2.090E+13*	*8.069E+11*	*7.365E+11*
1.66E+00	*to*	*2.00E+00*	*6.828E+02*	*3.440E+12*	*1.311E+03*	*3.843E+02*
2.00E+00	*to*	*2.50E+00*	*3.014E+07*	*1.414E+13*	*1.931E+07*	*1.762E+07*
2.50E+00	*to*	*3.00E+00*	*2.575E+04*	*2.225E+11*	*1.650E+04*	*1.506E+04*
3.00E+00	*to*	*4.00E+00*	*6.684E-06*	*1.983E+10*	*3.319E-05*	*5.504E-06*
4.00E+00	*to*	*5.00E+00*	*9.736E-29*	*1.138E+05*	*6.338E-29*	*0.000E+00*
5.00E+00	*to*	*6.50E+00*	*2.805E-29*	*4.558E+04*	*1.826E-29*	*0.000E+00*
6.50E+00	*to*	*8.00E+00*	*3.568E-30*	*8.929E+03*	*2.323E-30*	*0.000E+00*
8.00E+00	*to*	*1.00E+01*	*4.762E-31*	*1.894E+03*	*3.100E-31*	*0.000E+00*
*Total Gamma, g/(sec*FA)*			*6.153E+12*	*4.852E+15*	*3.907E+12*	*3.465E+12*
Total Neutron Source Term, n/(sec*FA)						
Raw ORIGEN-ARP source for uniform burnup						*3.371E+06*
Treated with peaking factor 1.215 and k-eff=0.4 (dry)						*6.826E+06*
Treated with peaking factor 1.215 and k-eff=0.65 (wet)						*1.170E+07*

All Indicated Changes are in response to RAI 6-8

Table 6-19a
PWR Source Term for the EOS-HSM, HLZC 5, Zone 1, 0.7 kW/FA (Normal)

Burnup (GWd/MTU)			*24.54*	*50*	*24.54*	*24.54*
Enrichment (wt. % U-235)			*1.8*	*3.1*	*1.8*	*1.8*
Cooling Time (yr)			*5.000*	*24.860*	*5.000*	*5.000*
Gamma Source Term, g/(sec*FA)						
E_{min}, MeV	***to***	***E_{max}, MeV***	***Bottom Nozzle***	***In-core***	***Plenum***	***Top Nozzle***
1.00E-02	*to*	*5.00E-02*	*1.745E+11*	*6.875E+14*	*1.169E+11*	*4.051E+10*
5.00E-02	*to*	*1.00E-01*	*1.408E+10*	*2.015E+14*	*8.930E+09*	*7.869E+09*
1.00E-01	*to*	*2.00E-01*	*1.292E+10*	*1.254E+14*	*8.335E+09*	*1.928E+09*
2.00E-01	*to*	*3.00E-01*	*8.456E+08*	*3.811E+13*	*5.500E+08*	*9.491E+07*
3.00E-01	*to*	*4.00E-01*	*2.480E+09*	*2.518E+13*	*1.612E+09*	*1.232E+08*
4.00E-01	*to*	*6.00E-01*	*5.093E+10*	*2.093E+13*	*3.315E+10*	*8.717E+06*
6.00E-01	*to*	*8.00E-01*	*2.742E+10*	*1.327E+15*	*2.163E+10*	*7.238E+08*
8.00E-01	*to*	*1.00E+00*	*9.757E+10*	*1.365E+13*	*2.063E+10*	*5.572E+10*
1.00E+00	*to*	*1.33E+00*	*3.903E+12*	*2.149E+13*	*2.470E+12*	*2.280E+12*
1.33E+00	*to*	*1.66E+00*	*1.102E+12*	*2.208E+12*	*6.975E+11*	*6.438E+11*
1.66E+00	*to*	*2.00E+00*	*6.486E+02*	*6.470E+10*	*1.274E+03*	*3.779E+02*
2.00E+00	*to*	*2.50E+00*	*2.637E+07*	*3.335E+09*	*1.669E+07*	*1.540E+07*
2.50E+00	*to*	*3.00E+00*	*2.253E+04*	*5.679E+08*	*1.426E+04*	*1.316E+04*
3.00E+00	*to*	*4.00E+00*	*5.139E-06*	*4.256E+07*	*2.552E-05*	*4.232E-06*
4.00E+00	*to*	*5.00E+00*	*2.987E-29*	*1.436E+07*	*1.944E-29*	*0.000E+00*
5.00E+00	*to*	*6.50E+00*	*8.606E-30*	*5.763E+06*	*5.602E-30*	*0.000E+00*
6.50E+00	*to*	*8.00E+00*	*1.095E-30*	*1.130E+06*	*7.125E-31*	*0.000E+00*
8.00E+00	*to*	*1.00E+01*	*1.461E-31*	*2.400E+05*	*9.509E-32*	*0.000E+00*
*Total Gamma, g/(sec*FA)*			*5.386E+12*	*2.463E+15*	*3.379E+12*	*3.031E+12*
Total Neutron Source Term, n/(sec*FA)						
Raw ORIGEN-ARP source for uniform burnup						*4.170E+08*
Treated with peaking factor 1.215 and k-eff=0.4 (dry)						*8.444E+08*

All Indicated Changes are in response to RAI 6-8

Table 6-19b
PWR Source Term for the EOS-HSM, HLZC 5, Zone 2, 0.5 kW/FA (Normal)

Burnup (GWd/MTU)			*18.285*	*4.558*	*18.285*	*18.285*
Enrichment (wt. % U-235)			*1.8*	*0.7*	*1.8*	*1.8*
Cooling Time (yr)			*5.000*	*2.000*	*5.000*	*5.000*
Gamma Source Term, g/(sec*FA)						
E_{min}, MeV	***to***	***E_{max}, MeV***	***Bottom Nozzle***	***In-core***	***Plenum***	***Top Nozzle***
1.00E-02	*to*	*5.00E-02*	*1.356E+11*	*1.148E+15*	*9.010E+10*	*3.144E+10*
5.00E-02	*to*	*1.00E-01*	*1.095E+10*	*3.762E+14*	*6.829E+09*	*6.115E+09*
1.00E-01	*to*	*2.00E-01*	*9.930E+09*	*3.779E+14*	*6.380E+09*	*1.499E+09*
2.00E-01	*to*	*3.00E-01*	*6.494E+08*	*9.494E+13*	*4.210E+08*	*7.374E+07*
3.00E-01	*to*	*4.00E-01*	*1.903E+09*	*7.512E+13*	*1.235E+09*	*9.575E+07*
4.00E-01	*to*	*6.00E-01*	*3.899E+10*	*2.496E+14*	*2.538E+10*	*6.783E+06*
6.00E-01	*to*	*8.00E-01*	*2.097E+10*	*4.000E+14*	*1.646E+10*	*5.387E+08*
8.00E-01	*to*	*1.00E+00*	*8.011E+10*	*4.424E+13*	*1.662E+10*	*4.573E+10*
1.00E+00	*to*	*1.33E+00*	*3.036E+12*	*3.614E+13*	*1.889E+12*	*1.771E+12*
1.33E+00	*to*	*1.66E+00*	*8.574E+11*	*1.217E+13*	*5.334E+11*	*5.002E+11*
1.66E+00	*to*	*2.00E+00*	*5.999E+02*	*2.164E+12*	*1.217E+03*	*3.667E+02*
2.00E+00	*to*	*2.50E+00*	*2.051E+07*	*8.459E+12*	*1.276E+07*	*1.197E+07*
2.50E+00	*to*	*3.00E+00*	*1.753E+04*	*1.430E+11*	*1.090E+04*	*1.023E+04*
3.00E+00	*to*	*4.00E+00*	*3.127E-06*	*1.280E+10*	*1.553E-05*	*2.575E-06*
4.00E+00	*to*	*5.00E+00*	*3.270E-30*	*3.560E+04*	*2.129E-30*	*0.000E+00*
5.00E+00	*to*	*6.50E+00*	*9.423E-31*	*1.424E+04*	*6.134E-31*	*0.000E+00*
6.50E+00	*to*	*8.00E+00*	*1.198E-31*	*2.786E+03*	*7.801E-32*	*0.000E+00*
8.00E+00	*to*	*1.00E+01*	*1.599E-32*	*5.904E+02*	*1.041E-32*	*0.000E+00*
*Total Gamma, g/(sec*FA)*			*4.193E+12*	*2.825E+15*	*2.586E+12*	*2.357E+12*
Total Neutron Source Term, n/(sec*FA)						
Raw ORIGEN-ARP source for uniform burnup						*1.072E+06*
Treated with peaking factor 1.215 and k-eff=0.4 (dry)						*2.171E+06*

All Indicated Changes are in response to RAI 6-8

Table 6-19c
PWR Source Term for the EOS-HSM, HLZC 5, Zone 3, 2.4 kW/FA (Normal)

Burnup (GWd/MTU)			*50*	*62*	*50*	*50*
Enrichment (wt. % U-235)			*3.1*	*3.8*	*3.1*	*3.1*
Cooling Time (yr)			*3.332*	*4.167*	*3.332*	*3.332*
Gamma Source Term, g/(sec*FA)						
E_{min}, MeV	***to***	***E_{max}, MeV***	***Bottom Nozzle***	***In-core***	***Plenum***	***Top Nozzle***
1.00E-02	*to*	*5.00E-02*	*4.336E+11*	*2.648E+15*	*2.933E+11*	*7.280E+10*
5.00E-02	*to*	*1.00E-01*	*2.565E+10*	*7.729E+14*	*1.719E+10*	*1.414E+10*
1.00E-01	*to*	*2.00E-01*	*2.940E+10*	*6.602E+14*	*1.923E+10*	*3.470E+09*
2.00E-01	*to*	*3.00E-01*	*1.971E+09*	*1.835E+14*	*1.293E+09*	*1.705E+08*
3.00E-01	*to*	*4.00E-01*	*6.254E+09*	*1.284E+14*	*4.080E+09*	*2.213E+08*
4.00E-01	*to*	*6.00E-01*	*1.244E+11*	*2.120E+15*	*8.098E+10*	*2.582E+07*
6.00E-01	*to*	*8.00E-01*	*6.652E+10*	*4.743E+15*	*5.000E+10*	*1.284E+09*
8.00E-01	*to*	*1.00E+00*	*4.949E+11*	*9.255E+14*	*9.115E+10*	*2.819E+11*
1.00E+00	*to*	*1.33E+00*	*6.982E+12*	*2.403E+14*	*4.686E+12*	*4.096E+12*
1.33E+00	*to*	*1.66E+00*	*1.972E+12*	*8.202E+13*	*1.323E+12*	*1.157E+12*
1.66E+00	*to*	*2.00E+00*	*2.421E+05*	*3.082E+12*	*5.204E+05*	*1.609E+05*
2.00E+00	*to*	*2.50E+00*	*4.718E+07*	*5.914E+12*	*3.166E+07*	*2.768E+07*
2.50E+00	*to*	*3.00E+00*	*4.031E+04*	*2.323E+11*	*2.705E+04*	*2.365E+04*
3.00E+00	*to*	*4.00E+00*	*1.331E-05*	*2.159E+10*	*6.607E-05*	*1.096E-05*
4.00E+00	*to*	*5.00E+00*	*2.027E-27*	*4.932E+07*	*1.319E-27*	*0.000E+00*
5.00E+00	*to*	*6.50E+00*	*5.840E-28*	*1.980E+07*	*3.801E-28*	*0.000E+00*
6.50E+00	*to*	*8.00E+00*	*7.427E-29*	*3.884E+06*	*4.834E-29*	*0.000E+00*
8.00E+00	*to*	*1.00E+01*	*9.912E-30*	*8.246E+05*	*6.452E-30*	*0.000E+00*
*Total Gamma, g/(sec*FA)*			*1.014E+13*	*1.251E+16*	*6.567E+12*	*5.626E+12*
Total Neutron Source Term, n/(sec*FA)						
Raw ORIGEN-ARP source for uniform burnup						*1.441E+09*
Treated with peaking factor 1.215 and k-eff=0.4 (dry)						*2.918E+09*

All Indicated Changes are in response to RAI 6-8

Table 6-19d
PWR Source Term for the EOS-HSM, HLZC 5, Zone 4, 0.85 kW/FA (Normal)

Burnup (GWd/MTU)			*28.71*	*28.71*	*28.71*	*28.71*
Enrichment (wt. % U-235)			*1.8*	*1.8*	*1.8*	*1.8*
Cooling Time (yr)			*5.000*	*5.000*	*5.000*	*5.000*
Gamma Source Term, g/(sec*FA)						
E_{min}, MeV	***to***	***E_{max}, MeV***	***Bottom Nozzle***	***In-core***	***Plenum***	***Top Nozzle***
1.00E-02	*to*	*5.00E-02*	*1.994E+11*	*1.130E+15*	*1.343E+11*	*4.636E+10*
5.00E-02	*to*	*1.00E-01*	*1.610E+10*	*3.306E+14*	*1.033E+10*	*9.001E+09*
1.00E-01	*to*	*2.00E-01*	*1.484E+10*	*2.755E+14*	*9.608E+09*	*2.205E+09*
2.00E-01	*to*	*3.00E-01*	*9.722E+08*	*7.708E+13*	*6.339E+08*	*1.086E+08*
3.00E-01	*to*	*4.00E-01*	*2.853E+09*	*5.469E+13*	*1.856E+09*	*1.410E+08*
4.00E-01	*to*	*6.00E-01*	*5.864E+10*	*6.241E+14*	*3.817E+10*	*9.964E+06*
6.00E-01	*to*	*8.00E-01*	*3.159E+10*	*1.819E+15*	*2.500E+10*	*8.492E+08*
8.00E-01	*to*	*1.00E+00*	*1.076E+11*	*2.575E+14*	*2.305E+10*	*6.149E+10*
1.00E+00	*to*	*1.33E+00*	*4.461E+12*	*9.264E+13*	*2.857E+12*	*2.608E+12*
1.33E+00	*to*	*1.66E+00*	*1.260E+12*	*2.712E+13*	*8.069E+11*	*7.365E+11*
1.66E+00	*to*	*2.00E+00*	*6.828E+02*	*1.260E+12*	*1.311E+03*	*3.843E+02*
2.00E+00	*to*	*2.50E+00*	*3.014E+07*	*2.397E+12*	*1.931E+07*	*1.762E+07*
2.50E+00	*to*	*3.00E+00*	*2.575E+04*	*9.448E+10*	*1.650E+04*	*1.506E+04*
3.00E+00	*to*	*4.00E+00*	*6.684E-06*	*8.760E+09*	*3.319E-05*	*5.504E-06*
4.00E+00	*to*	*5.00E+00*	*9.736E-29*	*8.559E+06*	*6.338E-29*	*0.000E+00*
5.00E+00	*to*	*6.50E+00*	*2.805E-29*	*3.435E+06*	*1.826E-29*	*0.000E+00*
6.50E+00	*to*	*8.00E+00*	*3.568E-30*	*6.738E+05*	*2.323E-30*	*0.000E+00*
8.00E+00	*to*	*1.00E+01*	*4.762E-31*	*1.431E+05*	*3.100E-31*	*0.000E+00*
*Total Gamma, g/(sec*FA)*			*6.153E+12*	*4.692E+15*	*3.907E+12*	*3.465E+12*
Total Neutron Source Term, n/(sec*FA)						
Raw ORIGEN-ARP source for uniform burnup						*2.457E+08*
Treated with peaking factor 1.215 and k-eff=0.4 (dry)						*4.975E+08*

All Indicated Changes are in response to RAI 6-8

Proprietary Information on Pages 6-97 through 6-109
Withheld Pursuant to 10 CFR 2.390.

Proprietary Information on Pages 6-123 through 6-125
Withheld Pursuant to 10 CFR 2.390.

Table 6-60
Distribution of BWR Assemblies from 2013 EIA GC-859 Database

Burn-Up, GWd/MTU	Assembly Averaged Initial ^{235}U Enrichment, wt.%																																							
	0.6	0.7	0.8	0.9	1.0	1.1	1.2	1.3	1.4	1.5	1.6	1.7	1.8	1.9	2.0	2.1	2.2	2.3	2.4	2.5	2.6	2.7	2.8	2.9	3.0	3.1	3.2	3.3	3.4	3.5	3.6	3.7	3.8	3.9	4.0	4.1	4.2	4.3	4.4	4.5
1																			1	2																					
2		50																	1	5											1										
3		365				2										2			7									1												
4		579														3	11		6	1									2											
5		298				1									1	2	19		11	38									8	1	2	6					1			
6		44		32		9									1	22	39		17	2	1	1	1				3				2	10								
7				40		135									2	57	3	2	19	20		1				1	3	1	4			4								
8				132	6	99									1	28	9	1	7	27			1				5		8					2						
9				156	17	103						2			21	50	27		31	29	9		2				7	1			2									
10				4	23	272				116		6	1		3	74	32		33	96	30		6				8			4	11					1				
11				8	70	305			8	144	8	8			2	95	54	1	29	84	7		14			2	32	2	2	3	4		1							
12				7	13	76			12	77		304			2	227	50	9	4	7	4		36		1	12	71		3		10		2	2						
13				52						168	4	171			12	441	105	2	4	14	26		110	2	2	11	114		6		15		7	5						
14				58						114	20	508			27	140	115	1	4	30	23		37	2	1	2	54	3	7	1	34	1	6	9	1		1			
15				15						24	128	197		2	137	141	108	3	9	25	8	2	14		2		57	1	4	8	30		6	17		1				
16				14							161	197	3		51	263	116	13	13	22	2	2	26	1		1	4		2	4	36		29	17						
17				18						32	50	289	12	6	53	662	95	35	4	35	5	17	12		1	2				6	62		46	7	1	1				
18				3						28	61	151	49		140	808	144	46	1	27	32	7	20			3			2	12	57		64	6						
19				5					1	8	80	249	57	6	275	726	154	92	4	121	52	19	4	1		2	1		5	9	24		3	6						
20									3		60	59	30	18	99	1047	229	111	9	417	96	20	7			1			5	13	11		3	10	1		1			
21									7		21	27	7	57	137	774	309	135	20	261	131	54	38	1		6	1	5	6	15	6		7	4	1					
22									1		35	20	3	4	85	943	209	143	44	264	164	112	82	7	1	3	4	6	7	6	1		21	7	4					
23									1		22	16	1		90	746	187	49	202	541	246	94	111	15	3	17	5	1	32	1		3	29	5	2	2				
24									8		26	24	4		80	574	302	75	224	609	434	223	203	12	5	32	3	1	48			5	34		1	3	1				
25									21	3	20	9	4	6	76	522	335	51	210	559	400	395	317	21	5	80	3	7	35			5	30	1	1					
26									7	5	16	8	1	17	103	460	152	45	300	649	439	442	474	83	30	52	11	6	34			3	92							
27											2	16	1	11	92	402	150	40	257	551	536	435	550	200	58	67	37	6	22			3	78	3	2	2				
28											6	6	1	27	3	274	181	31	265	492	752	457	1006	185	149	86	16	26	4	1		10	35	1		4				
29												7	1	15	8	169	139	35	273	348	988	289	1110	271	229	110	43	40	15			1	28		3					
30										1				24	12	126	60	7	135	183	925	276	1184	484	377	112	44	124	53	2			13		1	2				
31														24	4	38	41		144	60	797	229	1084	487	334	156	150	147	119	29	2	50	8	1	10	8				
32														3		24	17	2	36	76	686	206	1002	711	381	213	270	399	229	50	22	38	18	2	36	42		1		
33											4					9	5	1	12	76	507	177	707	879	497	391	207	484	297	54	14	74	53	3	15	1	4		
34																7			6	20	197	114	631	865	671	406	418	525	251	94	9	161	78	9	7	10	8		
35															24				1	8	105	89	307	612	451	495	776	431	310	152	18	63	125	22	11	6		1		
36																			24	4	3	81	127	404	470	731	1094	495	427	179	21	29	130	29	52	43	11	1		
37														4				1	14	4	2	34	79	269	373	892	1120	613	512	193	65	95	65	46	70	47	12	14		
38														14					11	6	1	4	36	286	468	565	909	594	484	196	72	184	160	211	220	90	68	13		
39														3						16	7	16	33	225	421	436	824	359	455	234	104	309	232	369	193	158	128	19	1	
40																					2		18	54	149	305	736	342	393	286	180	429	263	359	241	115	164	27		
41										1										4	2		34	25	77	132	508	454	381	284	381	500	356	405	405	147	165	91	1	
42																							7	47	41	111	346	263	287	506	385	532	365	709	632	368	196	39	2	
43																					1		7	51	19	72	288	151	245	430	266	407	507	761	1032	568	228	64	15	
44																					4			16	4	20	172	70	234	240	174	453	474	867	1537	1043	361	49	47	
45																									8	31	162	20	121	171	293	521	358	790	1192	1244	294	54	57	
46																										14	87	27	57	99	301	504	379	760	1009	913	242	37	8	
47																										3	62	27	20	94	226	460	364	704	1053	1180	158	43	8	
48																										1	24	18	5	81	134	266	219	674	1001	934	93	21	13	
49																											3	18	17	41	113	309	230	597	923	910	79	27	22	
50																											2	17	18	19	39	187	234	424	721	824	72	1	1	
51																											2	39	4	20	26	150	95	219	519	670	29	1		
52																											2	22		6	18	47	41	101	288	382	4			
53																											1	24		8	24	9	38	26	101	147				
54																												4		32	8	2		9	22	18				
55																														8					2	1				
56																																								
Enr.–>	0.6	0.7	0.8	0.9	1.0	1.1	1.2	1.3	1.4	1.5	1.6	1.7	1.8	1.9	2.0	2.1	2.2	2.3	2.4	2.5	2.6	2.7	2.8	2.9	3.0	3.1	3.2	3.3	3.4	3.5	3.6	3.7	3.8	3.9	4.0	4.1	4.2	4.3	4.4	4.5

Note: The heavy line represents the lower enrichment boundary from Table 6-7.

Table 6-61
Distribution of PWR Assemblies from 2013 EIA GC-859 Database

Burn-Up, GWd/MTU	Assembly Averaged Initial ^{235}U Enrichment, wt.%																																												
	0.2	0.3	0.4	0.7	0.8	0.9	1.1	1.2	1.3	1.4	1.5	1.6	1.7	1.8	1.9	2.0	2.1	2.2	2.3	2.4	2.5	2.6	2.7	2.8	2.9	3.0	3.1	3.2	3.3	3.4	3.5	3.6	3.7	3.8	3.9	4.0	4.1	4.2	4.3	4.4	4.5	4.6	4.7	4.8	4.9	5.0
1																																														
2																																														
3		16									1								2																											
4																																							8						
5															3																1					5			16						
6															1	1				1				1			2			3	4								8						
7												1												1	2	8	5	2		1	4				9	5									
8									8	1	1					1									11	9					4		8		11	7									
9									13	7					2	1									16		2	2	3	8	20		24		9	1					2	2			
10									4				4												6	80		1	5	10	4		4			6					10	2			
11	4								4			20				13				2					13	8				11		2	32		5	7					4				
12		4					16		4	6	18	50	20	6		29	11		1	33		1			9	8	3			1	4	2			10	8				15	5	3			
13		4		2						17	8	60	49	7	39	13	4	1	2	34					1	14	1	3	1	2	2			2	12				5	2	2			
14				2						23	24	152		61	56	15	10			49					4		1			7	1		2	1	16		4		12					
15									8	5	14	84		122	36	22	48			8					15	1	5			2	16		1	2	5	11		4		14			7		
16									16		16	1		155	126	58	58	32		14		1	3		1			2		1				1		9		1		29			5		
17											2			53	90	147	230	27	9	23		14	3	1	8	1	1	2		1	22	1				1		4		25			4		
18								4	4			5		8	140	96	333	95	15			17	6	5			15		11	3	35	1	1			11	10	8			4		12		
19													1	4	39	17	242	158	2	16		17	22	11	1	1	52	10	3		1	3	9	1	1	7		12	1		12				
20				4			1	3		1				18	20	23	240	149		11	13	37	21	5	1	55	47	11	19	3		2	7	1		17		5		4				4	
21											2			15	40	19	107	52	15	39	34	84	19	3	8	13	68	3	3	5	1	2	20	1	1	20	8			1					
22						1		8			7	6		13	12	20	57	8	25	85	49	50	13	9	8	14	36	16	2	15	3	3	2	4	11	22	11			1				12	
23												2		6	6	26	83	55	80	7	42	38	22	19	23	11	44	11	3	15	39		12	4	7	24	2	1		1	1				
24								4						19	11	42	66	48	24	18	47	96	42	44	28	17	49	11	12	15	8	3	5	6	37	20	3	3	1	3		3			11	
25												1		4	8	32	61	64	54	15	59	124	52	34	18	68	77	20	5	39	2	2		14	17	47	25	3	3	3				23	
26														4	3	33	45	36	111	56	73	225	108	77	68	88	89	28	14	59	12	7		9	23	34	29	20	4	3		4	2	20	
27											4	1			20	31	18	24	72	102	99	239	96	102	79	155	76	110	9	65	5	22	1	16	32	26	23	10	4	1		15	4	4		
28											5	4				7	23	42	41	136	47	257	86	135	118	164	141	68	45	37	8	10	3	11	26	58	12	6		4		9				
29										1	3	5			2		10	27	49	21	48	293	141	183	141	259	184	76	61	93	26	49	16	19	27	27	36	9	3	5	1		2		12	
30											1	2				1	15	16	26	5	58	160	135	235	183	340	179	122	53	77	24	44	29	24	83	41	9	4	4	1	4	3	1		4	
31										1				4		2	16	1	14	5	43	106	122	247	162	351	235	209	108	157	48	48	38	17	63	34	6	11	4	2		4			4	
32														11	15	3	12				27	102	141	164	271	349	306	345	186	161	54	72	35	15	78	122		9	8	8	1				5	
33												1				2	9			9	28	48	86	163	212	330	306	364	213	239	79	75	50	34	143	153	19	10	2	3	2	9				
34																4	5	1	1	9	12	99	61	155	144	299	366	342	255	237	188	97	84	111	178	107	24	23	19	34		1			4	
35														1		2	3		5	1	2	48	112	116	80	234	356	441	291	309	172	169	109	111	228	193	40	26	28	20	7				
36																		4	2	3	5	53	75	68	96	333	252	442	339	398	181	270	103	183	154	162	63	44	31	41	13	4				
37														1		1			17	1	1	45	28	32	50	232	255	370	407	381	244	348	141	154	166	264	50	37	12	32	4	2	4			
38						1								4					4		1	38	22	26	37	128	312	266	337	442	279	318	183	233	267	212	71	100	35	41	23	17	1	3		
39				2																		12	12	27	44	71	123	217	375	450	411	397	278	247	203	299	116	84	47	46	28	10	3	5		
40				2															1			14	2	7	25	80	127	223	375	346	364	348	409	348	340	255	164	109	86	89	22	17	1	6	3	
41																						15	1	8	4	34	69	192	187	292	275	421	327	422	290	408	244	135	98	144	27	32	17	5	16	
42																						1		7	8	11	59	120	231	241	256	319	430	443	451	440	255	285	107	160	60	13	39	9	4	
43																					1			4	23	37	35	164	161	235	262	404	440	392	421	604	337	378	153	180	62	68	34	10	8	
44																				2	1				14	41	58	96	122	205	405	463	480	549	708	383	517	210	187	84	82	61	7	15	
45																						1		1	2	8	11	43	93	110	136	275	242	494	593	944	437	627	194	237	97	88	75	14	50	
46																					1	1		3	2	2	6	34	70	81	153	190	279	342	496	963	563	865	295	448	203	51	94	8	50	
47																						1		1	1	2	1	10	69	103	105	142	196	211	438	941	646	1035	456	627	235	141	151	27	41	
48																									2	4	3	3	21	34	72	120	93	143	255	782	464	1085	431	541	266	216	159	44	55	
49																			1							6	1	2	22	35	29	101	121	137	142	440	309	858	319	725	312	270	215	85	106	
50																					2						4	9	9	34	40	67	107	116	93	267	351	639	433	617	388	276	243	94	102	
51																										1	1		2	16	16	23	55	63	72	278	200	529	246	566	439	336	265	97	110	
52																					1				1				12	17	6	21	67	60	83	164	152	341	305	430	384	356	333	123	86	
53																											2		2	5	4	17	19	40	63	66	77	213	212	402	267	314	459	115	119	
54																													2	2	4	12	23	22	49	35	46	82	118	187	176	262	435	100	144	
55																													4			13	23	13	19	27	40	41	51	112	111	182	371	48	180	
56																													2				2	19	24	18	19	15	19	23	40	119	175	133	218	
57																													1	1				3	9	4	12	3	13	16	9	44	70	41	96	
58																									1						1	5	2	1	7		1	2		1		4	2	10	41	
59																															3		1		2			3	1	4		1	2		46	
60																																							1	3					
61																																							2						
62																																													
Enr.-->	0.2	0.3	0.4	0.7	0.8	0.9	1.1	1.2	1.3	1.4	1.5	1.6	1.7	1.8	1.9	2.0	2.1	2.2	2.3	2.4	2.5	2.6	2.7	2.8	2.9	3.0	3.1	3.2	3.3	3.4	3.5	3.6	3.7	3.8	3.9	4.0	4.1	4.2	4.3	4.4	4.5	4.6	4.7	4.8	4.9	5.0

Note: The heavy line represents the lower enrichment boundary from Table 6-7.

7. CRITICALITY EVALUATION

NOTE: The referenced basket types throughout this chapter are based on the boron content in the poison plates. The term "basket types" in this chapter differs from the definition of the basket types in Chapter 1. The correlations between the basket types used in this chapter and the basket types identified in Chapter 1 are clarified below. *Note that damaged and failed fuel can only be loaded in the basket types A4L or B4L.*

	Basket Type Identification in Chapter 1 and Technical Specifications *[7-8]*	**Basket Type Identification in Chapter 7**
EOS-37PTH	A1/A2/A3/*A4H/A4L/A5*	A
	B1/B2/B3/*B4H/B4L/B5*	B
EOS-89BTH	A1/A2/A3	M1-A
	B1/B2/B3	M1-B
	C1/C2/C3	M2-A

The design criteria for the NUHOMS® EOS System dry shielded canisters (DSCs) require that the fuel loaded in the EOS-37PTH and EOS-89BTH DSCs remain subcritical under normal, off-normal and accident conditions as defined in 10 CFR Part 72. The criticality analyses performed to demonstrate that these DSCs *loaded with intact, damaged or failed fuel in the EOS-37PTH DSC, or loaded with intact fuel in the EOS-89BTH DSC* satisfy the stated requirements are presented in this chapter. *Failed fuel shall be loaded into a failed fuel canister (FFC) and include failed fuel assemblies (FAs), rods, rod segments, pellets, and debris.*

The DSCs consist of a shell assembly, an internal basket assembly, and extruded aluminum open section transition rails that provide the transition to a cylindrical exterior surface to match the inside surface of the shell. The EOS-37PTH DSC is designed to store and transport up to 37 pressurized water reactor (PWR) FAs with or without control components (CCs) while the EOS-89BTH is designed to store and transport up to 89 boiling water reactor (BWR) FAs with and without channels. The DSCs are of variable length to match the length of the fuel and CCs, as applicable, to be stored. The basket is composed of interlocking slotted plates to form an egg-crate type structure. The egg-crate structure forms a grid of 37 or 89 fuel compartments that house the spent fuel assemblies (SFAs). The egg-crate structure is composed of steel alloy, aluminum alloy, and poison plates.

All indicated Changes are in response to RAI 7-1

EOS-37PTH Only

- Non-fuel assembly hardware that extends into the active fuel regions, such as BPRAs, CRAs, APSRAs, CEAs, and NSAs, are conservatively assumed to exhibit the neutronic properties of $^{11}B_4C$ (no credit taken for B-10 content). There is negligible neutron absorption from any of this hardware and it is collectively referred to as CCs.
- Water in the EOS-37PTH DSC cavity contains soluble boron at optimum density. The soluble boron is mixed with the moderator. By varying the moderator density from 50% to 100% of full density, the density of water at which the reactivity is maximized is determined.
- The maximum planar average initial fuel enrichment is modeled as uniform everywhere throughout the assembly. Natural uranium blankets and axial or radial enrichment zones are modeled as enriched uranium at the planar average initial enrichment.
- The portion of the DSC corresponding to the axial length of the active fuel is modeled for the criticality analysis. The axial ends of the DSC are not modeled.

In addition, the damaged and failed FA criticality calculations also employ the following assumptions for the EOS-37PTH DSC:

- *Single-ended shear assumes one row of fuel rods not axially severed is displaced to a new location.*
- *Double-ended shear assumes that the selected sheared row displaced with a single-ended shear is further split axially to result in an "extra" row of fuel rods in the axial region where the severed fuel rod pieces are displaced to.*
- *Bent or bowed fuel rods assume that the fuel is intact but that the rod pitch is allowed to vary from its nominal fuel rod pitch.*
- *Fuel assembly lattices with less fuel rod assume missing fuel rods.*
- *Full fuel rod lattices assume that guide and instrument tubes are replaced with fuel rods (failed fuel assumption).*
- *De-cladded fuel rods assume severe cladding damage (failed fuel assumption).*
- *No credit is taken for FFCs (failed fuel assumption).*
- *Both damaged and failed FAs are modeled as failed (total of 12), which is highly conservative because damaged and failed fuel cannot be stored in the same DSC.*

The following assumptions are employed in the criticality evaluation for failed FA debris in the EOS-37PTH DSC:

- *No credit is taken for FFC or any secondary containers.*
- *A total of four failed fuel locations is considered; remaining locations are modeled with intact fuel, see Figure 7-25.*

All Indicated Changes are in response to RAI 7-3

Proprietary Information on This Page
Withheld Pursuant to 10 CFR 2.390

Table 7-51
EOS-37PTH Maximum Planar Average Initial Enrichment
(Applicable for Damaged and Failed Fuels)

(4 Pages)

PWR Fuel Class	***Maximum Planar Average Initial Enrichment (wt. % U-235) as a Function of Soluble Boron Concentration and Basket Type (Fixed Poison Loading) With and Without CCs***								
	Minimum Soluble Boron (ppm)	***Basket Type***							
		A4L				***B4L***			
		w/o CCs		***w/ CCs***		***w/o CCs***		***w/ CCs***	
		Intact Fuel	***Damaged /Failed Fuel***	***Intact Fuel***	***Damaged /Failed Fuel***	***Intact Fuel***	***Damaged /Failed Fuel***	***Intact Fuel***	***Damaged /Failed Fuel***
WE 17x17 Class	***2000***	*4.35*	*4.20*	*4.35*	*4.15*	*4.50*	*4.15*	*4.45*	*4.25*
	2100	*4.50*	*4.20*	*4.45*	*4.20*	*4.65*	*4.25*	*4.60*	*4.40*
	2200	*4.60*	*4.40*	*4.55*	*4.35*	*4.75*	*4.45*	*4.70*	*4.55*
	2300	*4.70*	*4.45*	*4.65*	*4.50*	*4.85*	*4.65*	*4.85*	*4.60*
	2400	*4.85*	*4.45*	*4.80*	*4.60*	*5.00*	*4.65*	*4.95*	*4.75*
	2500	*4.95*	*4.65*	*4.90*	*4.70*	*5.00*	*5.00*	*5.00*	*4.95*
CE 16x16 Class	***2000***	*5.00*	*4.75*	*5.00*	*4.70*	*5.00*	*5.00*	*5.00*	*5.00*
	2100	*5.00*	*5.00*	*5.00*	*5.00*	-	-	-	-
	2200	-	-	-	-	-	-	-	-
	2300	-	-	-	-	-	-	-	-
	2400	-	-	-	-	-	-	-	-
	2500	-	-	-	-	-	-	-	-

All Indicated Changes are in response to RAI 7-1

Table 7-51
EOS-37PTH Maximum Planar Average Initial Enrichment
(Applicable for Damaged and Failed Fuels)

(4 Pages)

PWR Fuel Class	*Minimum Soluble Boron (ppm)*	*Maximum Planar Average Initial Enrichment (wt. % U-235) as a Function of Soluble Boron Concentration and Basket Type (Fixed Poison Loading) With and Without CCs*							
		Basket Type							
		A4L				*B4L*			
		w/o CCs		*w/ CCs*		*w/o CCs*		*w/ CCs*	
		Intact Fuel	*Damaged /Failed Fuel*	*Intact Fuel*	*Damaged /Failed Fuel*	*Intact Fuel*	*Damaged /Failed Fuel*	*Intact Fuel*	*Damaged /Failed Fuel*
BW 15x15 Class	*2000*	4.25	4.05	4.20	4.00	4.40	4.10	4.35	4.15
	2100	4.40	4.10	4.30	4.15	4.55	4.20	4.45	4.25
	2200	4.50	4.25	4.45	4.15	4.65	4.35	4.60	4.30
	2300	4.60	4.35	4.55	4.30	4.80	4.40	4.70	4.50
	2400	4.75	4.40	4.65	4.45	4.90	4.55	4.85	4.50
	2500	4.85	4.55	4.75	4.65	5.00	4.75	4.90	4.75
	2600	(1)	(1)	(1)	(1)	5.00	5.00	(1)	(1)
WE 15x15	*2000*	4.45	4.10	4.40	4.10	4.55	4.30	4.55	4.25
	2100	4.60	4.15	4.55	4.15	4.65	4.50	4.65	4.35
	2200	4.70	4.25	4.65	4.35	4.80	4.55	4.80	4.45
	2300	4.85	4.35	4.75	4.45	5.00	4.50	4.95	4.50
	2400	4.95	4.50	4.90	4.50	5.00	4.90	5.00	4.80
	2500	5.00	4.75	5.00	4.65	5.00	5.00	5.00	5.00

All Indicated Changes are in response to RAI 7-1

Table 7-51
EOS-37PTH Maximum Planar Average Initial Enrichment
(Applicable for Damaged and Failed Fuels)

(4 Pages)

PWR Fuel Class	***Minimum Soluble Boron (ppm)***	***Maximum Planar Average Initial Enrichment (wt. % U-235) as a Function of Soluble Boron Concentration and Basket Type (Fixed Poison Loading) With and Without CCs***							
		Basket Type							
		A4L				***B4L***			
		w/o CCs		***w/ CCs***		***w/o CCs***		***w/ CCs***	
		Intact Fuel	***Damaged /Failed Fuel***	***Intact Fuel***	***Damaged /Failed Fuel***	***Intact Fuel***	***Damaged /Failed Fuel***	***Intact Fuel***	***Damaged /Failed Fuel***
CE 15x15 Assembly Class	***2000***	*4.60*	*4.25*	*4.55*	*4.20*	*4.75*	*4.35*	*4.70*	*4.30*
	2100	*4.70*	*4.45*	*4.65*	*4.40*	*4.85*	*4.50*	*4.85*	*4.35*
	2200	*4.85*	*4.50*	*4.80*	*4.45*	*5.00*	*4.60*	*4.95*	*4.60*
	2300	*5.00*	*4.55*	*4.90*	*4.65*	*5.00*	*5.00*	*5.00*	*4.80*
	2400	*5.00*	*5.00*	*5.00*	*4.85*	*5.00*	*5.00*	*5.00*	*5.00*
	2500	-	-	*5.00*	*5.00*	-	-	-	-
CE 14x14 Assembly Class	***2000***	*5.00*	*5.00*	*5.00*	*4.50*	*5.00*	*5.00*	*5.00*	*4.95*
	2100	-	-	*5.00*	*4.95*	-	-	*5.00*	*5.00*
	2200	-	-	*5.00*	*5.00*	-	-	-	-
	2300	-	-	-	-	-	-	-	-
	2400	-	-	-	-	-	-	-	-
	2500	-	-	-	-	-	-	-	-

All Indicated Changes are in response to RAI 7-1

Table 7-51
EOS-37PTH Maximum Planar Average Initial Enrichment
(Applicable for Damaged and Failed Fuels)

(4 Pages)

PWR Fuel Class	***Minimum Soluble Boron (ppm)***	***Maximum Planar Average Initial Enrichment (wt. % U-235) as a Function of Soluble Boron Concentration and Basket Type (Fixed Poison Loading) With and Without CCs***							
		Basket Type							
		A4L				***B4L***			
		w/o CCs		***w/ CCs***		***w/o CCs***		***w/ CCs***	
		Intact Fuel	***Damaged /Failed Fuel***	***Intact Fuel***	***Damaged /Failed Fuel***	***Intact Fuel***	***Damaged /Failed Fuel***	***Intact Fuel***	***Damaged /Failed Fuel***
WE 14x14 Class	***2000***	*5.00*	*5.00*	*5.00*	*5.00*	*5.00*	*5.00*	*5.00*	*5.00*
	2100	-	-	-	-	-	-	-	-
	2200	-	-	-	-	-	-	-	-
	2300	-	-	-	-	-	-	-	-
	2400	-	-	-	-	-	-	-	-
	2500	-	-	-	-	-	-	-	-

Note:
1. Not analyzed.

All Indicated Changes are in response to RAI 7-1

Components	UFSAR Sections
EOS-TC loaded with EOS-37PTH DSC (Side and corner drop)	Appendices 3.9.1 - 3.9.3 and 3.9.5
EOS-TC loaded with EOS-89BTH DSC (Side and corner drop)	Appendices 3.9.1 - 3.9.3 and 3.9.5
EOS-37PTH DSC, PWR Fuel Cladding (Side and corner drop)	Appendix 3.9.6
EOS-89BTH DSC, BWR Fuel Cladding (Side and corner drop)	Appendix 3.9.6

All stresses are within allowable limits in both drop scenarios for the TC108, EOS-37PTH DSC and EOS-89BTH DSC. The largest strain in the basket is *0.9%* and 0.6 % for the EOS-TC108 loaded with EOS-37PTH DSC and EOS-89BTH DSC, respectively. The maximum stresses and strains in the fuel cladding for the side and corner drops remain below the applicable yield strength, therefore there is no fuel deformations. 72.48

The strain is limited in effect given the mode of deformation as the basket plates maintain their general shape. This deformation is limited and the position of the fuel assemblies is maintained from their initial positions relative to each other. The deformations of the basket plates are approximately uniform in the direction of impact and the fuel does not change configuration. Therefore, these deformations do not have an effect on criticality control.

Accident Dose Calculation

Based on analysis results presented in Appendix 3.9.3, Sections 3.9.3.3 and 3.9.3.4, the accidental EOS-TC drop scenarios do not breach the EOS-37PTH or the EOS-89BTH DSC confinement boundaries. The function of EOS-TC lead shielding is not compromised by these drops. The EOS-TC neutron shield, however, may be damaged in an accidental drop.

Dose rates are computed at 100 m from the EOS-TC with the neutron shield removed, which is the minimum allowed distance to the site boundary. As presented in Chapter 6, Table 6-54, the maximum dose rate at 100 m from an EOS-TC during a loss of neutron shield and lead slump in an accidental drop accident is 2.15 mrem/hr. *Based on the discussion in Section 6.2.8, the maximum accident dose rate is doubled to 4.3 mrem/hr.* If an 8-hour recovery time is assumed, the dose to an individual at the site boundary is *4.3**8 =*35* mrem, which is significantly below the 10 CFR 72.106 dose limit of 5 rem.

All Indicated Changes are in response to RAI 6-6

A.1.2 General Description and Operational Features of the NUHOMS® MATRIX

A.1.2.1 NUHOMS® MATRIX CHARACTERISTICS

The NUHOMS® MATRIX provides a staggered two-tiered self-contained modular structure for storage of spent fuel canistered in an EOS-37PTH or EOS-89BTH DSC. The HSM-MX is constructed from reinforced concrete and structural steel. Contact doses for the HSM-MX are designed to be as low as reasonably achievable (ALARA). The key design parameters of the HSM-MX are listed in Table A.1-1.

In lieu of a separate roof and separate shield walls, those features are integral to the monolith in the HSM-MX.

The HSM-MXs provide an independent, passive system with substantial structural capacity to ensure the safe dry storage of spent fuel assemblies (SFAs). To this end, the HSM-MXs are designed to ensure that normal transfer operations and postulated accidents or natural phenomena do not impair the DSC or pose a hazard to the public or plant personnel. Postulated accidents and natural phenomena affecting the HSM-MX are described in detail in Chapter A.12.

The HSM-MX provides a means of removing spent fuel decay heat by a combination of radiation, conduction, and convection. Ambient air enters the HSM-MX through ventilation inlet openings located on the lower tier of the HSM-MX, circulates around the DSC and the heat shields, then exits through the outlets of the HSM-MX. The HSM-MX is designed to remove up to 50.0 kW of decay heat from the bounding EOS-37PTH DSC, when loaded in an HSM-MX lower compartment.

Decay heat is rejected from the DSC to the HSM-MX air space by convection and then removed from the HSM-MX by natural circulation airflow. Heat is also radiated from the DSC surface to the heat shields and HSM-MX walls and roof, where the natural convection airflow and conduction through the walls and roof aid in the removal of the decay heat. The passive cooling system for the HSM-MX is designed to preserve fuel cladding integrity by maintaining SFA peak cladding temperatures below acceptable limits during long-term storage. *The* outlet vent covers installed on the top of the HSM-MX *are designed* to mitigate the effect of sustained winds.

Configurations of systems to be stored in the HSM-MX are determined based on heat load, basket type, etc. These configurations are detailed in Table 1-2.

The HSM-MXs are installed on a load-bearing foundation, which consists of a reinforced concrete basemat on a subgrade suitable to support the loads. The HSM-MXs are not tied to the basemat.

Dimensions of the HSM-MX components described in the text and provided in figures and tables of this UFSAR are, in general, nominal dimensions for general system description purposes. Actual design dimensions are contained in the drawings in Section A.1.3.

Proprietary and Security Related Information for Drawing MX01-5000-SAR, Rev. 0B Withheld Pursuant to 10 CFR 2.390

A.1.8 Supplemental Data

A.1.8.1 GENERIC STORAGE ARRAYS

The DSC containing the SFAs is transferred to, and stored in, compartments of the HSM-MX. Multiple compartments are grouped together to form a staggered, two-tiered monolithic structure known as the HSM-MX. Multiple compartments are grouped together to form arrays whose size is determined to meet plant-specific needs. The HSM-MX is arranged within the ISFSI site on a concrete basemat(s) with the entire area enclosed by a security fence. Modules may be placed in a single-row array or in a back-to-back array for site dose and footprint optimization. Like the EOS-HSM, the decay heat within the HSM-MX DSC compartment is primarily removed by internal natural circulation flow though the inlet/outlet vents and conduction through the HSM-MX walls.

Figure A.1-1 and Figure A.1-2 show typical HSM-MX expansion layouts at ISFSIs that are capable of modular expansion to any capacity.

The expansion option shown in Figure A.1-1 allows the array to be expanded with a construction joint splitting the upper compartment at the end of the array. A minimum of five compartments are required in a monolith. End shield walls shall be installed at this location in the interim period between expansions; the shield walls will be removed to allow for expansion of the array. Two empty compartments (one upper and one lower), in addition to the partial empty compartment, are required at the end of an array during the interim period before expansion. At the end of the array, the end wall will be the same thickness as the wall at the beginning of the first array, and all compartments may be filled.

Figure A.1-2 shows the expansion joint used at ~100 feet into the array. This joint addresses the thermal growth due to cyclic temperatures in ambient conditions. When an array is expanded at the expansion joint, two empty compartments (one top and one bottom) are required at the end of the interim array prior to expansion. When the expansion joint is used, and construction continues past the expansion joint, the construction joint configuration can be used to further expand the array, or the array can terminate with an end wall the same thickness as the wall at the beginning of the first array. If using the construction joint configuration, the same requirements described above for the construction joint apply.

These are typical layouts only and do not represent limitations in number of modules, number of rows, and orientation of modules in rows. Back-to-back module configurations require expansion in sets of pairs. Expansion can be accomplished, as necessary, by the licensee, provided the criteria of 10 CFR 72.104, 10 CFR 72.106 and Chapter 14 are met. The parameters of interest in planning the installation layout are the configuration of the HSM-MX array and an area in front of each HSM-MX to provide adequate space for loading operations. Illustrations of typical HSM-MX ISFSI layouts are provided in Figure A.1-4 through Figure A.1-6.

Table A.1-1
Key Design Parameters of the NUHOMS® MATRIX Components

Horizontal Storage Module (HSM-MX):	
Overall length	23'-1" single array
	41'-4" back-to-back array
Overall width	36'-6"
Overall height (two-tiers *without vent covers*)	*27'-1 3/8"*
Total weight not including DSC (kips) (max. concrete density of 160 pcf.)	*2,450* (single array)
	4,125 (double array)
Materials of construction	Reinforced concrete and structural steel
Heat removal	Conduction, convection, and radiation

Note: Dimensions are based on a single monolith of five compartments (see Figure A.1-2).

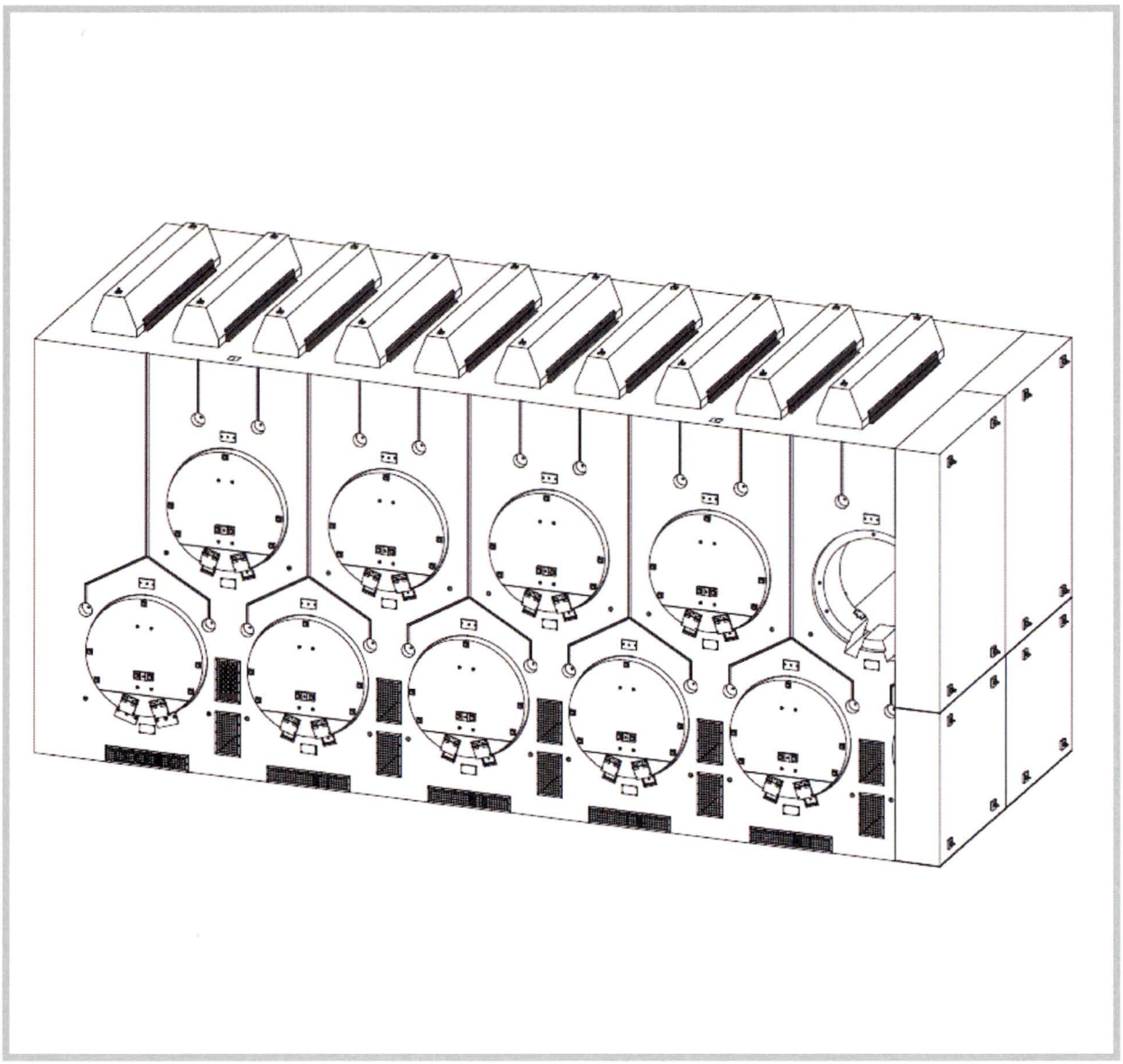

Figure A.1-1
NUHOMS® MATRIX *Construction Joint Expansion*

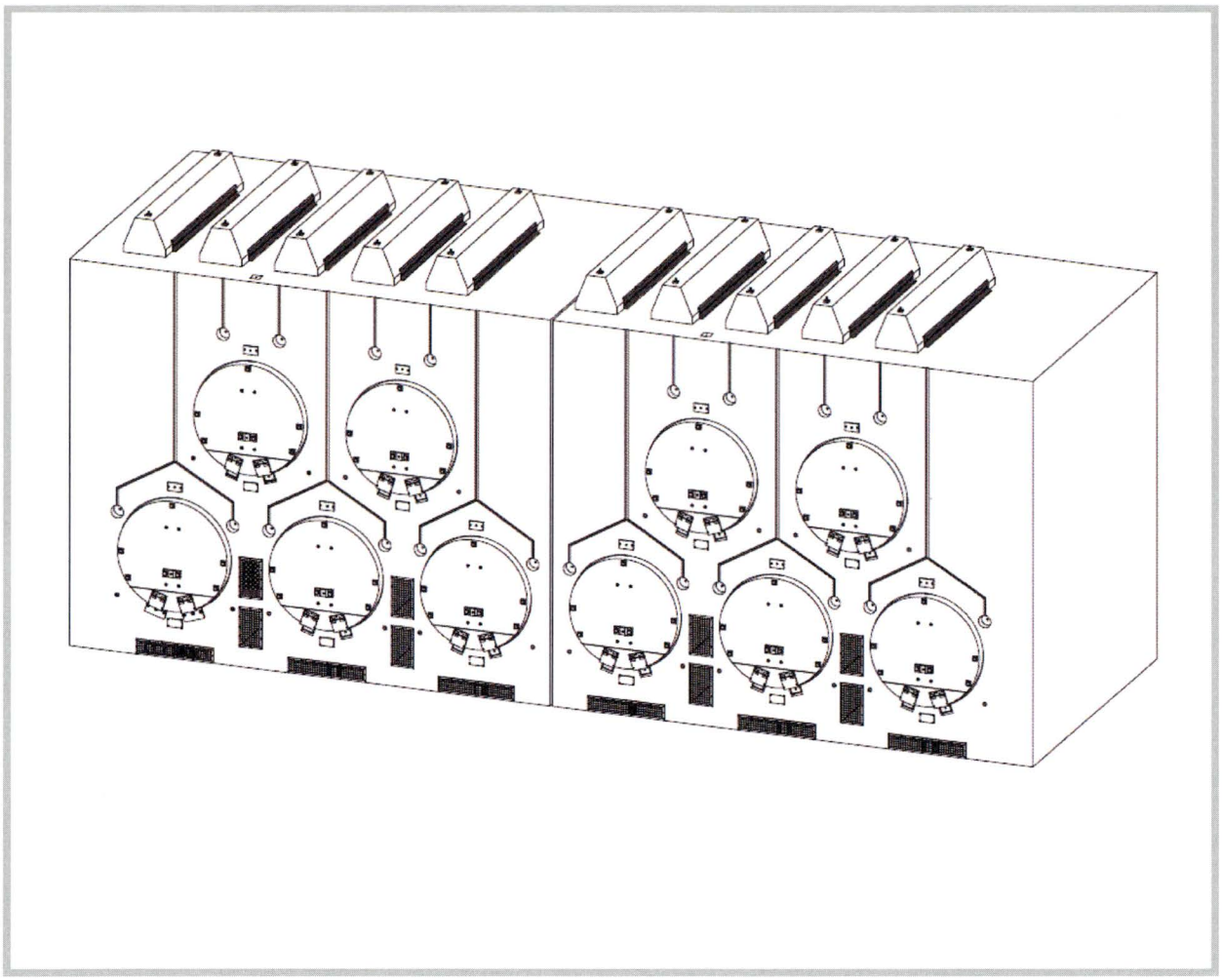

Figure A.1-2
NUHOMS® MATRIX *Expansion Joint*

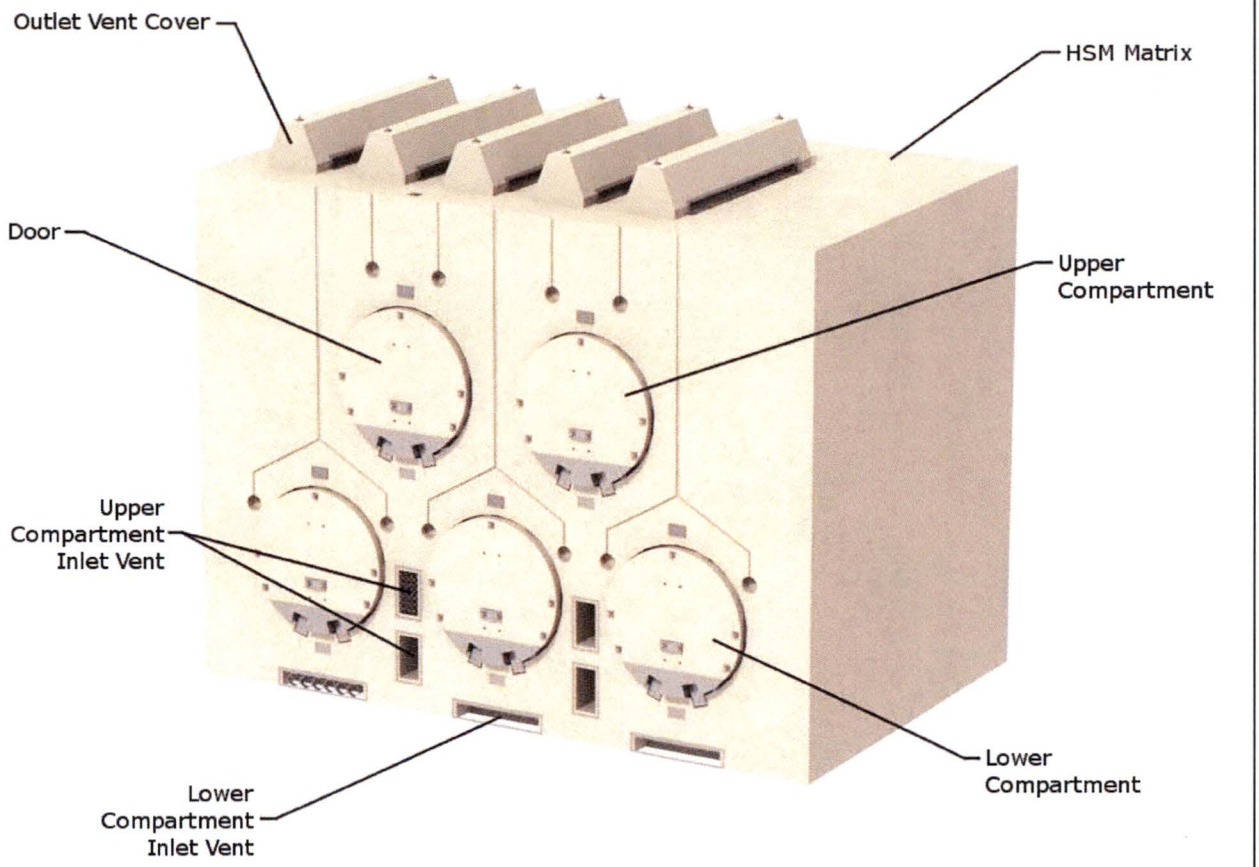

Figure A.1-7
NUHOMS® MATRIX System Components and Structures

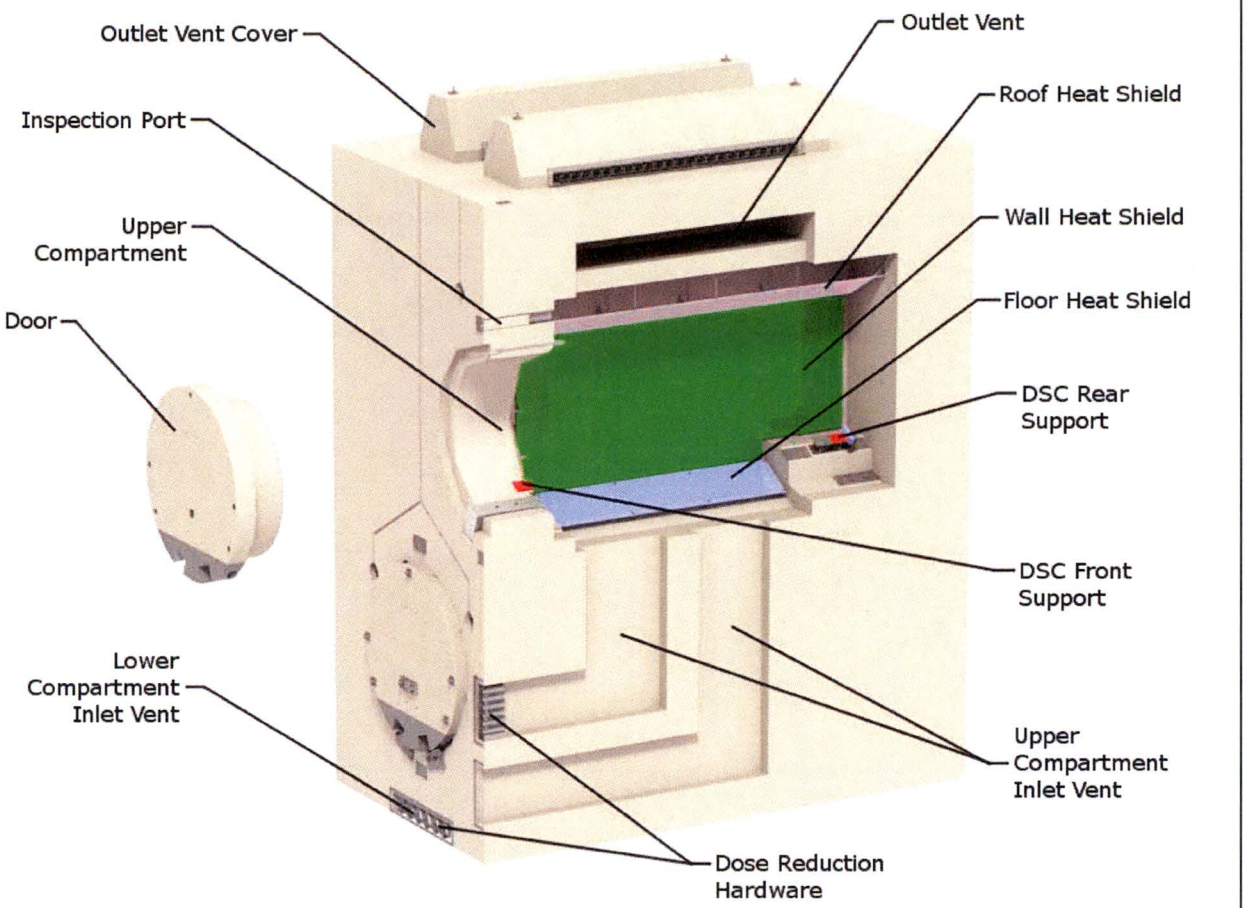

Figure A.1-8
NUHOMS® MATRIX System Components and Structures

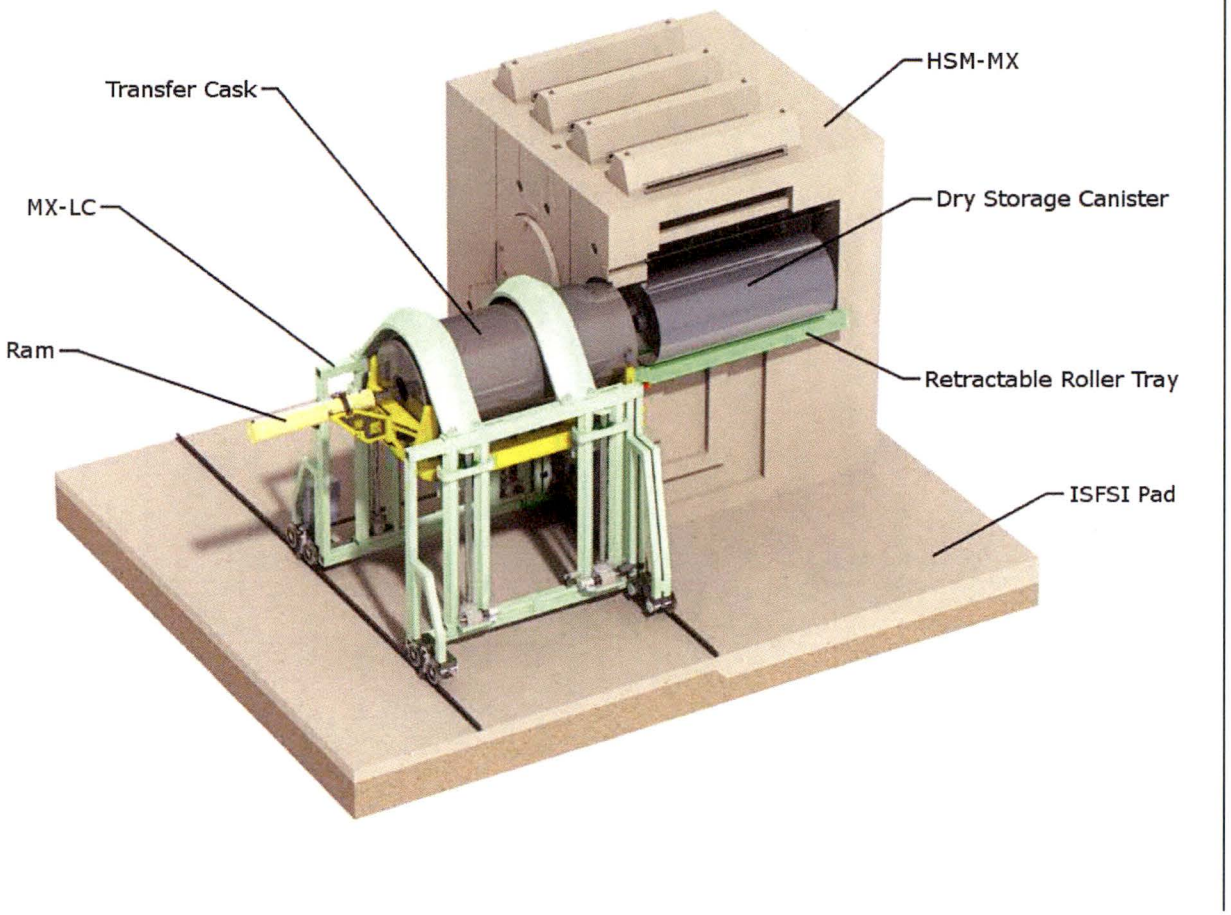

Figure A.1-9
NUHOMS® MATRIX System Components, Structures, and Transfer Equipment

A.2.3.3 Water Level (Flood) Design

HSM-MX inlet vents are blocked when the depth of flooding is greater than 0.25 m (10 in.) for the lower compartment, and 2.29 m (7 ft-6 in.), for the upper compartments, above the level of the ISFSI basemat. The DSC in the lower and upper compartments are wetted when flooding exceeds a depth of 1.3 m (4 ft-2 in.), and 4.4 m (14 ft-5 in.), respectively, above ISFSI basemat. Greater flood heights result in submersion of the DSC and blockage of the HSM-MX outlet vents.

The DSC and HSM-MX are conservatively designed for an enveloping design basis flood. The flood is postulated to result from natural phenomena such as tsunamis and seiches, as specified by 10 CFR 72.122(b) [A.2-6]. A bounding assumption of a 15-meter (50-foot) flood height and water velocity of 4.6 m/sec (15 fps) is used for the flood evaluation. The HSM-MX is evaluated for the effects of the 4.6 m/sec (15 fps) water current impinging upon the side of the submerged HSM-MX. The DSC is subjected to an external pressure equivalent to a 15-meter (50-foot) head of water. These evaluations are presented in Section A.12.3.5. The effects of water reflection on DSC criticality safety are addressed in Chapter 7. Due to its short-term, infrequent use, the onsite EOS transfer cask (EOS-TC) is not explicitly evaluated for flood effects. Independent spent fuel storage installation procedures should ensure that the EOS-TC is not used for DSC transfer during flood conditions.

The plant-specific design basis flood (if the possibility for flooding exists at a particular ISFSI site) should be evaluated by the licensee and shown to be enveloped by the flooding conditions used for this generic evaluation of the HSM-MX.

A.2.3.4 Seismic Design

The seismic design criteria for the HSM-MX are based on the NRC RG 1.60 [A.2-13] response spectra anchored at a zero period acceleration (ZPA) of 0.85g in the horizontal direction and 0.80g in the vertical direction and enhanced frequency content above 9 Hz. The horizontal and vertical components of the design response spectra corresponding to a maximum horizontal ground acceleration of 1.0g are shown in Figure A.2-1. The seismic structural evaluations consider both stability evaluation and stress qualification of the HSM-MX. The stability criteria for seismic loading are based on the stability response of a *five-compartment construction joint option of the HSM-MX module without the side shield walls attached.*

The HSM-MX has no anchorage to the concrete basemat. The stability analyses consider the effects of sliding and rocking motions, and determine the maximum possible sliding of *the HSM-MX*. The HSM-MX will neither slide nor overturn at design ZPA of 0.*48*g in the horizontal direction and 0.*32*g in the vertical direction.

The licensee shall determine if, based on ISFSI-specific site investigations, a soil-structure interaction (SSI) analyses ought to be performed to assess potential site-specific amplifications. The SSI evaluations are based on ISFSI site-specific parameters (free-field accelerations, strain-dependent soil properties, HSM-MX array configurations, etc.). The SSI response spectra at the base of the HSM-MXs are to be bounded by the HSM-MX design basis seismic criteria response spectra, i.e., the RG 1.60 response spectra shape, with enhanced spectral accelerations above 9 Hz, and anchored at 0.85g horizontal and 0.80g vertical directions. The licensee shall reconcile spectral accelerations from the SSI analysis response spectra that exceed the seismic criteria spectra (if any); 5% damped response spectra may be used in making these determinations.

Since the DSC can be considered to act as a large diameter pipe for the purpose of evaluating seismic effects, the "Equipment and Large Diameter Piping System" category in NRC RG 1.61 [A.2-16], Table 1 is applicable. Therefore, a damping value of 3% of critical damping for the design bases safe shutdown earthquake is used. Similarly, from the same RG table, a damping value of 7% of critical damping is used for the reinforced concrete structural components of the HSM-MX.

The seismic criteria for the MX-LC are based on Figures 1 and 2 of NRC Regulatory Guide 1.60 [A.2-13], *with enhanced spectral accelerations above 9 Hz, and* anchored at 0.85g zero period acceleration (ZPA) in the horizontal direction and 0.80g ZPA in the vertical direction. The seismic structural calculations consider both a stability evaluation and stress qualification of the MX-LC for seismic loading criteria. The stability evaluations address the MX-LC rails and use of any shims under the MX-LC rails due to unevenness in the basemat and approach slab foundation.

The seismic criteria for the MX-RRTs is based on Figures 1 and 2 of NRC Regulatory Guide 1.60 [A.2-13], *with enhanced spectral accelerations above 9 Hz, and* anchored at 0.85g ZPA in the horizontal direction and 0.80g ZPA in the vertical direction. As required, the seismic structural calculations shall consider both a stability evaluation and stress qualification for the seismic loading criteria.

A.2.3.5 Snow and Ice Loading

No change to Section 2.3.5.

A.2.3.6 Tsunami

No change to Section 2.3.6.

A.2.3.7 Lightning

A lightning strike will not cause a significant thermal effect on the HSM-MX, MX-LC, MX-RRT, or stored DSC. The effects on the HSM-MX resulting from a lightning strike are discussed in Section 12.3.7.

A.2.4 Safety Protection Systems

A.2.4.1 General

No change to Section 2.4.1.

A.2.4.2 Structural

A.2.4.2.1 EOS-DSC Design Criteria

No change to Section 2.4.2.1.

A.2.4.2.2 HSM-MX Design Criteria

The principal design criteria for the HSM-MX, both *the concrete and steel* structures, are presented in Table 2-7.

The reinforced concrete HSM-MX is designed to meet the requirements of ACI 349-06 [A.2-3]. The ultimate strength method of analysis is utilized with the appropriate strength reduction factors as described in Appendix A.3.9.4. The load combinations specified in Section 6.17.3.1 of American National Standards Institute (ANSI) 57.9-1984 [A.2-20] are used for combining normal operating, off-normal, and accident loads for the HSM-MX. All seven load combinations specified are considered and the governing combinations are selected for detailed design and analysis. The resulting HSM-MX load combinations and the appropriate load factors are presented in Appendix A.3.9.4. The effects of duty cycle on the HSM-MX are considered and found to have negligible effect on the design.

A.2.4.2.3 EOS-TC Design Criteria

No change to Section 2.4.2.3.

Thermal analysis is based on fuel assemblies with decay heat up to 50.0 kW per DSC for the EOS-37PTH and up to 34.4 kW per DSC for the EOS-89BTH. Zoning is used to accommodate high per assembly heat loads. The heat load zoning configurations for the DSCs are shown in Figure 1A through Figure 1I and Figure 2 of the Technical Specifications [A.2-18] for 37PTH and 89BTH DSC, respectively. Among the various HLZCs presented in Figure 1 for EOS-37PTH DSC, only HLZC # 7 through 9 presented in Figure 1G through Figure 1I are applicable for storage in HSM-MX. Similarly for the EOS-89BTH, among the various HLZCs presented in Figure 2 for EOS-89BTH DSC, only HLZC # 3 is permitted for storage in the HSM-MX.

The thermal analyses for storage are performed for the environmental conditions listed in Table A.2-2. The remainder of the environment conditions are provided in Table 2-9.

Peak clad temperature of the fuel at the beginning of the long-term storage does not exceed 400 °C for normal conditions of storage, and for short-term operations, including DSC drying and backfilling. Fuel cladding temperature shall be maintained below 570 °C (1058 °F) for accident conditions involving fire or off-normal storage conditions.

For onsite transfer in the EOS-TC, air circulation may be used, as a recovery action, to facilitate transfer operations in the EOS-37PTH DSC as described in the Technical Specifications [A.2-18].

A.2.4.4 Shielding/Confinement/Radiation Protection

The HSM-MX provides the bulk of the radiation shielding for the DSCs. The HSM-MX designs can be arranged in either a single-row or a back-to-back arrangement. The nominal thickness of the HSM-MX roof is (50) inches for biological shielding. Additionally, the front wall has a minimum thickness of 39 inches. Sufficient shielding is provided by thick concrete side walls between HSM-MXs in an array to minimize doses in adjacent HSM-MXs during loading and retrieval operations. Section A.11.3 provides a summary of the offsite dose calculations for representative arrays of design basis HSM-MXs providing assurance that the limits in 10 CFR 72.104 and 10 CFR 72.106(b) are not exceeded.

There are no radioactive releases of effluents during normal and off-normal storage operations. Also, there are no credible accidents that cause significant releases of radioactive effluents from the DSC. Therefore, there are no off-gas or monitoring systems required for the HSM-MX.

A.2.4.5 Criticality

No change to Section 2.4.5.

A.2.4.6 Material Selection

No change to Section 2.4.6.

A.3.4 General Standards for NUHOMS® MATRIX System

A.3.4.1 Chemical and Galvanic Reaction

No change to Section 3.4.1 for the EOS System. Chemical and galvanic reactions for the HSM-MX System are presented in Chapter A.8.

A.3.4.2 Positive Closure

No change to Section 3.4.2.

A.3.4.3 Lifting Devices

No change to Section 3.4.3.

A.3.4.4 Heat

A.3.4.4.1 Summary of Pressures and Temperatures

Temperatures and pressures for the HSM-MX are described in Chapter A.4. The thermal evaluations for storage and transfer conditions are performed in Chapter A.4 for normal, off-normal, and accident conditions. The internal pressure evaluation is performed in Chapter A.4, Section *A.4.5.*

Maximum temperatures for the various components of the HSM-MX, loaded with an EOS-37PTH DSC or an EOS-89BTH DSC under normal, off-normal and accident conditions are summarized in *Chapter A.4, Section A.4.5* for all the applicable heat zone loading configurations provided in Appendix A, Technical Specification [A.3-5].

These temperatures are used for the structural evaluations documented in Appendices A.3.9.1 and A.3.9.4. Stress allowables for the components are a function of component temperature. The temperatures used to perform the structural analyses are based on actual calculated temperatures or conservatively selected higher temperatures.

A.3.4.4.2 Differential Thermal Expansion

No change to Section 3.4.4.2.

A.3.4.4.2.1 Minimum Gaps within the Interlocking Slots

No change to Section 3.4.4.2.1.

A.3.4.4.2.2 Axial Gaps between the Basket Assembly Plates

No change to Section 3.4.4.2.2.

A.3.4.4.2.3 Radial Gap between the Basket Assembly and the DSC Shell

No change to Section 3.4.4.2.3.

A.3.4.4.2.4 Axial Gaps between Fuel Assemblies and the DSC Cavity

No change to Section 3.4.4.2.4.

A.3.4.4.2.5 Axial Gap between the Basket Assembly and the DSC Cavity

No change to Section 3.4.4.2.5.

A.3.4.4.2.6 Axial Gap between the Transition Rails and the DSC Cavity

No change to Section 3.4.4.2.6.

A.3.4.4.2.7 Axial Gap between the TC125/TC135 Cavity and the DSC Shell

No change to Section 3.4.4.2.7.

A.3.4.4.2.8 Axial Gap between the Rear DSC support, Axial Retainer and the HSM-MX cavity

A gap of 0.5 inch is provided between the rear DSC Support and the HSM-MX to accommodate any thermal growth. This section verifies that there is no interference when the rear DSC support increases from room temperature to accident temperature.

The maximum temperature of the rear DSC support is assumed to be 350°F. A mean thermal expansion coefficient of 7.0×10^{-6} in/in/°F for 350°F is used. The thermal growth of the rear DSC support is determined as:

$$\Delta L_{rs}=L_{cold}\times\alpha\times\Delta T$$

$$\Delta L_{rs}=21.5\times7.0\times10^{-6}\times(350-70)=0.042\ in.$$

The maximum thermal growth between the rear DSC Support and the HSM-MX is 0.042 inch and is less than the initial 0.5-inch gap.

Therefore, there is sufficient clearance for free thermal expansion between the rear DSC supports and HSM-MX.

A gap is provided between the axial retainer and DSC to accommodate any thermal growth. Shims are used to *adjust the gap to be 0.1875 inch initially. The bounding thermal expansion temperature ranges from the normal operating temperature to the blocked vent accident temperature. The largest average temperature difference for the DSC is 396 °F - 293 °F = 103 °F. The axial retainer is conservatively assumed to experience the same temperature difference. The average HSM concrete temperature difference is 207 °F - 152 °F = 55 °F. Conservatively, a higher temperature difference of 105 °F is applied to the DSC and axial retainer, and a lower temperature difference of 50 °F is applied to the HSM concrete. Thermal expansion coefficients of 7.5 x 10-6 in/in/°F and 10.1 x 10-6 in/in/°F for 350 °F are used for the Axial Retainer and the DSC, respectively. The instantaneous coefficients of thermal expansion are used here as the initial temperatures are above 70 °F. A thermal expansion coefficient of 5.5 x 10-6 in/in/°F is used for the HSM concrete. The growth of the HSM is subtracted from the growth of the DSC and axial retainer as it increases the gap.*

$$\Delta L = L_{DSC} \times \alpha_{DSC} \times \Delta T_{DSC} + L_{AR} \times \alpha_{AR} \times \Delta T_{AR} - L_{HSM} \times \alpha_{HSM} \times \Delta T_{HSM}$$

$$\Delta L = 199.5 \times 10.1 \times 10^{-6} \times (105) + 36.5 \times 7.5 \times 10^{-6} \times (105) - (199.5 + 36.5) \times 5.5 \times 10^{-6} \times (50) = 0.175 \text{ in}$$

The maximum thermal growth between the axial retainer and DSC is *0.175* inch and is less than a *0.1875* inch gap.

A.3.4.5 Cold

No change to Section 3.4.5.

A.3.6 Normal Conditions of Storage and Transfer

This section presents the structural analysis of the EOS-37PTH DSC/ EOS-89BTH DSCs, the HSM-MX and the EOS-TC subjected to normal conditions of storage and transfer. The analyses performed evaluate the components for the design criteria described in Section A.3.1.1.

Numerical analyses have been performed for the normal and accident conditions. In general, numerical analyses have been performed for the regulatory events. The analyses are summarized in this section.

The detailed structural analyses of the HSM-MX are included in Appendices A.3.9.1 through A.3.9.7.

A.3.6.1 EOS-37PTH DSC/89BTH DSC

Details of the structural analysis of the DSC shell assemblies are provided in Appendix A.3.9.1, while the structural analysis for basket assemblies are provided in Appendix 3.9.2. There are no changes to the analysis described for the DSC shell except that the DSC shell is analyzed for dead weight and seismic load combinations, which are affected when the DSC is loaded into *the* HSM-MX and are provided in Appendix A.3.9.1. The design or loading conditions for the basket remain the same when loaded into the DSC shell and, therefore, results for the basket from Appendix 3.9.2 remain the same and are applicable.

A.3.6.2 HSM-MX

The HSM-MX design is able to accommodate different DSC lengths. For the structural evaluation, *the* HSM-MX with the longest DSC bounds all sizes. The following table shows how the bounding loads are used for structural evaluation of the HSM-MX.

Component	Weight (kips)	Thermal Heat Load
EOS-37PTH DSC (Loaded Weight)	134	50 kW
EOS-89BTH DSC (Loaded Weight)	120	43.6 kW
Bounding HSM-MX (Double Array)	*4,125* (2)	50 kW for lower compartment and 41.8 kW for upper compartment (1)

Notes:

1. The thermal loading condition of the HSM-MX is based on the most conservative thermal loading configuration.
2. For stability evaluation, several different combinations of DSC and HSM bounding weights are considered.

Table A.3-1
Summary of HSM-MX Weight and Center of Gravity

Component	Description	
Empty HSM-MX	Total Weight (kips)	
	Single Array	2,448
	Double Array	4,125
	Center of Gravity from Bottom in Vertical Direction (inches)	
	Single Array	176.42
	Double Array	178.79
HSM-MX Loaded with EOS-37PTH DSC	Maximum Weight (kips)	
	Single Array	3,048
	Double Array	5,325
	Center of Gravity from Bottom in Vertical Direction (inches)	
	Single Array	168.68
	Double Array	169.39
HSM-MX Loaded with EOS-89BTH DSC	Maximum Weight (kips)	
	Single Array	3,053
	Double Array	5,335
	Center of Gravity from Bottom in Vertical Direction (inches)	
	Single Array	168.63
	Double Array	169.33

Notes:

1. The weight and center of gravity values listed in the table are corresponding to the maximum concrete density of 160 pcf.
2. The weight values are for the HSM-MX having three lower compartments and two upper compartments.

A.3.9.1.2.7.6 Seismic Load during Storage

The model described in Section A.3.9.1.2.7.1 for dead weight in HSM-MX is used and updated to reflect the effect of the vertical 0.8g load, transverse 1.7g load, axial (longitudinal) 1.7g load, and the internal pressure load of 20 psig.

Two elastic-plastic runs are performed for this load:

1. 0.8g vertical + 1.7g transverse + 1.7g axial with the weight of DSC internals modeled by equivalent pressure application on TSP with addition of internal pressure of 20 psig.
2. 0.8g vertical + 1.7g transverse + 1.7g axial with the weight of DSC internals modeled by equivalent pressure application on IBCP with addition of internal pressure of 20 psig.

The compound effect of dead weight, 0.8g vertical and 1.7g transverse, is modeled by multiplying the pressure from the dead weight case by a conservative factor of 4.

Seismic axial forces away from the HSM-MX door (load case 1 above) are resisted by the rear plates located at the ends of the DSC rear supports. The OTCP is recessed from the edge of the DSC shell, thus, the rear plate bears against the bottom edge of the DSC shell. The nodes of the top end of DSC shell, which come into contact with the rear stop plate, are restrained in the axial direction.

Seismic axial forces toward the HSM-MX door (load case 2 above) are resisted by the front axial retainers. The retainer is a steel bar located horizontally through the HSM-MX door. The retainer bears against the OBCP. The nodes of the OBCP, which bear against the area of the axial retainer bar, are restrained in the axial direction.
Figure A.3.9.1-4 shows the pressure load applied to the DSC while supported by the HSM-MX DSC supports.

The DSC shell and the OBCP experience compressive bearing stress in the vicinity of the axial retainer and rear plate. The bearing stresses experienced by the DSC shell and OBCP need not be evaluated for Service Level D loads.

A.3.9.1.2.7.7 Cask Drop

No change to Section 3.9.1.2.7.7.

The DSC weld stresses are summarized in Table A.3.9.1-3. The maximum weld stress ratio is 0.87 and occurs at the DSC shell to ITCP weld for Load Combination 9. The maximum radial weld stress is summarized in Table A.3.9.1-4. The maximum radial stress between the DSC and OTCP is 4.22 ksi. Therefore, the flaw size evaluation from Section 3.9.1.5 still remains valid.

Table A.3.9.1-5 summarizes the stress results for the controlling load combination. The maximum component stress ratio remains the same as in the original analysis and is equal to 0.92 in the grapple ring support. The second maximum component stress ratio is equal to 0.87 and occurs in the confinement boundary area of the DSC shell during load combination 9 (storage condition in the HSM-MX, dead weight normal conditions).

The structural integrity of the DSC shell, including closure welds, is maintained since the maximum stress ratio is less than 1. Therefore, it is concluded that the EOS DSC is structurally adequate under all anticipated load conditions for service during the transfer and storage in the HSM-MX.

A.3.9.1.7 References

A.3.9.1-1 ANSYS Computer Code and User's Manual, Release 14.0, Release 14.0.3 and Release 17.1

A.3.9.1-2 CoC 1042 Appendix A, NUHOMS® EOS System Generic Technical Specifications, Amendment 1.

Table A.3.9.1-1
EOS-37PTH/EOS-89BTH DSC Shell Assembly Loads and Load Combinations
(2 Sheets)

Loading Type	DSC Orientation	Load for Analysis	Load Combination	Service Level	Load Combination No.
Dead Weight (DW)	Horizontal[3] Vertical[3]	1g down	DW + Pressure+ 65 inch Accident Drop	D	7A
Internal pressure-Off-Normal		20 psig[9]			
Accident Side/corner drop[17]		65 inch drop			7B
Dead Weight (DW)	Horizontal	1g down	DW + Accident Pressure	D	8
Internal pressure-Accident		130 psig[3][9][10]			
Dead Weight (DW)	Horizontal [11]	1g down	DW + Pressure+ Thermal	A	9
Internal Pressure-Off-Normal		20 psig			
Thermal-Off Normal		Thermal-Off Normal			
Dead Weight (DW)	Horizontal [11]	1g down	DW + Pressure+ Seismic (S)	D	10
Internal Pressure-Off-Normal		20 psig			
Seismic (S)		S=±1.7g(axial) ±1.7g(transverse ±0.8g(vertical)[16]			
Test Pressure at fabricator—23 psig[12]	Vertical	23 psig internal pressure	23 psig (15x1.5=23 psig) internal pressure	Test	11
External pressure	Horizontal	See Note [14]		D	12

Notes

1. DSC in Transfer cask in vertical orientation. Only inner top cover is installed.
2. Use bounding thermal case for normal operations of transfer cask in vertical orientation.
3. DSC in Transfer Cask; Transfer Cask is in horizontal orientation. In case of End drop, the orientation is vertical supported by IBS in case of Bottom End drop and TSP in case of Top End drop.
4. Not used.
5. The push loads are applied at the canister bottom surface within the grapple ring support.

Table A.3.9.1-2
DSC Results - Load Combinations
(2 Sheets)

Load Combination Number	Service Level	Loads	Components		Stress Category [ksi]				
					P_m	P_m+P_b	P_L	P_m(or P_L)+P_b+Q	P_m(or P_L)+P_b+Q+P_e
9	A	DW+IP (20psi)	DSC Shell (Confinement)	Stress Intensity	6.77	12.11	18.07	27.90	45.44
				Allowable Stress	17.50	26.25	26.25	52.50	52.50
				Stress Ratio	0.39	0.46	0.69	0.53	0.87
			DSC Shell (Non-Confinement)	Stress Intensity	4.99	6.87	7.46	11.61	31.00
				Allowable Stress	17.50	26.25	26.25	52.50	52.50
				Stress Ratio	0.29	0.26	0.28	0.22	0.59
			OTCP	Stress Intensity	1.81	7.01	2.99	8.46	15.08
				Allowable Stress	17.50	26.25	26.25	52.50	52.50
				Stress Ratio	0.10	0.27	0.11	0.16	0.29
			ITCP	Stress Intensity	1.96	7.12	3.62	10.96	17.30
				Allowable Stress	17.50	26.25	26.25	52.50	52.50
				Stress Ratio	0.11	0.27	0.14	0.21	0.33
			OBCP	Stress Intensity	1.10	2.71	1.91	5.61	20.15
				Allowable Stress	17.50	26.25	26.25	52.50	52.50
				Stress Ratio	0.06	0.10	0.07	0.11	0.38
			IBCP	Stress Intensity	2.87	4.72	5.23	8.20	24.42
				Allowable Stress	17.50	26.25	26.25	52.50	52.50
				Stress Ratio	0.16	0.18	0.20	0.16	0.47

Table A.3.9.1-2
DSC Results - Load Combinations
(2 Sheets)

Load Combination Number	Service Level	Loads	Components		Stress Category[ksi]		
					P_m	P_m+P_b	P_L
10	D	DW+ Seismic+ IP(20psi)	DSC Shell (Confinement)	Stress Intensity	22.10	29.10	34.00
				Allowable Stress	44.38	57.06	57.06
				Stress Ratio	0.50	0.51	0.60
			DSC Shell (Non-Confinement)	Stress Intensity	20.10	22.60	20.30
				Allowable Stress	44.38	57.06	57.06
				Stress Ratio	0.45	0.40	0.36
			OTCP	Stress Intensity	7.13	13.00	14.30
				Allowable Stress	44.38	57.06	57.06
				Stress Ratio	0.16	0.23	0.25
			ITCP	Stress Intensity	5.53	11.20	9.27
				Allowable Stress	44.38	57.06	57.06
				Stress Ratio	0.12	0.20	0.16
			OBCP	Stress Intensity	19.80	26.70	5.60
				Allowable Stress	44.38	57.06	57.06
				Stress Ratio	0.45	0.47	0.10
			IBCP	Stress Intensity	11.10	16.10	18.60
				Allowable Stress	44.38	57.06	57.06
				Stress Ratio	0.25	0.28	0.33

Table A.3.9.1-3
DSC Weld Stress Results- Load Combinations

Load Combination Number	Service Level	Loads	Weld Components	Stress Category	Stress Intensity [ksi]	Allowable Stress [ksi]	Stress Ratio
9	A	DW+IP (20psi)	DSC-ITCP	P_L	16.50	23.2	0.71
				$P_L+P_b+Q+P_e$	40.19	46.3	0.87
			DSC-OTCP	P_L	11.57	23.2	0.50
				$P_L+P_b+Q+P_e$	30.24	46.3	0.65
			DSC-OBCP	P_L	5.46	23.2	0.24
				$P_L+P_b+Q+P_e$	25.77	46.3	0.56
10	D	DW+ Seismic + IP (20psi)	DSC-ITCP	P_L	25.0	46.9	0.53
			DSC-OTCP	P_L	38.8	46.9	0.83
			DSC-OBCP	P_L	17.30	46.9	0.37

Table A.3.9.1-4
DSC-OTCP Maximum Radial Weld Stress (S_x) Results- Load Combinations

Load Combination Number	Service Level	Loads	Maximum Radial Stress [ksi]
9	A	DW+IP (20psi)	0.14
10	D	DW+Seismic +IP(20psi)	(4.22)

Table A.3.9.1-5
Controlling DSC Load Combination Results Summary

Components / Welds	Controlling Load Combination [1]		Service Level	Max. Stress Ratio
	Number	Description		
DSC Shell Containment	9	DW + IP + Thermal	A	0.87
DSC Shell Non Containment	5	DW + Ram Retrieval+ IP + Thermal	A/B	0.85
OTCP	8	DW + Accident P	D	0.45
ITCP	8	DW + Accident P	D	0.45
OBCP	5	DW + Ram Retrieval + IP + Thermal	A/B	0.78
IBCP	4	DW + Ram Insert + IP + Thermal	A/B	0.47
Grapple Support	5	DW + Ram Retrieval + IP + Thermal	A/B	0.92
Grapple Ring	5	DW + Ram Retrieval + IP + Thermal	A/B	0.81
OTCP-DSC Shell Weld	10	DW + IP + max (HS_TOP, HS_BOT)	D	0.83
ITCP-DSC Shell Weld	9	DW + IP	A	0.87
OBCP-DSC Shell Weld	5	DW + Ram Retrieval + IP + Thermal	A/B	0.75

Note: [1] See Table A.3.9.1-1 for the load combination description.

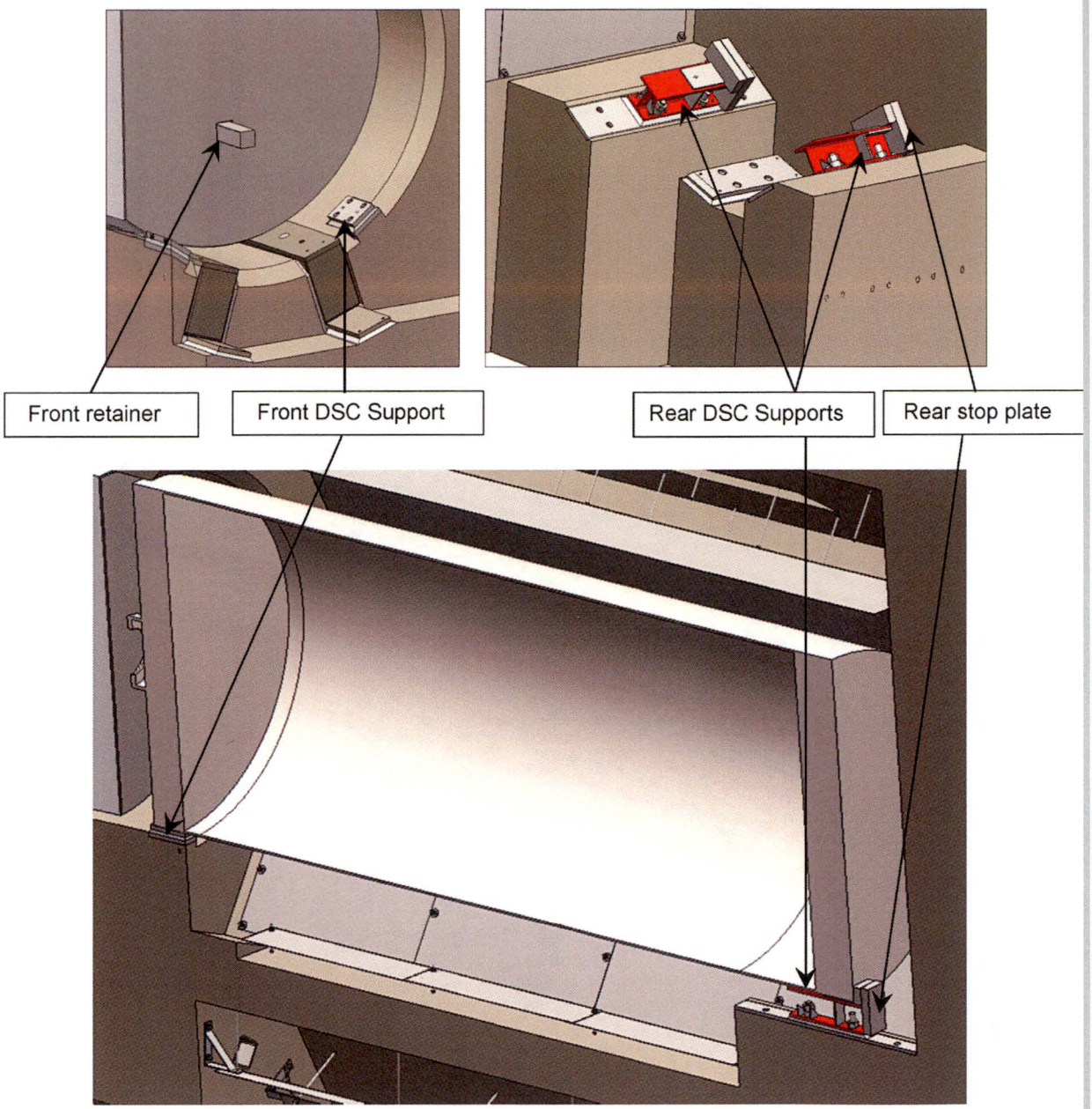

Figure A.3.9.1-1
DSC Supports and Axial Retainers

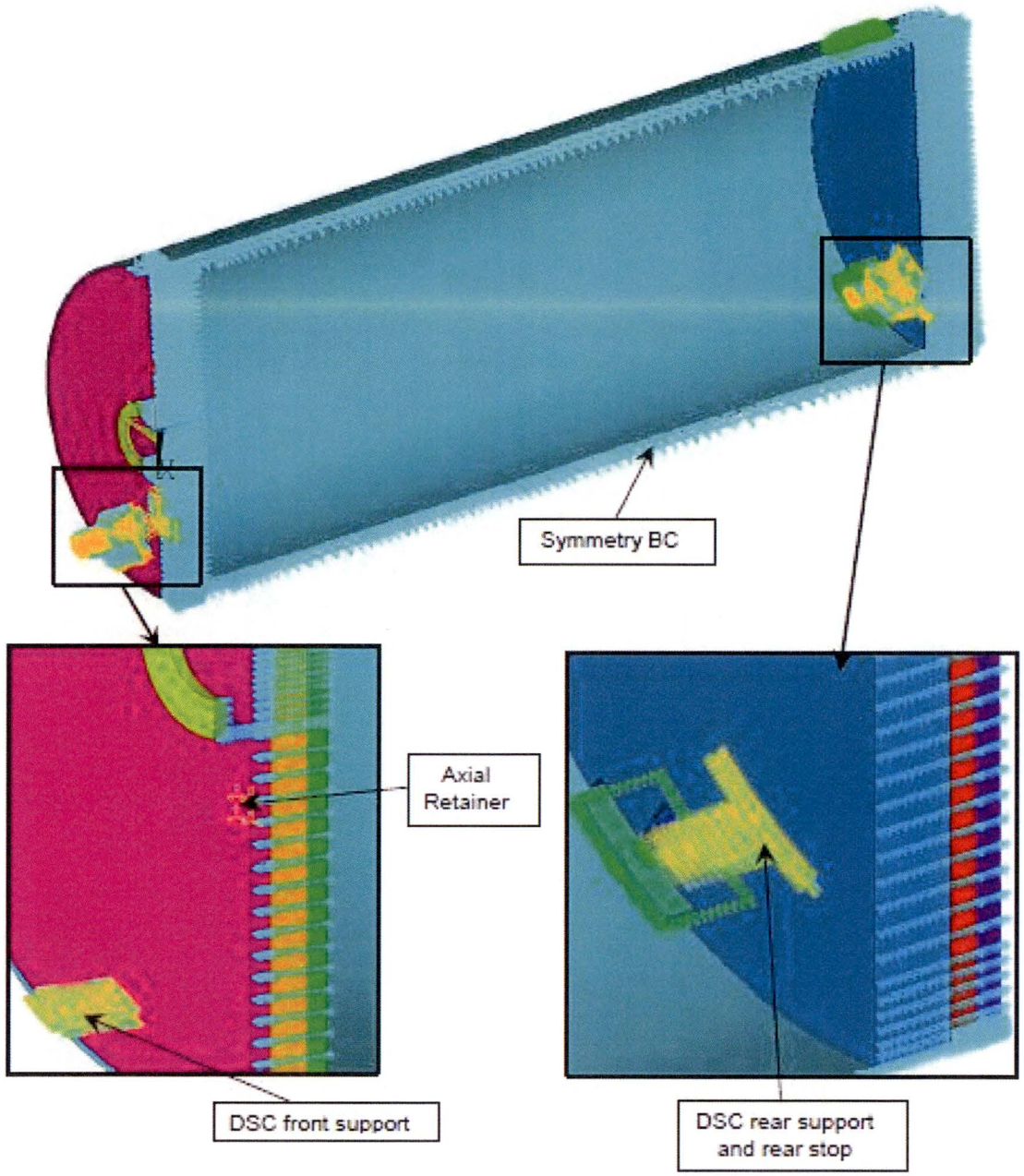

Figure A.3.9.1-3
DSC Boundary Conditions in HSM-MX

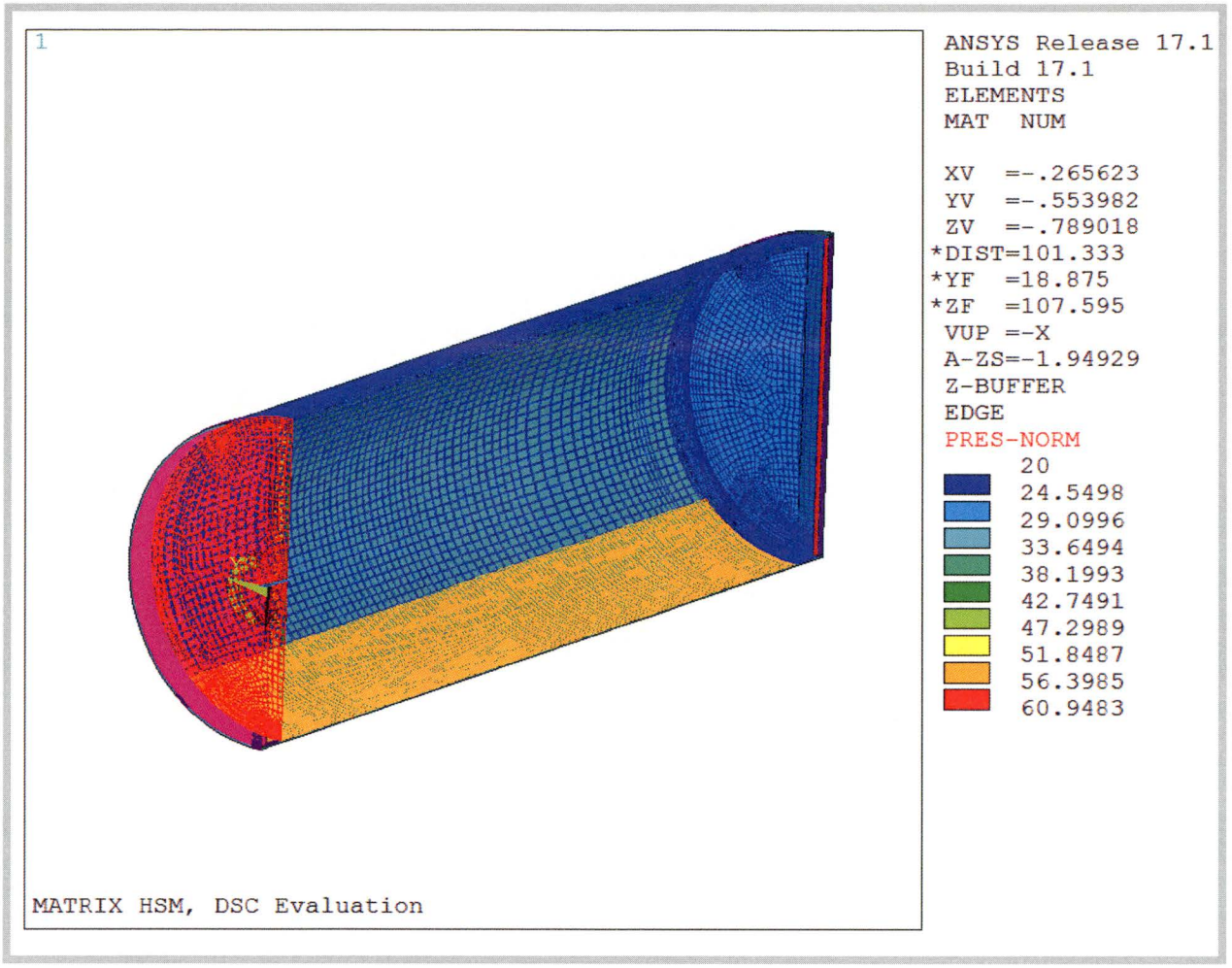

Figure A.3.9.1-4
Internals Seismic Equivalent Pressures with Internal Pressure, Load Case 2

A.3.9.4 HSM-MX STRUCTURAL ANALYSIS

The purpose of this appendix is to present the structural evaluation of the NUHOMS® MATRIX (HSM-MX) due to all applied loads during storage and transfer operations.

A.3.9.4.1 General Description

General description and operational features for the HSM-MX is provided in Appendix A.1. The HSM-MX is a freestanding, staggered reinforced concrete structure, designed to provide environmental protection and radiological shielding for the EOS-37PTH/EOS-89BTH DSC. The drawings of the HSM-MX, showing different components and overall dimensions, are provided in Appendix A.1.3

The HSM-MX is one of the three main components of the NUHOMS® MATRIX System. The system consists of the dual purpose (Transportation/Storage) EOS-37PTH/EOS-89BTH DSC, the HSM-MX, and the onsite transfer cask (EOS-TC) with associated ancillary equipment.

The HSM-MX overpack system comprises the MATRIX Horizontal Storage Modules, the MATRIX retractable roller tray (MX-RRT), the MATRIX loading crane (MX-LC) and associated trailer interface for storing dry shielded canisters (DSCs).

The HSM-MX is a staggered, two-tiered, high density, high-heat rejection, storage overpack that provides a self-contained modular structure for storage of DSCs. The HSM-MX is constructed from reinforced concrete and structural steel. The thick concrete roof and walls of the HSM-MX provide substantial neutron and gamma shielding. The monolithic structure increases resistance to earthquakes and offers significant self-shielding. The MX-RRT delivers the DSC from the transfer cask to the HSM-MX and places it on the front and rear DSC supports.

The HSM-MX can be arranged in both single-row or back-to-back row arrays.

For thermal protection of the HSM-MX concrete, stainless steel heat shields are installed inside the HSM-MX. The primary function of the heat shields is to limit the temperature of the surrounding concrete walls. The heat shields guide the cooling airflow through the HSM-MX.

A.3.9.4.2 Material Properties

The material properties used in the analysis and design of the HSM-MX and its components are discussed in detail in Chapter 8 and Appendix A.8.

A.3.9.4.3 Design Criteria

No change to Section 3.9.4.3.

A.3.9.4.7.3 HSM-MX Normal Operational Handling Load (R_o) Analysis

Normal operation assumes the canister is sliding over the MX-RRT due to a hydraulic ram force of up to 135,000 lbs (insertion) and 80,000 lbs (extraction) applied at the grapple ring and resisted by an axial load of 70,000 lb (insertion) and 40,000 lb (extraction) developing at each side of the MX-RRT supports. Here the total resisting axial load of 140,000 lbs is greater than the hydraulic ram force of 135,000 lbs. Only the insertion load is applied in the ANSYS FEM, since the extraction load is bounded by the insertion load. In addition, the DSC weight is applied to the MX-RRT support locations on both sides (4 points).

A.3.9.4.7.4 HSM-MX Normal Operating Thermal (T_o) Stress Analysis

The normal operating thermal (T_o) loads on the HSM-MX include the effect of design basis heat load of up to 50 kW generated by the DSC, plus the effect of normal ambient temperature. To evaluate the effects of normal thermal loads on the HSM-MX, heat transfer analyses for a range of normal ambient temperatures (-20 °F and 100 °F) are performed with a DSC heat load of 50 kW. The normal thermal cold condition (-20 °F) is bounded by the off-normal thermal cold condition (-40 °F). Therefore, the off-normal thermal cold condition is used in place of the normal thermal cold condition. The ambient condition that causes the maximum temperature and maximum gradients in the concrete components is used in the analysis. The normal thermal hot condition is the governing case for this load case. The HSM-MX thermal stress analysis was performed using thermal profiles and maximum temperatures that bound those reported in *Section A.4.5*. The ANSYS FEM described in Section A.3.9.4.6.2 is used for the normal thermal load analysis.

A.3.9.4.7.5 HSM-MX Design Basis Wind Load (W) Analysis

The DSCs inside the HSM-MX are not affected by wind load. The concrete structure forces and moments due to the design basis wind load (W) are bounded by the result of tornado generated wind load discussed in Section A.3.9.4.9.1. Therefore, no separate analysis is performed for this case.

A.3.9.4.8 Off-Normal Operation Structural Analysis

This section describes the design basis off-normal events for the HSM-MX components and presents analyses that demonstrate the adequacy of the design safety features of the HSM-MX.

The off-normal operating loads for which the HSM-MX components are designed include off-normal handling load and off-normal thermal load.

4. Automobile traveling through the air not more than 25 ft above the ground and having contact area of 20 sq. ft, Weight = 4000 lbs, Impact Horizontal Velocity = 195 fps.

Stability and stress analyses are performed to determine the response of the HSM-MX to tornado wind pressure loads. The stability analyses are discussed in detail in Appendix A.3.9.7. The stress analyses are performed using the ANSYS FEM of the HSM-MX to determine design forces and moments. These conservative analyses envelope the effects of wind pressures on the HSM-MX in other array configurations. Thus, the requirements of 10 CFR 72.122 are met.

The HSM-MX is qualified for maximum design basis tornado (DBT) generated design wind loads of 238 psf and 167 psf on the windward and leeward HSM-MX walls (See Table A.3.9.4-1 and Table A.3.9.4-2), respectively, and a pressure drop of 3 psi.

An HSM-MX array is protected by *end side walls,* shield walls, or an adjacent module. For an HSM-MX array, the module on the windward end of the array has *either an end side wall or* an end shield wall to protect the module from tornado missile impacts. The *end walls are* also subjected to the 238 psf windward pressure load. The 167 psf suction load is applicable to the end *side* wall on the opposite end module in the array. A suction of 355 psf is also applied to the roof of each HSM-MX in the array.

For the stress analyses, the DBT wind pressures are applied to the HSM-MX as uniformly distributed loads. The bending moments and shear forces at critical locations in the HSM-MX concrete components are calculated by performing an analysis using the ANSYS analytical model of the HSM-MX as described in Section A.3.9.4.6. The wind and tornado loads are identified as load combination C2 and C5 as provided in Table A.3.9.4-5. The demand to capacity ratios in terms of reinforcement areas for the bounding load combinations are presented in Table A.3.9.4-6 for each of the HSM-MX components.

Conservatively, the design basis extreme wind pressure loads are assumed to be equal to those calculated for the DBT (based on 360 mph wind speed) in the formulation of HSM-MX load combination results.

In addition, the adequacy of the HSM-MX to resist tornado missile loads is checked using the modified National Defense Research Committee (NDRC) empirical formulae [A.3.9.4-10] for local damage evaluation, and response chart solution method [A.3.9.4-13] for global response. These evaluations are described in Section A.3.9.4.10.5.

A.3.9.4.9.2 Earthquake (Seismic) Load (E) Analysis

The design basis seismic load used for analysis of the HSM-MX components is as discussed in Section A.2.3.4. Based on NRC Regulatory Guide 1.61 [A.3.9.4-3], a damping value of 4% is used for seismic analysis of steel structural components and a damping value of 7% is used for seismic analysis of concrete components of the HSM-MX. An evaluation of the frequency content of the loaded HSM-MX is performed to determine the amplified accelerations associated with the design basis seismic response spectra for the HSM-MX. The results of the frequency analysis of the HSM-MX structure (which includes a simplified model of the DSC) yield a lowest frequency of *23.94* Hz in the transverse direction and *24.08* Hz in the longitudinal direction. The lowest vertical frequency exceeds 45 Hz; therefore, the spectral acceleration is not amplified in the vertical direction. Thus, based on the *enhanced* Regulatory Guide 1.60 response spectra amplifications, the corresponding seismic accelerations used for the design of the HSM-MX are *1.33*g and *1.33*g in the transverse and longitudinal directions, respectively, and 0.800g in the vertical direction. The resulting amplified accelerations are given in Table A.3.9.4-3.

An equivalent static analysis of the HSM-MX is performed using the ANSYS FEM described in Section A.3.9.4.6.1 by applying the amplified seismic accelerations load. The dominant frequencies are lower for the double row array in the X *and Y* direction*s*, whereas the single row array has a lower frequency in the Z direction. Therefore, the spectral accelerations to be used in seismic analysis are taken from the double row array model for the X *and Y* direction*s*, and from the single row array model for the Z direction.

The responses for each orthogonal direction are combined using the square root of the sum of the squares (SRSS) method. The resulting moments and forces due to the combined seismic load are included in the HSM-MX load combination results.

For sites having a higher zero period acceleration than analyzed, the reinforcement requirement may need to be reviewed, and additional rebar may be added for such sites.

The stability evaluation of the HSM-MX due to seismic load is discussed in Appendix A.3.9.7.

Seismic analysis of the HSM-MX heat shields consists of a modal time-history analysis of the HSM-MX using the seismic acceleration load corresponding to the ISRS with ±15% peak-broadening and the frequency response of each type of heat shield. The ground motion time histories used in the modal time-history analysis of the HSM-MX are based on four earthquakes,

- Hector Mine,
- Chi-Chi,
- Denali,
- Mianzhuqingping.

- Case 2: Flood water flowing transversely from the right side wall to the left side wall of the module or vice versa.

The ANSYS FEM described in Section A.3.9.4.6.1 is used for the structural evaluation. The results for the flood load case are obtained by enveloping results from the above load cases.

The stability evaluation of the HSM-MX due to flood load is discussed in Appendix A.3.9.7.

A.3.9.4.9.4 Accident Blocked Vent Thermal (T_a) Stress Analysis

The postulated accident thermal event occurs due to blockage of the air inlet and outlet vents under off-normal ambient temperatures range from -40 °F to 117 °F. The HSM-MX thermal stress analysis was performed using the thermal profiles and maximum temperatures reported in *Section A.4.5*.

The ANSYS FEM described in Section A.3.9.4.6.2 is used for the structural analysis for the accident blocked vent condition.

A.3.9.4.10 Structural Evaluation

The load categories associated with normal operating conditions, off-normal conditions and postulated accident conditions are described previously. The load combination results and design strengths of HSM-MX components are presented in this section.

A.3.9.4.10.1 HSM-MX Concrete Components

To determine the required strength (internal axial forces, shear forces, and bending moments) for each HSM-MX concrete component, linear elastic finite element analyses are performed for the normal, off-normal, and accident loads using the analytical models described in Sections A.3.9.4.6.1 and A.3.9.4.6.2 for mechanical and thermal loads, respectively.

The concrete design loads are multiplied by load factors and combined to simulate the most adverse load conditions. The load combinations listed in Table A.3.9.4-5 are used to evaluate the concrete components. The demand to capacity ratios (in terms of reinforcement areas) for the bounding load combinations are presented in Table A.3.9.4-6 for each HSM-MX component. The reinforcement directions are shown in Figure A.3.9.4-5. The thermal stresses of HSM-MX concrete components used in the load combination results are based on thermal results that bound those reported in *Section A.4.5*.

The required longitudinal reinforcement areas for the critical sections of concrete are calculated in accordance with the requirements of ANSI 57.9 [A.3.9.4-8] and ACI 349-06 [A.3.9.4-9], including the strength reduction factors defined in ACI 349-06, Section 9.3. The longitudinal reinforcement areas provided for the HSM-MX concrete components exceed the required reinforcement areas as shown in Table A.3.9.4-6.

A.3.9.4.10.2 HSM-MX Shield Door

The shield door is free to grow in the radial direction when subjected to thermal loads. Therefore, there are no stresses in the door due to thermal growth. The dead weight, differential pressure, flood and seismic loads cause insignificant stresses in the door compared to stresses due to missile impact load. Therefore, the door is evaluated only for the missile impact load.

The minimum thickness of a concrete component to prevent perforation and scabbing are 18.5 inches and 27.7 inches, respectively. Thus, the 28-inch thick door is adequate to protect from local damage due to missile impact. The computed maximum ductility ratio for the door is less than 2, which satisfies the ductility requirement if compared against the allowable ductility ratio of 10 as per ACI 349-06 [A.3.9.4-9]. Therefore, the concrete door meets the ductility requirement and is adequate to protect from the global effect of missile impact.

A.3.9.4.10.3 HSM-MX Heat Shield

The heat shield panels are connected by bolts and threaded studs to the support brackets and surrounding concrete walls. The HSM-MX heat shield consists of different variations such as lower cavity side heat shield (LSHS), lower cavity top heat shield (LTHS), upper cavity bottom heat shield (UBHS), upper cavity side heat shield (USHS) and upper cavity top heat shield (UTHS).

The heat shield panels consists of 12 gauge 0.1054-inch thick stainless steel.

The maximum interaction ratio for the combined axial and bending stress for all bolts is *0.98*, which is less than 1.0, in the UBHS and maximum bending stress in the panel is *30.0* ksi, which is less than the allowable stress of 32.2 ksi.

The maximum temperature used in the stress analysis of the heat shields bounds the maximum temperatures reported in *Section A.4.5*. Expansion due to off-normal and accident condition for all heat shields will not be restrained by the supporting elements.

A.3.9.4.10.4 HSM-MX DSC Axial Retainer

The DSC axial retainer consists of a 3.5 in x 3.5 in solid steel square rod. The axial retainer slides horizontally through the HSM-MX door and stops the forward motion of the DSC towards the door. The anchor plate of the axial retainer (2 ½ in. thick, *in the middle and 2 in. thick near the edge* 6 in. x 15 in. plate), which is bolted to the door, supports the axial motion of the retainer and transfers the DSC seismic load to the door. The motion towards the back wall is controlled by the rear stop plate.

The calculated compressive strength of the axial retainer rod is 280.3 kips which is greater than the equivalent force of *270.5* kips, due to seismic load. The maximum seismically induced shear load in the anchor plate is *135.3* kips. The allowable shear strength of the anchor plate is 498.6 kips. The bounding seismically induced moment in the anchor plate is *507.2* in-kips. The allowable flexural strength of the anchor plate at that location is 714.0 in-kips. Hence, the DSC axial retainer design is adequate to perform its intended function.

A.3.9.4.10.5 Evaluation of Concrete Components for Missile Loading

Missile impact effects are assessed in terms of local damage and overall structural response. Local damage that occurs in the immediate vicinity of the impact area is assessed in terms of penetration, perforation, spalling and scabbing. Evaluation of local effects is essential to ensure that protected items (the DSC and fuel) would not be damaged by a missile perforating a protective barrier, or by secondary missiles such as scabbing particles. Evaluation of overall structural response is essential to ensure that protected items are not damaged or functionally impaired by deformation or collapse of the impacted structure.

The tornado-generated missiles are conservatively assumed to strike normal to the surface with the long axis of the missile parallel to the line of flight to maximize the local effects. Plastic deformation to absorb the energy input by the tornado-generated missile load is desirable and acceptable, provided that the overall integrity of the structure is not impaired. Due to complex physical process associated with missile impact effects, the HSM-MX structure is primarily evaluated conservatively by application of empirical formulae.

A.3.9.4.10.5.1 Local Damage Evaluation

Local missile impact effects consist of (a) missile penetration into the target, (b) missile perforation through the target, and (c) spalling and scabbing of the target. This also includes punching shear in the region of the target. Per F.7.2.3 of ACI 349-06 [A.3.9.4-9], if the concrete thickness is at least 20% greater than that required to prevent perforation, the punching shear requirement of the code need not be checked.

The following enveloping missiles are considered for local damage:

- Utility wooden pole
- Armor piercing artillery shell

Where,

e = perforation thickness, in.

In order to provide an adequate margin of safety the design thickness $t_d = 1.2e$ [A.3.9.4-9]

C. Modified NDRC formula for scabbing thickness [A.3.9.4-10]:

$$\frac{s}{d} = 7.91\left(\frac{x}{d}\right) - 5.06\left(\frac{x}{d}\right)^2 \text{, for } x/d \leq 0.65$$

$$\frac{s}{d} = 2.12 + 1.36\left(\frac{x}{d}\right) \text{, for } 0.65 \leq x/d \leq 11.75$$

Where,

s = scabbing thickness, in.

In order to provide an adequate margin of safety the design thickness $t_d = 1.2s$ [A.3.9.4-9]

The concrete targets of the HSM-MX that may be subjected to local damage due to missile impact are:

- *24*-inch thick roof panel
- *44*-inch thick roof side wall
- 39-inch thick (minimum) front wall
- 36-inch thick end shield wall
- 36-inch thick end shield wall with 11-inch thick (minimum) side wall (upper compartment)
- 44-inch thick end wall (lower compartment)
- *82*-inch thick end wall (upper compartment)
- 44-inch thick rear wall (for the case of single row array)

The minimum thickness of concrete target components listed above is *36 inches and 24 inches for horizontal and vertical missiles impacts, respectively*. So, the required perforation thickness and required scabbing thickness are compared against *36 inches and 24 inches for horizontal and vertical missiles impacts, respectively,* to ensure the adequacy of design.

Local Impact Effects of Utility Wooden Pole Missile

Per section 6.4.1.2.5 of [A.3.9.4-10], utility wooden pole missiles do not have sufficient strength to penetrate a concrete target and that the scabbing thickness required for wood missiles is substantially less than that required for a steel missile with the same mass and velocity. Practically, wooden pole missiles do not appear to be capable of causing local damage to the 12-inch or thicker walls (also see Section 2.1.1 of [A.3.9.4-13]). Since none of the concrete targets are less than 12 inches thick, the postulated wood missiles do not cause any local damage to the HSM-MX concrete component.

Local Impact Effects of Armor Piercing Artillery Shell Missile

The penetration depth for this missile is calculated using the NDRC Formula as given in Section A.3.9.4.10.5.1 (a) and the parameters used in the formula are as listed below:

d = 8.0 in. effective diameter of missile

W = 276 lb weight of missile

v_o = 185 fps striking velocity of missile

f'_c = 5000 psi concrete compressive strength

K = 180/√5000 = 2.55 concrete penetrability factor

N = 0.84 projectile shape factor (blunt nosed)

Penetration depth, x = 4.6 in. for x/d (= 0.58) ≤ 2.0

Perforation thickness, e = 12.9 in. for x/d (= 0.58) ≤ 1.35

Required perforation thickness = *1.2**12.9 = 15.5 in. < *36* in.

Scabbing thickness, s = 23.1 in. for x/d (= 0.58) ≤ 0.65

Required scabbing thickness = 1.2*23.1 = 27.7 in. < *36* in.

Similarly, for vertical impact:

Required perforation thickness = 11.2 in. < 24 in

Required scabbing thickness = 22.7 in. < 24 in

Therefore, penetration and perforation of the concrete components of the HSM-MX do not occur due to this missile impact.

Local Impact Effects of 12-Inch Diameter Schedule 40 Steel Pipe Missile

The penetration depth for this missile is calculated using the NDRC Formula as given in Section A.3.9.4.10.5.1 and the parameters used in the formula are as listed below:

ϕ = 12.75 in. outer diameter of 12-inch dia. schedule 40 steel pipe.

A_c = 15.74 in^2 missile impact area (cross sectional area of steel)

$d = (4*15.74/\pi)^{1/2} = 4.5$ in. effective diameter of missile

W = 750 lb weight of missile

v_o = 154 fps striking velocity of missile

f'_c = 5000 psi concrete compressive strength

$K = 180/\sqrt{5000} = 2.55$ concrete penetrability factor

N = 0.72 projectile shape factor (flat nosed)

Penetration depth, x = 7.6 in. for $x/d\ (= 1.69) \leq 2.0$

Perforation thickness, e = 15.4 in. for $1.35 \leq x/d\ (= 1.69) \leq 13.5$

Required perforation thickness = 1.2*15.4 = 18.5 in. < *36* in.

Scabbing thickness, s = 19.9 in. for $0.65 \leq x/d\ (= 1.69) \leq 11.75$

Required scabbing thickness = 1 .2*19.9 = 23.9 in. < *36* in.

Similarly, for vertical impact:

Required perforation thickness = 14.8 in. < 24 in

Required scabbing thickness = 20 in. < 24 in

Therefore, penetration and perforation of the concrete components of the HSM-MX do not occur due to this missile impact.

A.3.9.4.10.5.2 Global Structural Response

When a missile strikes a structure, large forces develop at the missile-structure interface, which decelerate the missile and accelerate the structure. The response of the structure depends on the dynamic properties of the structure and the time dependent nature of the applied loading (interface force-time function). The force-time function is, in turn, dependent on the type of impact (elastic or plastic) and the nature and extent of local damage.

In an elastic impact, the missile and the structure deform elastically, remain in contact for a short period of time (duration of impact), and subsequently disengage due to the action of elastic interface restoring forces.

In a plastic impact, the missile or the structure (or both) may sustain permanent deformation or damage (local damage). Elastic restoring forces are small, and the missile and the structure tend to remain in contact after impact. Plastic impact is much more common than elastic impact, which is rarely encountered. Test data have indicated that the impact from all postulated tornado-generated missiles can be characterized as a plastic impact.

W_m = weight of missile (lb) = 750 lb

M_m = missile mass (lb-sec^2/ft) = W_m/g = 750 lb /32.2 ft/sec^2 = 23.29 lb-sec^2/ft

v_s = striking velocity of missile = 154 fps

Therefore,

F = 728 kip and t_i = 0.00986 sec

For the missile with vertical velocity F_{peak} = 485 kip

D. Automobile Missile

For automobile missile, the interface forcing function per 2.3.3 of [A.3.9.4-13] is as follows:

$F_t = 0.625\ v_c\ W \sin(20t)$ $\quad 0 < t \leq 0.0785$ sec

$F_t = 0$ $\quad t > 0.0785$ sec

Where,

F_t = force as a function of time (lb)

W = weight of automobile (lb) = 4000 lb

v_c = change in velocity during impact (conservatively = v_s) (fps) = 195 fps

Therefore,

F = 488 kip and t_i = 0.0785 sec

For the missile with vertical velocity, F_{peak} =325 kip

The lower compartment module left sidewall, top left sidewall, right shield wall, front wall, rear wall, roof and roof sidewall of the HSM-MX are evaluated for global response, since these components may interface with missile loading. The lower compartment module left side wall, upper compartment module left side wall and rear wall are idealized as a simply supported plate. The roof is idealized as a plate clamped to three sides and free at the other side adjacent to vent opening. The roof sidewall is idealized as a plate clamped to three sides and free at the other side facing the top. The yield resistance and fundamental period of vibration of concrete components are then determined based on the assumed idealized boundary condition using the equations given in Section 4.4 of [A.3.9.4-13]. *For the right shield wall and front wall, ANSYS finite element models are used to determine the yield resistance and fundamental period of vibration.* The calculated value of yield resistance, R_y, and fundamental period of vibration, T_n, for different concrete components are tabulated below.

Component	R_y (kip)	T_n (sec)
Lower Compartment Module Left Side Wall	*1659*	0.0048
Upper Compartment Module Left Side Wall	*3255*	*0.0025*
Right Shield Wall	*359.5*	*0.016*
Front Wall	*961.1*	*0.0079*
Rear Wall	1659	0.0030
Roof	*453.8*	*0.0040*
Roof Side Wall	*1659*	*0.0015*

In the response chart solution method, the structural response is determined by entering the chart with calculated values of C_T and C_R to determine the ductility ratio, μ, which is compared against the allowable ductility ratio as given in Appendix F of ACI 349-06 [A.3.9.4-9]. The dimensionless ratios, C_T and C_R, are defined as follows:

$$C_R = \frac{R_y}{F} \qquad C_T = \frac{t_i}{T_n}$$

The maximum value of ductility ratio of all seven components is found to be less than the allowable ductility ratio per ACI 349-06 [A.3.9.4-9], *which is 10 if flexure controls the design and 1.3 if shear controls the design.* Hence, the global response of HSM-MX is within deformation limit meeting the ductility requirement.

Each component is also evaluated for punching shear capacity with interfacing utility wooden pole missile and automobile missile. All the components have punching shear capacity greater than the peak missile interface force.

A.3.9.4.11 Conclusions

The load categories associated with normal operating conditions, off-normal conditions and postulated accident conditions are described and analyzed in previous sections. The load combination results for HSM-MX components important-to-safety are also presented. Comparison of the results with the corresponding design capacity shows that the design strength of the HSM-MX is greater than the strength required for the most critical load combination.

Table A.3.9.4-1
Design Pressures for Tornado Wind Flowing from Front Wall to Rear Wall and Vice Versa

Component	Velocity Pressure, q_v (psf)	External Pressure Coefficient, C_p	Internal Pressure Coefficient, (GC_{pi})	Max. Design Pressure, $q_v*(G*C_p-GC_{pi})$ (psf)
Windward (Front Row Front Wall)	276	0.80	±0.18	238
Leeward (Back Row Front Wall)		-0.47(1)		-160
Side (Right Side Wall)		-0.70		-214
Side (Left Side Wall)		-0.70		-214
Roof		-1.30		-355

Notes:

1. The C_p value is taken for L/B = 496"/*438*" ≈ *1.13*.
2. The gust effect factor, G=0.85 considering the HSM-MX as rigid.

Table A.3.9.4-2
Design Pressures for Tornado Wind Flowing from Right Side to Left Side Wall and Vice Versa

Component	Velocity Pressure, q_v (psf)	External Pressure Coefficient, C_p	Internal Pressure Coefficient, (GC_{pi})	Max. Design Pressure, $q_v*(G*C_p-GC_{pi})$ (psf)
Side (Front Row Front Wall)	276	-0.70	±0.18	-214
Side (Back Row Front Wall)		-0.70		-214
Windward (Right Side Wall)		0.80		238
Leeward (Left Side Wall)		-0.50(1)		-167
Roof		-1.30		-355

Notes:

1. The C_p value is taken for L/B = 431"/*438*" ≈ *0.88*
2. The gust effect factor, G=0.85 considering the HSM-MX as rigid.

Table A.3.9.4-3
Spectral Acceleration Applicable to Different Components of HSM-MX for Seismic Analysis

Direction	Frequency (Hz)	Spectral Acceleration Corresponding to Design ZPA (Design ZPA = 0.85g horizontal & 0.80g vertical)		
		at 3% Damping (for DSC)	at 4% Damping (for steel structure)	at 7% Damping (for concrete components)
X (Transverse)	*23.94*	*1.62*g	*1.53*g	*1.33*g
Y (Vertical)	*49.02*	0.80g	0.80g	0.80g
Z (Longitudinal)	*24.08*	*1.61*g	*1.52*g	*1.33*g

Table A.3.9.4-6
Demand to Capacity Ratios for HSM-MX Longitudinal Reinforcement Areas

Component Name	Thickness (in)	Reinforcement	$A_{s,provided}$ (in^2/in)	A_{sx}			A_{sy}			A_{sip}		
				$A_{sx,read}$ (in^2/in)	D/C_{asx}	Governing Load Combination	$A_{sy,read}$ (in^2/in)	D/C_{asy}	Governing Load Combination	$A_{sip,read}$ (in^2/in)	D/C_{asip}	Governing Load Combination[1]
Bottom Unit Front Wall Bottom	51	#9@7"	0.1429	0.1304	0.91	C4	0.0703	0.49	C4	0.1287	0.45	C1
Top Unit Front Wall Bottom	51	#9@8"	0.1250	0.0856	0.68	C4	0.0847	0.68	C4	0.1280	0.51	C1
Front Wall Top	39	#9@8"	0.1250	0.1023	0.82	C4	0.1142	0.91	C4	0.1589	0.64	C4
Bottom Unit Vent Wall	11.5	#5@8"	0.0388	0.0165	0.43	C4	0.0149	0.38	C4	0.0285	0.37	C1
Top Unit Side Vent Wall	11	#5@8"	0.0388	0.0122	0.31	C5	0.0172	0.44	C7	0.0276	0.36	C1
Bottom Unit Side Wall	37	#6@8"	0.0550	0.0243	0.44	C4	0.0239	0.43	C4	0.0925	0.84	C1
Bottom Unit End Side Wall	44	#9@8"	0.1250	0.0990	0.79	C4	0.0715	0.57	C7	0.1102	0.44	C1
Top Unit End Side Wall	82	#9@8"	0.1250	0.0449	0.36	C4	0.0570	0.46	C4	0.2047	0.82	C1
Bottom Unit Rear Wall Bottom	78	#9@8"	0.1250	0.0706	0.56	C4	0.0151	0.12	C4	0.1949	0.78	C1
Rear Wall	30	#9@8"	0.1250	0.0088	0.07	C4	0.0000	0.00	C1	0.1350	0.54	C4
Roof Top Panel	24	#7@9"	0.0667	0.0319	0.48	C2	0.0583	0.87	C5	0.0600	0.45	C1
Roof Bottom Panel	10	#5@8"	0.0388	0.0130	0.34	C5	0.0081	0.21	C7	0.0283	0.37	C3
Roof Side Panel	11	#5@8"	0.0388	0.0066	0.17	C5	0.0072	0.19	C2	0.0276	0.36	C1
Roof Side Panel	10.5	#5@9"	0.0344	0.0038	0.11	C5	0.0126	0.37	C7	0.0551	0.80	C5
Roof Side Wall	44	#9@8"	0.1250	0.0303	0.24	C5	0.1038	0.83	C2	0.1102	0.44	C1
Roof	50	#9@8"	0.1250	0.0973	0.78	C2	0.0711	0.57	C5	0.1250	0.50	C1
Inclined Slab	11.5	#5@8"	0.0388	0.0144	0.37	C4	0.0149	0.38	C4	0.0285	0.37	C1
Pedestal	23.89	#7@8"	0.0750	0.0242	0.32	C4	0.0410	0.55	C4	0.0600	0.40	C1

Note 1:

$A_{sip,required}$ is governed by minimum in-plane shear reinforcement requirement for most components. *C1* is shown for such components.

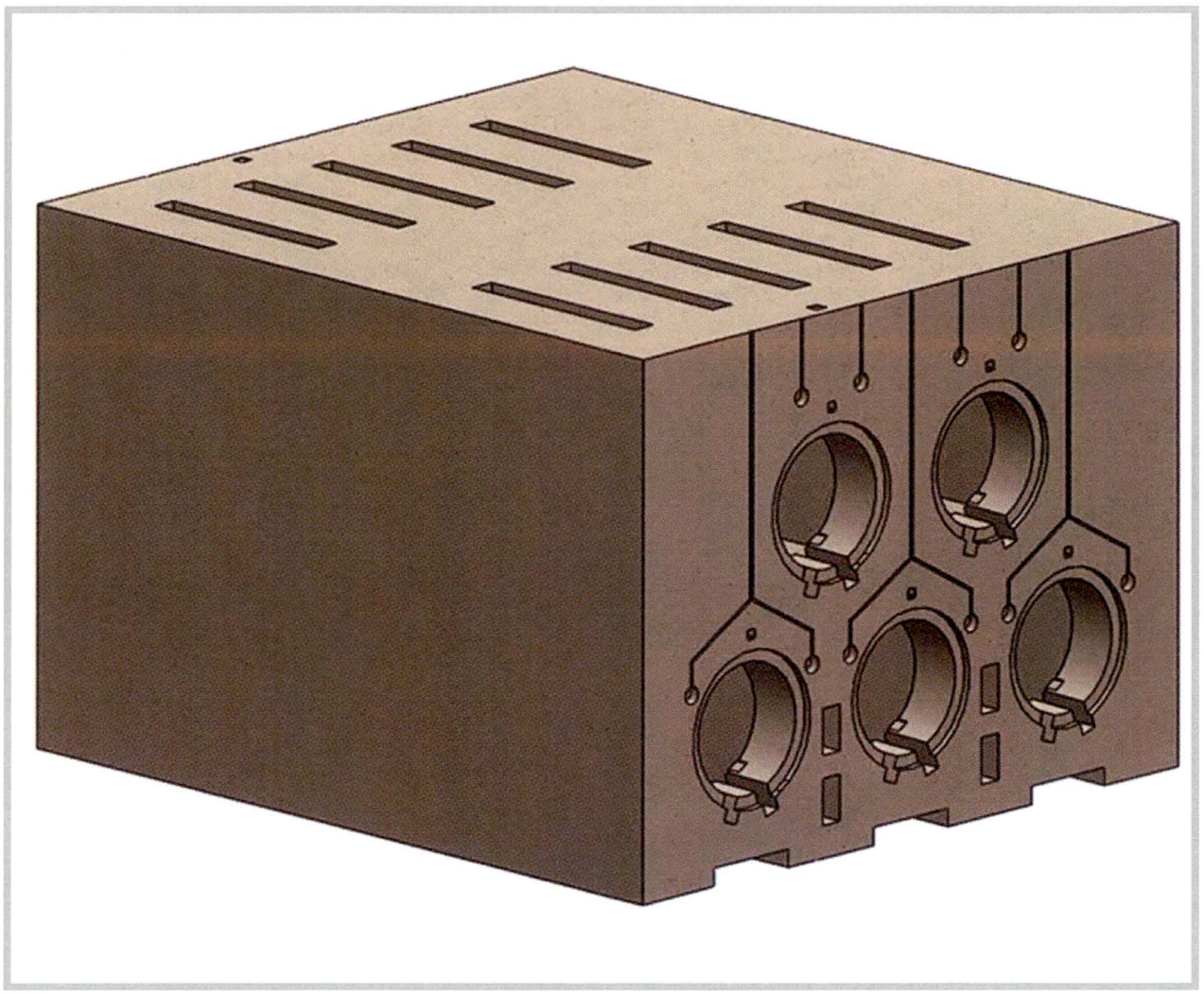

Figure A.3.9.4-1
HSM-MX (Back-to-Back) CAD Model

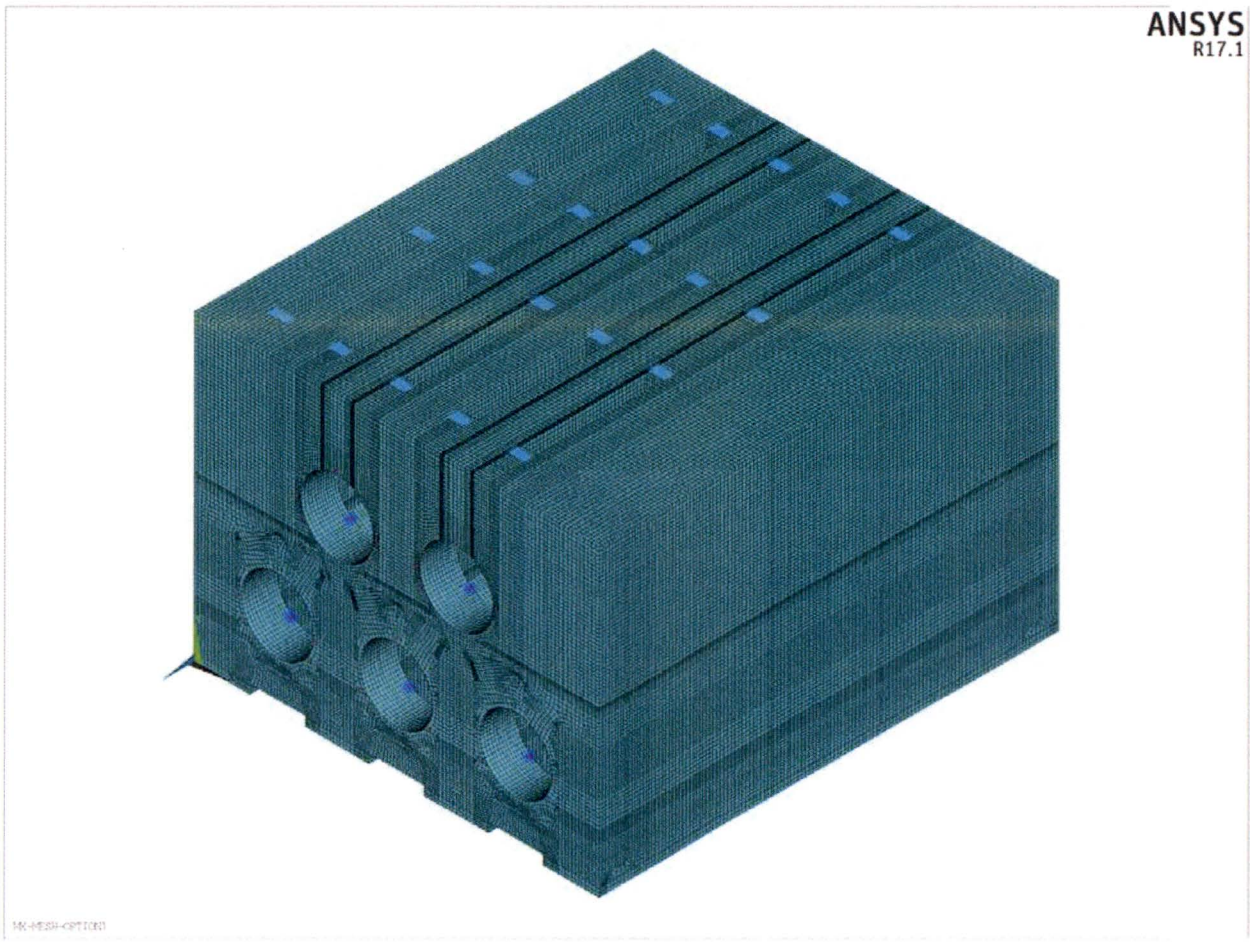

Figure A.3.9.4-2
HSM-MX (Back-to-Back) Meshed Model

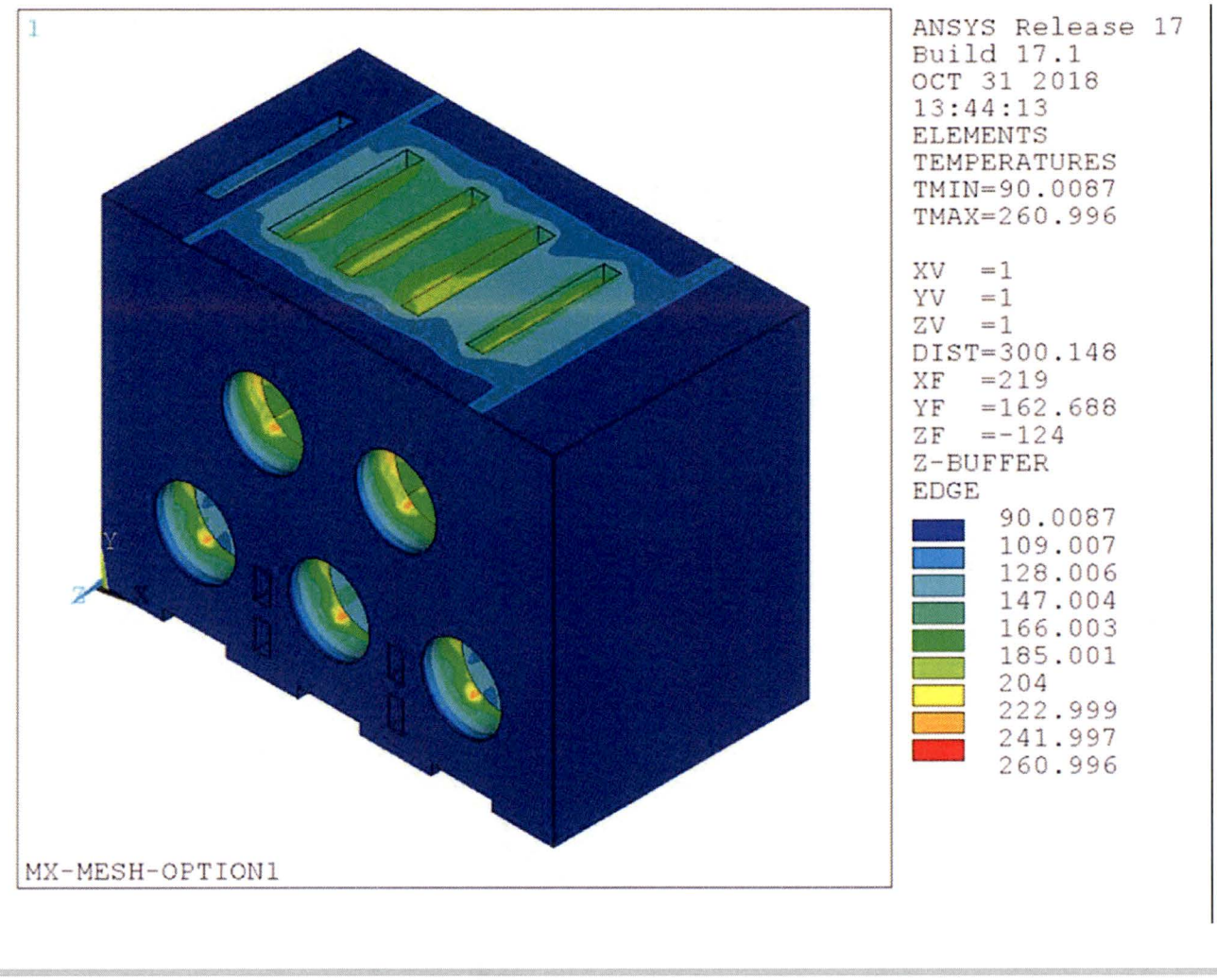

Figure A.3.9.4-3
Temperature Distribution of HSM-MX for Normal Thermal Hot Condition

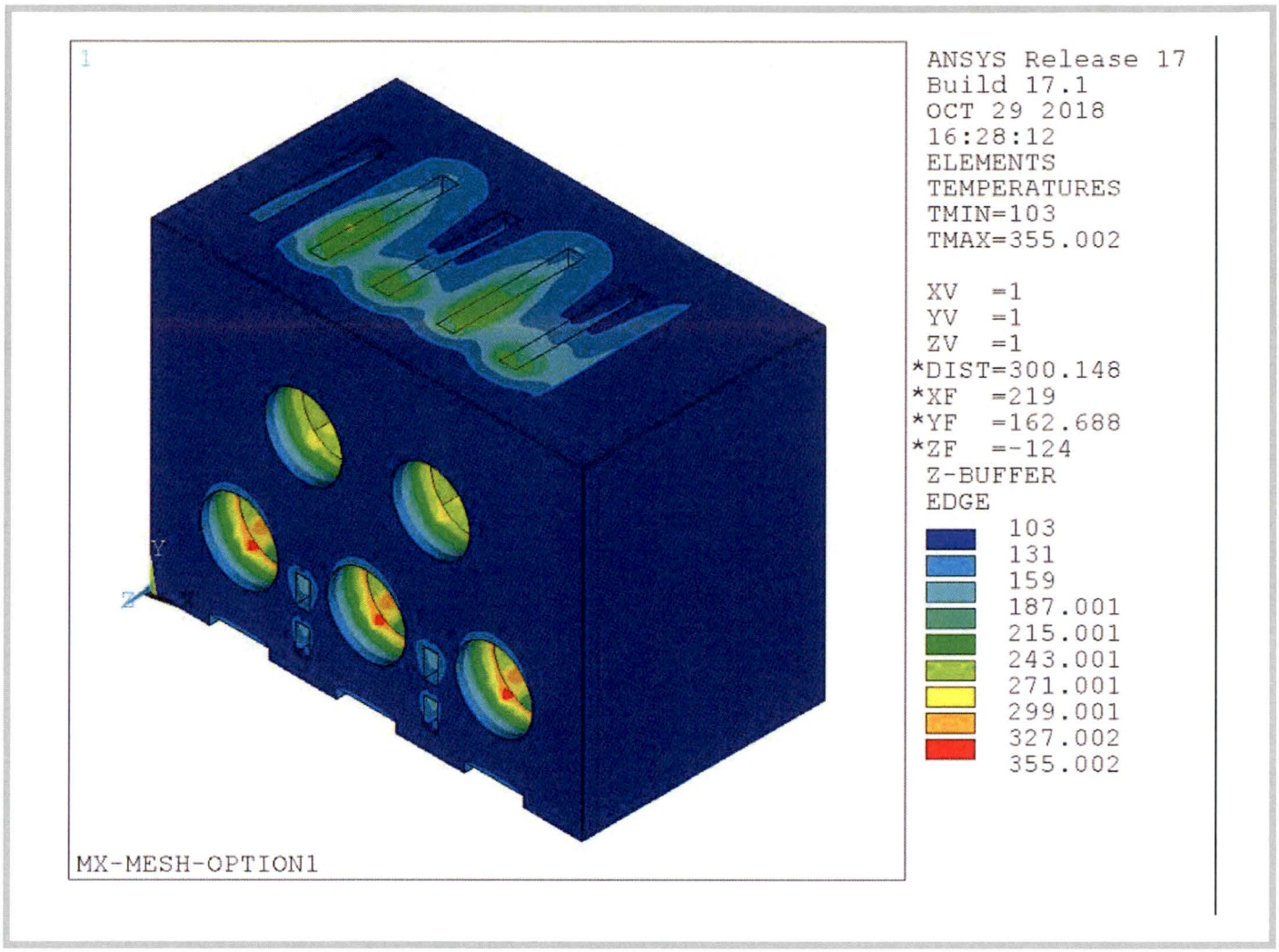

Figure A.3.9.4-4
Temperature Distribution of HSM-MXS for Blocked Vent Accident Thermal Condition

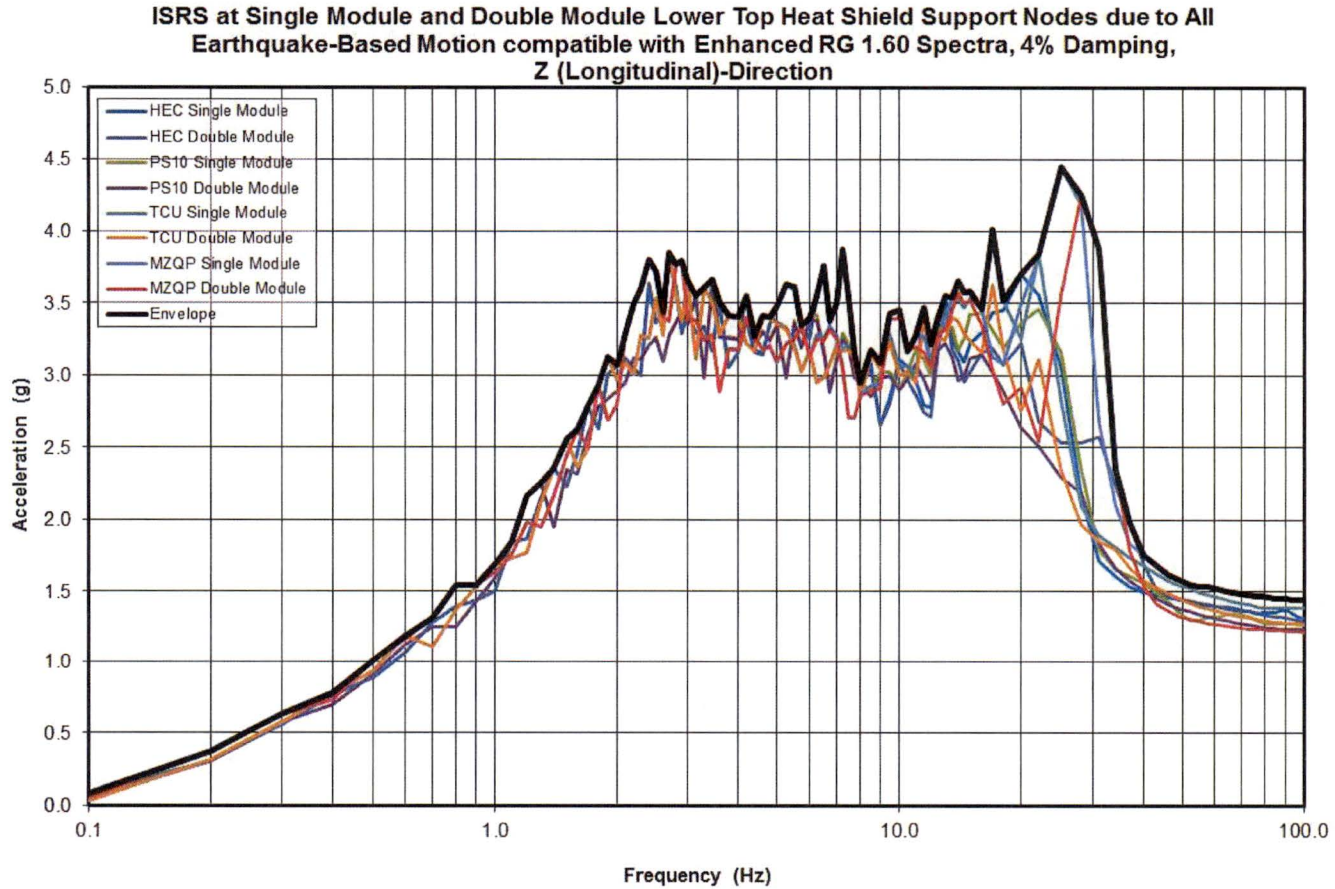

Figure A.3.9.4-13
Lower Top Heat Shield Support Node ISRS due to Envelope of Four Earthquake-Based Motions Compatible with Enhanced RG1.60 Spectra, 4% Damping, X-Direction

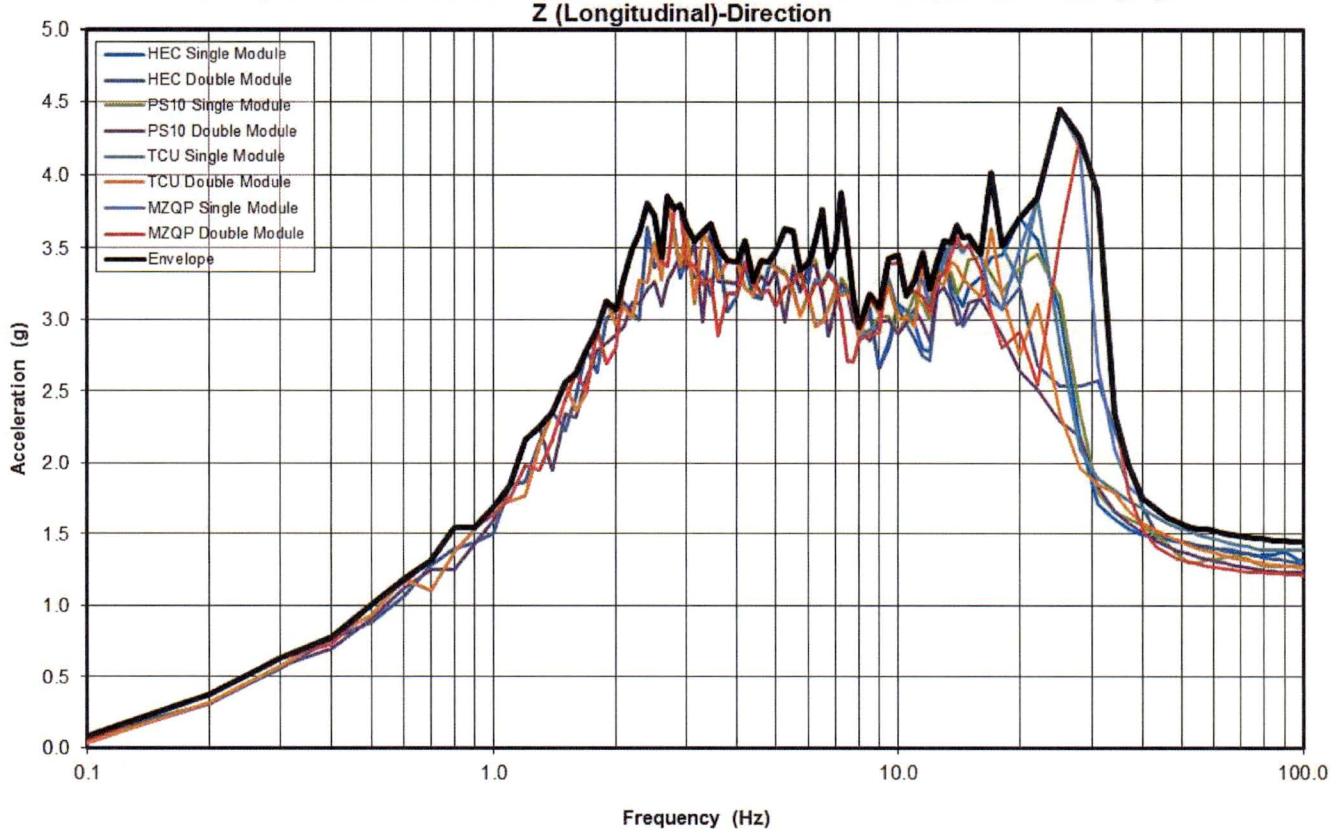

Figure A.3.9.4-14
Lower Top Heat Shield Support Node ISRS due to Envelope of Four Earthquake-Based Motions Compatible with Enhanced RG1.60 Spectra, 4% Damping, Y-Direction

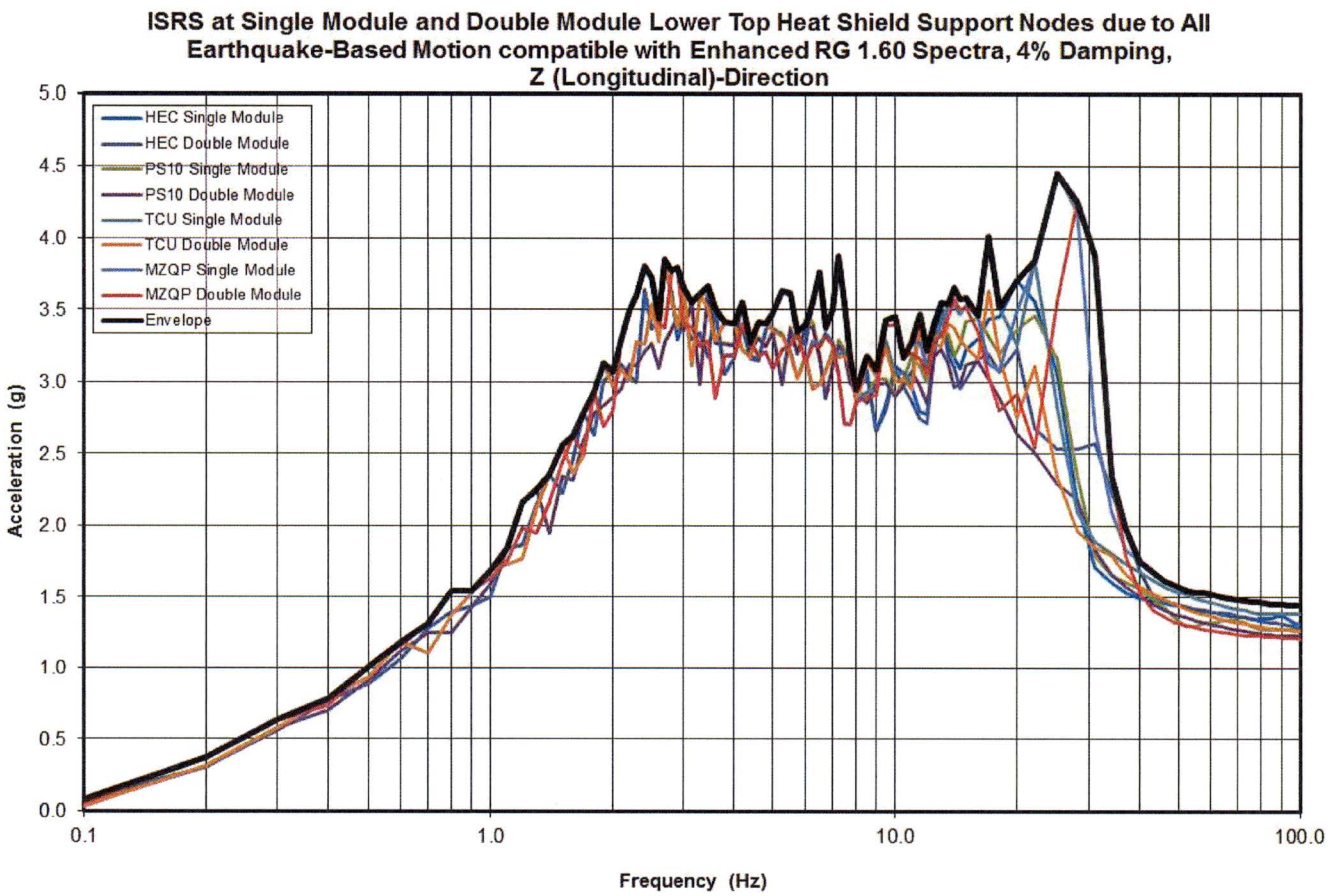

Figure A.3.9.4-15
Lower Top Heat Shield Support Node ISRS due to Envelope of Four Earthquake-Based Motions Compatible with Enhanced RG1.60 Spectra, 4% Damping, Z-Direction

A.3.9.7 NUHOMS® MATRIX STABILITY ANALYSIS

A.3.9.7.1 General Description

The system consists of the dual-purpose (transportation/storage) EOS-37PTH and EOS-89BTH DSCs, the HSM-MX and the onsite transfer cask (EOS-TC) with associated ancillary equipment. Each NUHOMS® MATRIX (HSM-MX) is designed to store DSCs containing up to either 37 pressurized water reactor (PWR) or 89 boiling water reactor (BWR) spent fuel assemblies (SFAs).

The HSM-MX is a staggered, two-tiered compartment, high density, high-heat rejection, storage overpack that provides a self-contained modular structure for storage of DSCs. The HSM-MX is constructed from reinforced concrete and structural steel. The thick concrete roof and walls of the HSM-MX provide substantial neutron and gamma shielding. The monolithic structure increases resistance to earthquakes and offers significant self-shielding. The NUHOMS® MATRIX retractable roller tray (MX-RRT) delivers the DSC from the transfer cask to the HSM-MX and places it on the DSC supports.

The HSM-MX storage modules can be arranged in both single row or back-to-back row arrays. *The HSM-MX assembly considered for the stability evaulaution is in a single row array, having three lower compartments and two upper compartments.*

A.3.9.7.1.1 HSM-MX Stability Evaluation

The sliding and overturning stability analyses due to design basis wind, flood, and massive missile impact loads are performed using hand calculations. A non-linear dynamic seismic stability analysis is performed using LS-DYNA [A.3.9.7-7].

A.3.9.7.1.2 Material Properties

The HSM-MX assembly is constructed of reinforced concrete and steel. The analyses consider rigid body motions. Therefore, the mechanical properties of the materials are not used as design inputs in the evaluations. The non-linear dynamic evaluation performed using LS-DYNA for the seismic loads, consists of simplified models of the HSM-MX and DSCs representative of their global masses and inertia properties.

A.3.9.7.1.3 Mass Properties

The mass properties of the HSM-MX are listed in Table A.3.9.7-1. Bounding values of concrete density (140 pcf) are considered for static analyses. Nominal concrete density of 150 pcf is considered for the non-linear dynamic seismic evaluation.

Where,

W_t = Total tornado load
W_w = Load from tornado wind effect
W_p = Load from tornado atmospheric pressure change effect
W_m = Load from tornado missile impact effect

Note that W_p is not applicable to the stability analysis as discussed in Section A.3.9.7.1.6. Thus, the load combination for tornado loading for this analysis is simplified to:

$$W_t = W_w + W_m$$

In addition, a 1.1 factor is added to Dead weight + Tornado load. (Table 3-3 of NUREG-1536 [A.3.9.7-3])

The envelope of a range of missiles from Chapter 2 is used for the missile impact load.

As shown in Table A.3.9.7-2, the automobile impact on to the HSM-MX has the maximum momentum and is considered as bounding evaluation.

A.3.9.7.1.7.3 Flood Input

The HSM-MX is evaluated for a flood height of 50 feet with a water velocity of 15 fps.

In addition, a 1.1 factor is added to Dead weight + Flood load (Table 3-3 of NUREG-1536 [A.3.9.7-3]).

A.3.9.7.2 HSM-MX Stability Analyses

The load categories associated with the HSM-MX stability analysis are described in the previous section. The analysis steps and results for each load category are presented in this section.

A.3.9.7.2.1 Design Basis Tornado Wind and Missile Loads

The HSM-MX is evaluated for forces created by drag as air impinges and flows past the HSM-MX with a maximum tornado wind speed of 360 mph.

For sliding and overturning analysis, it is assumed that the module is subjected to the load due to 238 psf windward pressure load acting on the front wall. The leeward side of the same module is subjected to a wind suction load of 167 psf. A suction of 355 psf is applied to the roof. These loads are shown in Table A.3.9.7-3.

In addition, missiles loads are combined with the tornado wind load per NUREG-800 [A.3.9.7-1] and NUREG-1536 [A.3.9.7-3].

Static Overturning Analysis due to Tornado Wind

The empty HSM-MX will rotate about B, shown in Figure A.3.9.7-1.

In the overturning analysis of the HSM-MX, the effects of tornado wind forces are first determined. An overturning moment is then calculated and is compared with a stabilizing moment. The safety factor against overturning computed for the HSM-MX due to tornado wind is *3.28*, which includes a factor of 1.1

Dynamic Overturning Analysis of Tornado Wind Concurrent with Massive Missile Impact Loading

A dynamic analysis based on the conservation of energy is conducted for the combined effects of wind and concurrent massive missile impact loading. The effects of the concurrent massive missile impact loads are used in determining the initial angular momentum from the conservation of angular momentum equation using the wind loads from the previous section. Then the angle of rotation is determined from the conservation of energy of the concurrent loading.

The wind loads are calculated conservatively for HSM-MX single array:

Horizontal $F_{hw} = (P_{windward} + P_{leeward})(L_{base})(h_{HSM})$

Vertical: $F_{vw} = (P_{roof})(L_{base})(w_{HSM})$

The concurrent wind loading is accounted for by reducing the inertia that resists motion in the denominator of the equation.

$$\omega_B = \frac{m_m \cdot d_m \cdot v_i}{m_m \cdot d_m^2 + I_{tot} - \left(\frac{F_{hw}}{g}\right)\left(\frac{h}{2}\right)^2 - \left(\frac{F_{vw}}{g}\right)\left(\frac{w}{2}\right)^2}$$

Where,

F_{hw} = Horizontal tornado wind load
F_{vw} = Vertical tornado wind load
ω_B = Angle of rotation
m_m = Mass of the missile
d_m = Distance from missile impact to floor
v_i = Initial missile velocity
I_{tot} = Total moment of inertia of HSM-MX
h = Height of HSM-MX
w = Width of HSM-MX

The conservation of energy is used for overturning.

Rotational Kinetic Energy = Change in Potential Energy – Work Done by Horizontal Wind force

$$\frac{I_{tot}\omega_B^2}{2} = (W - F_{vw}) \cdot r \cdot [\sin(\beta + \theta) - sin\beta] - F_{hw} \cdot r \cdot [\cos(\beta + \theta) - cos\beta]$$

Where,

θ = Angle of tipping
β = Angle from the horizontal to center of gravity (CG) of HSM-MX (*52.1°*)
r = Diagonal distance from CG to point B
I_{tot} = Total moment of Inertia of HSM-MX
W = Weight of the empty HSM-MX

The HSM-MX is stable against overturning as tip-over does not occur until the CG rotates past the edge (point B, Figure A.3.9.7-1) of the HSM-MX to an angle of more than 90°- *52.1°* = *37.9°*. *The* HSM-MX rotates a maximum of *0.000029* degrees, which includes a factor of 1.1 and is less than the *37.9* degrees required to overturn the module.

Time-Dependent Overturning Analysis of Tornado Wind Concurrent with Massive Missile Impact Loading

In addition to the dynamic overturning analysis, a time dependent analysis is used to ensure the absence of any overturning.

An approximate relationship for the deceleration of an automobile impacting a rigid wall is given by:

$$-\ddot{x} = 12.5g \cdot x \quad \text{Eq. D-1 of [A. 3.9.7-4]}$$

where,

$-\ddot{x}$ = *Deceleration (ft/sec^2)*
x = Distance automobile crushes into target (ft)

A force time history is obtained:

$$F = 0.625 V_s W_m sin20t \qquad Eq.\ D-6 \text{ of } [A.\ 3.9.7-4]$$

The overturning moment is:

$$M_{ot} = F \cdot d_m + \frac{F_{hw} h}{2}$$

Where,

d_m = Distance from missile impact to floor
h = Vertical height to the top of HSM-MX and is a function of rotation

The stabilizing moment is:

$$M_{st} = (W_{HSM} - F_{vw}) \cdot r cos(\beta + \theta)$$

Where,

W_{HSM}	=	Weight of the loaded HSM-MX
r	=	Diagonal distance from CG to point B
θ	=	Angle of rotation

The moment causing acceleration is:

$$M_{acc} = M_{ot} - M_{st}$$

The angular velocity is:

$$\omega_i = \left[\frac{M_{acc,i} + M_{acc,i-1}}{2} \cdot (t_i - t_{i-1})\right] / I_{tot} + \omega_{i-1}$$

Where,

i	=	Index for current time step
i-1	=	Index for previous time step
I_{tot}	=	Total moment of Inertia of HSM-MX

The angle of rotation is:

$$\theta_i = \left[\frac{\omega_i + \omega_{i-1}}{2} \cdot (t_i - t_{i-1})\right] + \theta_{i-1}$$

The angle of rotation is zero as the overturning moment due to missile impact and wind loading is less than the resisting moment.

Sliding Analysis for Tornado Wind Concurrent with Massive Missile Impact loading

The combined wind + missile impact case is considered for HSM-MX sliding analysis based on the conservation of energy.

First, the conservation of momentum is used for the sliding analysis.

$$V = \frac{m \cdot v_i}{M + m - F_{hw}/386.4}$$

Where,

V	=	Initial linear velocity of module after impact
v_i	=	Initial velocity of missile
m	=	Mass of the missile
M	=	Mass of the HSM-MX

Then using the conservation of energy:

$$Friction\ Energy = Initial\ Kinetic\ Energy\ of\ System + Work\ done\ by\ Wind$$

$$\mu \cdot (gM - F_{vw})d = \frac{(M+m)\cdot V^2}{2} + F_{hw}d$$

Where,

- μ = 0.6 coefficient of friction for concrete-to-concrete surfaces
- F_{vw} = Uplift force generated by DBT wind pressure on the roof
- d = Sliding distance of HSM-MX
- F_{hw} = Sliding force generated by DBT wind pressure

The sliding distance of the HSM-MX module is calculated to be *0.15* inches, which includes a factor of 1.1.

Time-Dependent Sliding Analysis for Tornado Wind Concurrent with Massive Impact Loading

In addition to the dynamic sliding analysis, a time dependent analysis is used to provide a bounding sliding displacement.

The total force causing sliding is:

$$F_{slide} = F + F_{hw}$$

The resisting force from friction is:

$$F_{resis} = \mu(W - F_{vw})$$

Therefore the force causing acceleration is:

$$F_{acc} = F_{slide} - F_{resis}$$

The velocity is:

$$v_i = \left[\frac{F_{acc,i} + F_{acc,i-1}}{2} \cdot (t_i - t_{i-1})\right] / m_{tot} + v_{i-1}$$

Where,

- i = Index for current time step
- i-1 = Index for previous time step
- m_{tot} = Total mass of empty HSM-MX

The sliding displacement is:

$$x_i = \left[\frac{v_i + v_{i-1}}{2} \cdot (t_i - t_{i-1})\right] + x_{i-1}$$

The sliding displacement is zero as the sliding force due to missile impact and wind loading is less than the resisting force.

A.3.9.7.2.2 Flood Loads

The HSM-MX is designed for a flood height of 50 feet and water velocity of 15 fps. The module is evaluated for the effects of a water current of 15 fps impinging on the side of a submerged HSM-MX. Under 50 feet of water, the inside of the module is rapidly filled with water. Therefore, the HSM-MX components are not evaluated for the 50 feet static head of water.

Calculation of the drag pressure due to design flood is shown in Appendix A.3.9.4.9.3.

Overturning Analysis

The factor of safety against overturning of an empty HSM-MX, for the postulated flooding conditions, is calculated by summing moments about the bottom outside corner of a single array HSM-MX. The factor of safety against overturning of the HSM-MX due to the postulated design basis flood water velocity is *1.98* inches, which includes a factor of 1.1.

Sliding Analysis

The factor of safety against sliding of a freestanding single array HSM-MX due to the maximum postulated flood water velocity of 15 fps is calculated using methods similar to those described above. The effective weight of the HSM-MX acting vertically downward, less the effects of buoyancy acting vertically upward is calculated. The factor of safety against sliding for a single array HSM-MX due to the postulated design basis flood water velocity is *1.42* inches, which includes a factor of 1.1.

A.3.9.7.2.3 Seismic Loads

The static sliding and overturning analysis for the seismic loads are performed to determine the maximum seismic accelerations before HSM-MX starts sliding or overturning. Non-linear dynamic analysis is performed using LS-DYNA for the earthquake inputs discussed in A.3.9.7.1.7.1 to determine the maximum sliding and overturning distances.

A.3.9.7.2.3.1 Low Seismic Load

HSM-MX static overturning analysis

The stabilizing moment due to the components dead weight and the overturning moment due to the seismic forces are calculated and compared. The 1.1 coefficient of the load combination (Table 3-3 of NUREG-1536 [A.3.9.7-3]) is conservatively applied to the overturning moment only. Both the maximum HSM-MX concrete density (160 pcf) with maximum DSC weight (to maximize the overturning moment) and minimum HSM-MX concrete density (140 pcf) with minimum DSC weight (to minimize the stabilizing moment) are considered. The overturning analysis is done considering the smallest distance from the HSM-MX center of gravity to HSM-MX corner point B (Figure A.3.9.7-1).

Table A.3.9.7-5 shows the results. The safety factor $M_{st}/1.1M_{ot}$ is less than 1, meaning the HSM-MX can have some lifting under the seismic loads. The non-linear dynamic analyses (Section A.3.9.7.2.3.2) estimate the amount of lifting for high seismic loads.

The maximum acceptable accelerations before any lifting occurs are $a_v = 0.40$g and $a_h = 0.60$g (assuming $a_v = \frac{2}{3}a_h$)

HSM-MX static sliding analysis

The resisting friction force and horizontal seismic force are calculated and compared. The 1.1 coefficient of the load combination (Table 3-3 of NUREG-1536 [A.3.9.7-3]) is conservatively applied to the horizontal seismic force only.

Resisting friction force: $F_{fr} = \mu W(1 - 0.4a_v)$ $\mu: Coefficient\ of\ friction$

Horizontal seismic force: $F_{hs} = a_h W$

Safety factor: $SF = F_{fr}/1.1F_{hs} = \mu(1 - 0.4a_v)/(1.1a_h)$

For static sliding analysis of the HSM-MX, the safety factor is independent of the weight considered. It only depends on the coefficient of friction and accelerations.

Table A.3.9.7-5 shows the results for a nominal coefficient of friction of 0.6 and gives a safety factor of 0.44. The HSM-MX will slide under 0.85g horizontal and 0.80g vertical loads. The non-linear dynamic analyses (Section A.3.9.7.2.3.2) estimate the amount of sliding for high seismic loads.

The maximum acceptable accelerations before any sliding occurs are $a_v = 0.32$g and $a_h = 0.48$g (assuming $a_v = \frac{2}{3}a_h$)

A.3.9.7.2.3.2 High Seismic Load

Non-Linear Dynamic Time-History Analyses of HSM-MX for High Seismic Loads

LS-DYNA Finite Element Model HSM-MX

A finite element model (FEM) of the HSM-MX monolithic expansion single array design loaded with five DSCs was created for use with LS-DYNA [A.3.9.7-7]. The HSM-MX unit and DSC are constructed with solid 4-node tetrahedral elements for meshing simplicity, whereas the IFSFI pad includes 8-node solids elements. All components are modeled with rigid materials for the stability analysis. The FEM includes the DSC axial retainers modeled with 0.5 inch gap to the DSC, the front and rear DSC supports with stop plates and five front doors and top vent covers.

The model does not include the metallic components (heat shields, etc.) which are not structurally important for the stability analysis. Their weight is accounted for in the total weight of the HSM-MX.

The HSM-MX rests on top of the ISFSI concrete pad and is free to slide or rock when subjected to the forces resulting from the prescribed pad seismic accelerations. In the FEM, contacts are defined between the HSM-MX and the ISFSI pad as well as between the DSCs with their front and rear DSC supports and parts of the HSM-MX concrete that could be in contact with the DSCs if they lift from their supports. Contact definitions are included between all interfacing parts using contacts algorithm in LS-DYNA.

Contacts are defined for the following interfaces:

- HSM-MX to basemat, no initial gap
- DSC to for supports, no initial gap
- DSC to rear stop plate, no initial gap
- DSC to HSM-MX front circular opening, initial 1.5" gap between DSC Ø75.5" and the door opening Ø78.5"
- DSC to front axial retainer, initial gap of 0.5"

Coefficient of Restitution

The coefficient of restitution is defined as the ratio of the velocity of a body immediately after impact to its velocity immediately prior to impact. A coefficient of restitution equal to 0 means a perfectly plastic impact in which the impacting body "sticks" to the impacted body. A coefficient of restitution equal to 1 means a perfectly elastic impact in which the impacting body bounces off the impacted body with no energy loss. For the case of concrete impacting against concrete, a reasonable coefficient of restitution is in the order of 0.1 since a concrete body does not "bounce" upon impacting on a concrete surface. For the LS-DYNA analyses, a coefficient of restitution of at least 0.8 is used as a conservative value. The coefficient of restitution is inputted into LS-DYNA analyses as the parameter viscous damping coefficient ((VDC) in percent of critical) of the surface-to-surface contact.

Non-Linear Dynamic Analyses

The seismic analyses inputs as described in Section A.3.9.7.1.7.1 consist of three components of acceleration in the form of earthquake time histories applied to the ISFSI pad. Thus, all nodal points of the pad move as prescribed by these input motions. Examples of the *input motion displacement, velocity and acceleration histories used in LS-DYNA analysis are shown* in Figure A.3.9.7-13, Figure A.3.9.7-14 and Figure A.3.9.7-15 *in the global X, Y, and Z directions, respectively, for the motion derived from the Hector Mine (HEC) earthquake.* The three components of the acceleration time histories are applied simultaneously in each of the three orthogonal directions. Each of the seven time history sets are analyzed with three different coefficients of friction (0.4, 0.6, and 0.8) for a total of 21 computer runs.

In order to obtain the sliding displacement of the HSM-MX relative to the pad, the change in X-lengths and change in Z-lengths (Figure A.3.9.7-4) between the four HSM-MX corner nodes and one ISFSI pad node are plotted over time.

Two uplift values are reported, one each for rotation about the global X and Z axes. For rocking about the X-axis, the change in the vertical (global Y) distance between the +Z and –Z node pairs is plotted and tabulated. For rocking about the Z axis, the change in the vertical distance between the +X and –X node pairs is plotted and tabulated.

The gaps between the DSCs and front axial retainers are verified against the DSC sliding on the support. Also, the loads on the DSC supports are verified against the uplift.

The maximum values over time for sliding and rocking movements from the seven time histories are used to get the "computed" response as the median value plus 1 standard deviation (shown in Table A.3.9.7-6). This methodology is in accordance with NUREG/CR-6865 [A.3.9.7-6]

A.3.9.7.2.4 Results

Table A.3.9.7-4 through Table A.3.9.7-6 show a summary of the results from the analyses performed in Section A.3.9.7.2.

For flood, wind, and missile impact, it is determined that the uplift and sliding values are small for the HSM-MX. Therefore, the DSC remains stable on the front and rear DSC supports inside the HSM-MX.

The maximum seismic acceleration before HSM-MX sliding or overturning occurs are 0.48g horizontal and 0.32g vertical for a coefficient friction of 0.6 between the HSM-MX and the ISFSI pad. The non-linear dynamic analysis shows a maximum resultant sliding of 12.5 inches and a maximum uplift of *0.13* inches for the set of seismic earthquake inputs.

A.3.9.7.4 References

A.3.9.7-1 NUREG-0800, Standard Review Plan, "Missiles Generated by Natural Phenomena," Revision 2, U.S. Nuclear Regulatory Commission, July 1981.

A.3.9.7-2 American Society of Civil Engineers, ASCE 7-10, "Minimum Design Loads for Buildings and Other Structures."

A.3.9.7-3 NUREG-1536 Revision 1, "Standard Review Plan for Spent Fuel Dry Storage Systems at a General License Facility," July 2010, U.S. Nuclear Regulatory Commission.

A.3.9.7-4 Bechtel Report BC-TOP-9A Rev. 2, "Topical Report – Design of Structures for Missile Impact," September 1974.

A.3.9.7-5 NUREG/CR-6728, "Technical Basis for Revision of Regulatory Guidance on Design Ground Motions: Hazard- and Risk-consistent Ground Motion Spectra Guidelines," October 2001, Prepared by Risk Engineering, Inc. for U.S. Nuclear Regulatory Commission.

A.3.9.7-6 NUREG/CR-6865, "Parametric Evaluation of Seismic Behavior of Freestanding Spent Fuel Dry Cask Storage Systems," February 2005, U.S. Nuclear Regulatory Commission.

U. S. Nuclear Regulatory Commission, Regulatory Guide 1.76, "Design Basis Tornado for Nuclear Power Plants," Revision 1, March 2007.

A.3.9.7-7 LS-DYNA Version 7.0.0, Rev. 79055, Livermore Software Technology Corporation (LSTC).

A.3.9.7-8 NRC Regulatory Guide 1.60, "Design Response Spectra for Seismic Design of Nuclear Power Plants," Rev. 1, December 1973.

A.3.9.7-9 U.S. Nuclear Regulatory Commission, Regulatory Guide 1.76, "Design Basis Tornado and Tornado Missiles for Nuclear Power Plants," Rev. 1, March 2007.

Table A.3.9.7-1
Sizes and Weight for Various HSM-MX Models

HSM-MX Module	Total Length of HSM-MX (in.)	Nominal Weight of Empty HSM-MX (kips)[1]
HSM-MX Single Array	277	*2.355*
HSM-MX Double Array	496	*3,945*

Notes:

(1) The nominal weights for the HSM-MX are based on concrete density of 150 pcf.

Table A.3.9.7-2
Missile Load Data for HSM-MX Stability Analysis

Missile	Mass (lbs.)	Dimensions	Velocity (fps)	Momentum (lbs-fps)
Utility Wooden Pole	1,124	13.5" Diameter 35' Long	180	202,320
Armor Piercing Artillery Shell	276	8" Diameter	185	51,060
Steel Pipe	750	12" Sch. 40 15' Long	154	115,500
Automobile	4,000	20 ft^2 Contact Area	195	780,000

Table A.3.9.7-3
Design Pressures for Tornado Wind Loading of HSM-MX

Wall Orientation[1]	Velocity Pressure (psf)	Ext. Pressure Coefficient [2]	Int. Pressure Coefficient [3]	Max/Min Design Pressure (psf) [4]
Front	276.4	0.680	± 0.18	237.7
Left	276.4	-0.595		-214.2
Rear[5]	276.4	-0.425		-167.2
Right	276.4	-0.595		-214.2
Top	276.4	-1.105		-355.2

Notes:

(1) Wind direction assumed to be from front. Wind loads from other directions may be found by rotating above table values to desired wind direction.

(2) These values are calculated using the external pressure coefficients from Figure 27.4-1 of [A.3.9.7-2] times the gust effect factor (0.85) from Section 26.9 of [A.3.9.7-2]

(3) Internal pressure coefficient taken from Table 26.11-1 of [A.3.9.7-2]

(4) These values are computed based on Equation 27.4-1 of [A.3.9.7-2]

(5) The bounding C_p of -0.5 from an L/B ratio of 0-1 is used for wind in all directions from Figure 27.4-1 of [A.3.9.7-2]

Table A.3.9.7-4
Summary of HSM-MX Sliding and Stability Results

Loading	Tornado Wind + Missile[1]		Flood	
Result	Maximum Sliding Distance (in)	Maximum Rocking Uplift (°)	Safety Factor against Sliding	Safety Factor against Tipping
HSM-MX Single Array	*0.15*	*0.000029*	*1.42*	*1.98*

Notes:

(1) 1.1 Factor Included.

Table A.3.9.7-5
Static analysis, Overturning and Sliding of the HSM-MX

	Concrete Density [pcf]		140	160
Overturning	Overturning Moment [in.kips]		*463,757*	*523,739*
	Stabilizing Moment [in.kips]		*344,115*	*383,056*
	Safety Factor[1]		*0.67*	*0.66*
	Max accelerations before overturning	$a_v = {}^2/_3\, a_h$	*0.41*	*0.40*
		a_h	*0.61*	*0.60*
Sliding	Horizontal Seismic Force [kips]		*2126*	*2408*
	Resisting Friction Force[3] [kips]		*1021*	*1156*
	Safety Factor[2]		0.44	
	Max accelerations before sliding	$a_v = {}^2/_3\, a_h$	0.32	
		a_h	0.48	

Notes:

(1) $SF=M_{st}/1.1M_{ot}$

(2) $SF=F_{fr}/1.1F_{hs}$

(3) Nominal Coefficient of friction 0.6

Table A.3.9.7-6
Summary of Displacement of HSM-MX relative to the ISFSI pad for nominal concrete density (150 pcf)

Earthquake	Coefficient of Friction	X-Displ. [in][2]	Z-Displ. [in][2]	Resultant [in][1]	X-Rocking [in]	Z-Rocking [in]
1. HEC	0.4	7.29	3.53	7.61	0.00	0.00
	0.6	2.45	2.08	2.55	0.00	0.02
	0.8	1.59	1.11	1.65	0.01	0.06
2. LCN	0.4	6.79	7.99	9.11	0.00	0.00
	0.6	3.83	5.52	6.65	0.00	0.02
	0.8	2.66	3.12	3.94	0.02	0.13
3. PS10	0.4	9.32	6.76	10.75	0.00	0.00
	0.6	5.13	3.36	6.12	0.00	0.07
	0.8	2.69	1.12	2.91	0.01	0.14
4. TAB	0.4	9.84	7.00	11.51	0.00	0.00
	0.6	5.39	3.78	6.48	0.00	0.02
	0.8	1.98	1.13	2.22	0.01	0.05
5. TCU	0.4	9.14	4.22	9.52	0.00	0.00
	0.6	3.73	1.40	3.77	0.00	0.02
	0.8	1.51	0.51	1.53	0.01	0.07
6. SHIF	0.4	8.49	9.57	12.77	0.00	0.00
	0.6	3.69	7.74	8.57	0.00	0.02
	0.8	2.35	4.63	5.19	0.01	0.10
7. MIAN	0.4	5.13	11.47	11.51	0.00	0.00
	0.6	3.19	7.69	8.11	0.00	0.02
	0.8	1.91	4.54	4.84	0.02	0.11
Maximum	0.4	9.84	11.47	12.77	0.00	0.00
	0.6	5.39	7.74	8.57	0.00	0.07
	0.8	2.69	4.63	5.19	0.02	0.14
Average	0.4	8.00	7.22	10.40	0.00	0.00
	0.6	3.92	4.51	6.04	0.00	0.03
	0.8	2.10	2.31	3.18	0.01	0.09
Median	0.4	8.49	7.00	10.75	0.00	0.00
	0.6	3.73	3.78	6.48	0.00	0.02
	0.8	1.98	1.13	2.91	0.01	0.10
Median + σ	0.4	10.16	9.80	12.50	0.00	0.00
	0.6	4.77	6.33	8.66	0.00	0.04
	0.8	2.46	2.88	4.41	0.01	0.13

(1) The resultant displacement is the square root of the sum of the squares of the X- and Z-displacements over time. This is not the resultant of the maximum X- and Z-Displacements

(2) Absolute values are reported = max(abs(u(t)))

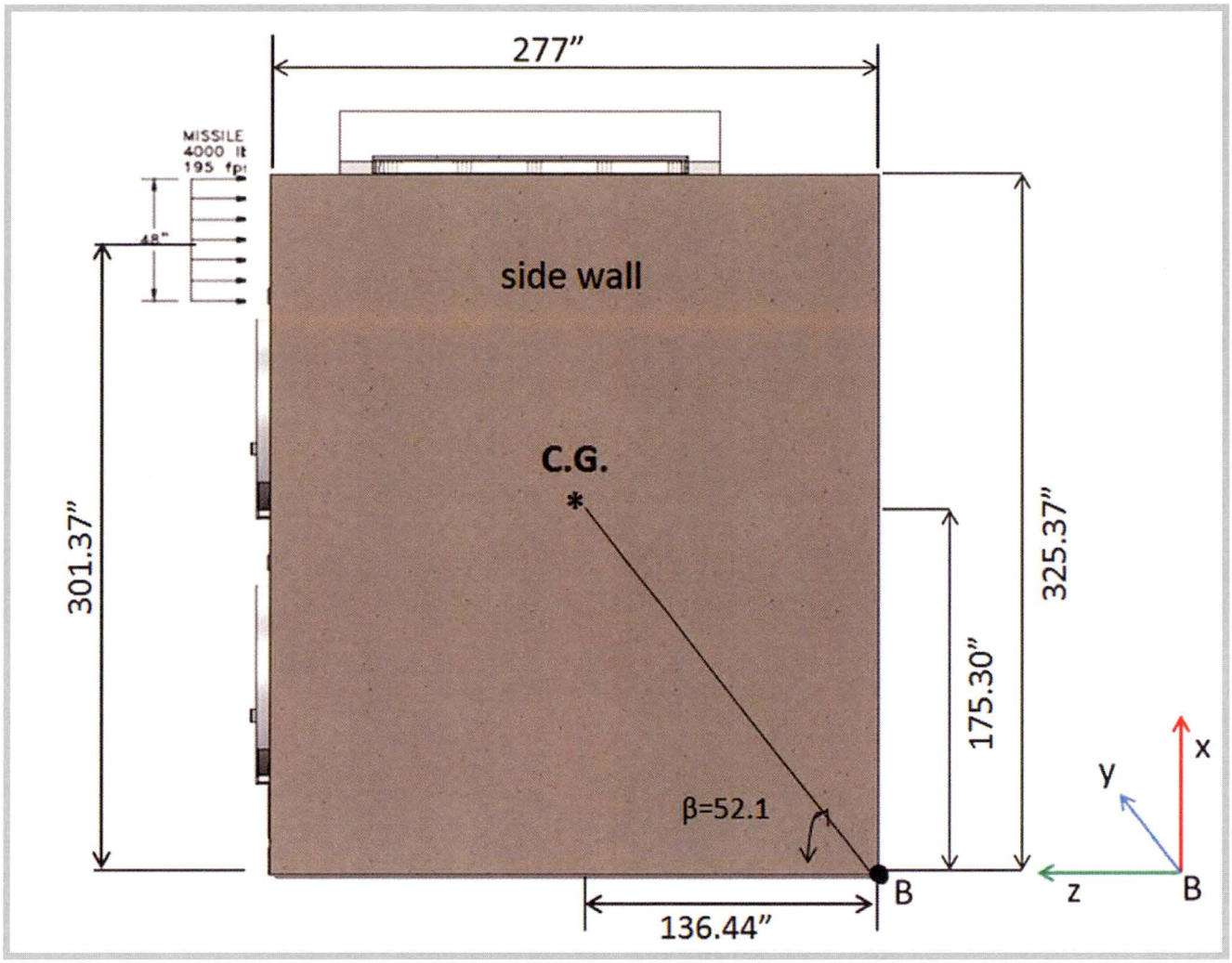

Figure A.3.9.7-1
HSM-MX Dimensions for Stability Analysis (Static)

Figure A.3.9.7-2
Not Used

Figure A.3.9.7-3
Not Used

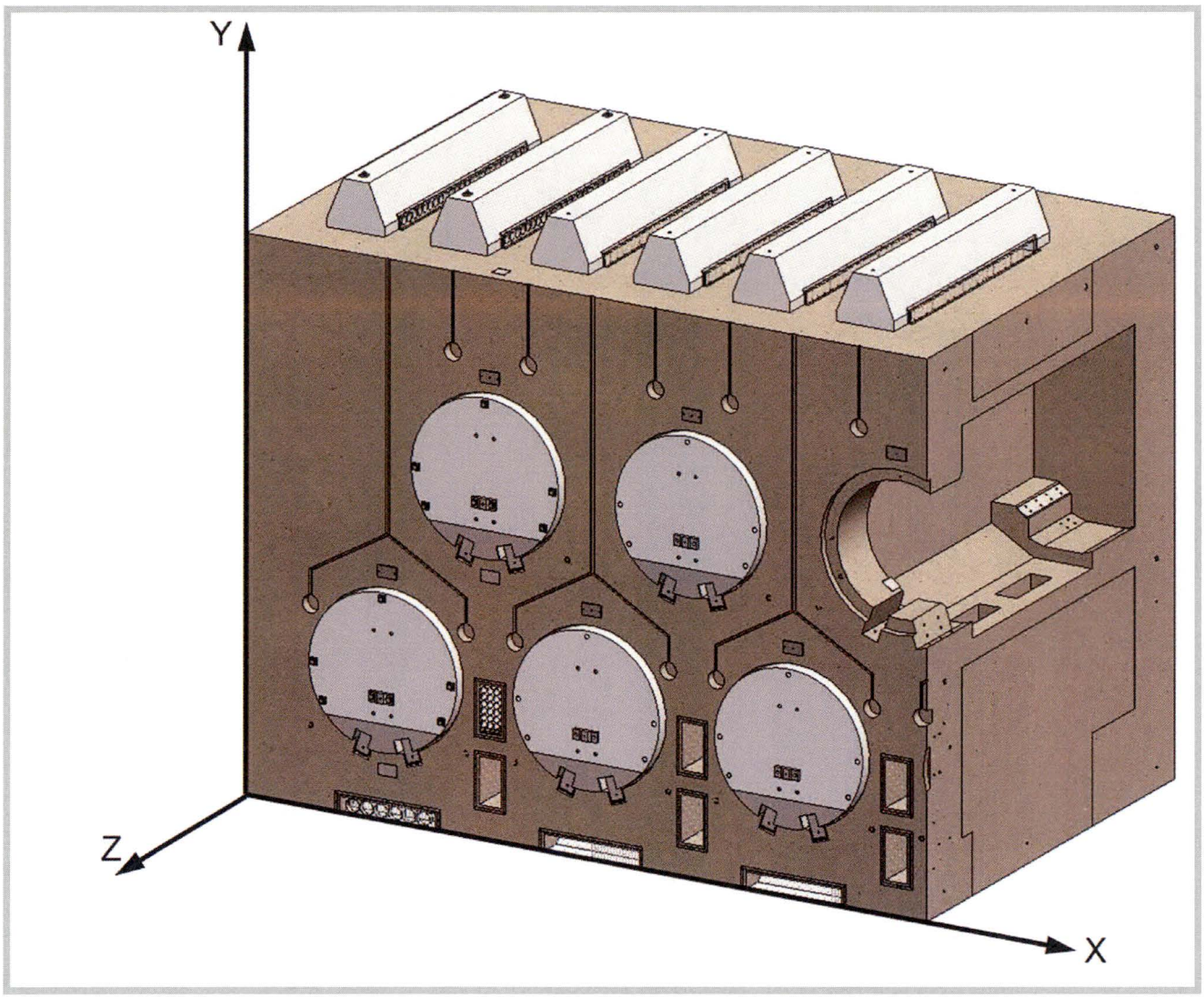

Figure A.3.9.7-4
HSM-MX Single Array Design with Five DSCs

Figure A.3.9.7-6
Not Used

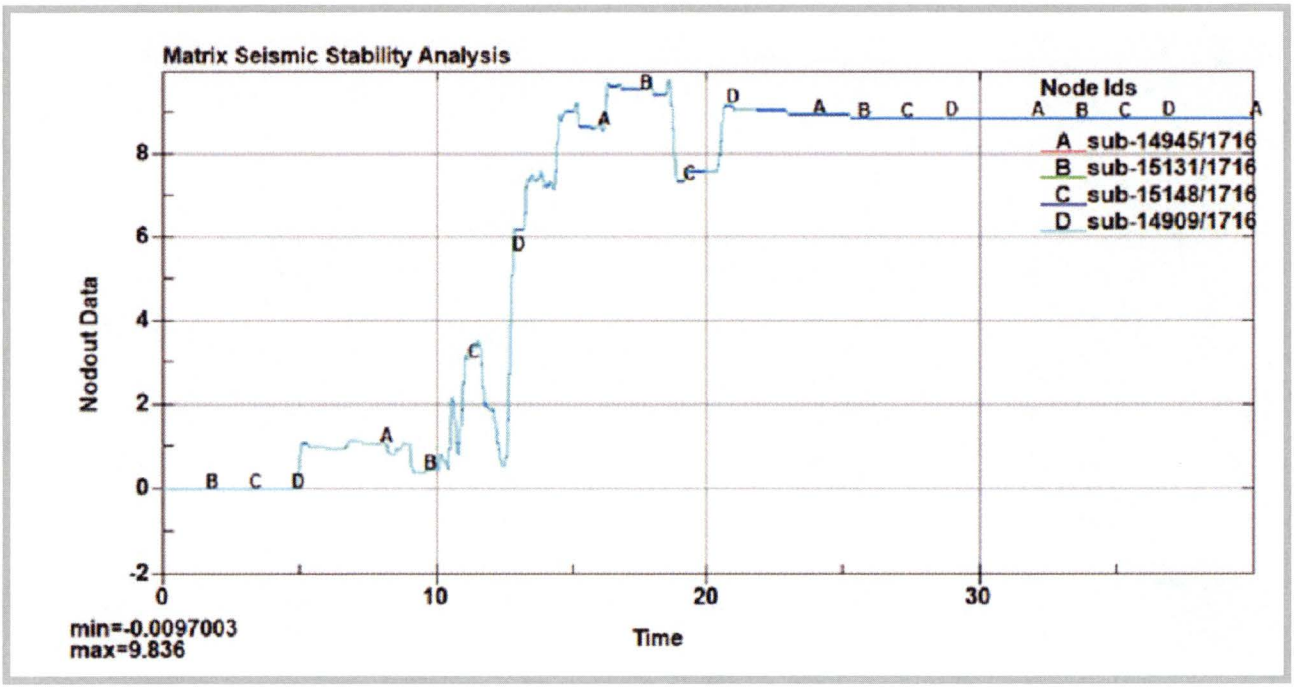

Figure A.3.9.7-7
***HSM-MX* Maximum X-Direction Sliding TAB, μ=0.4**

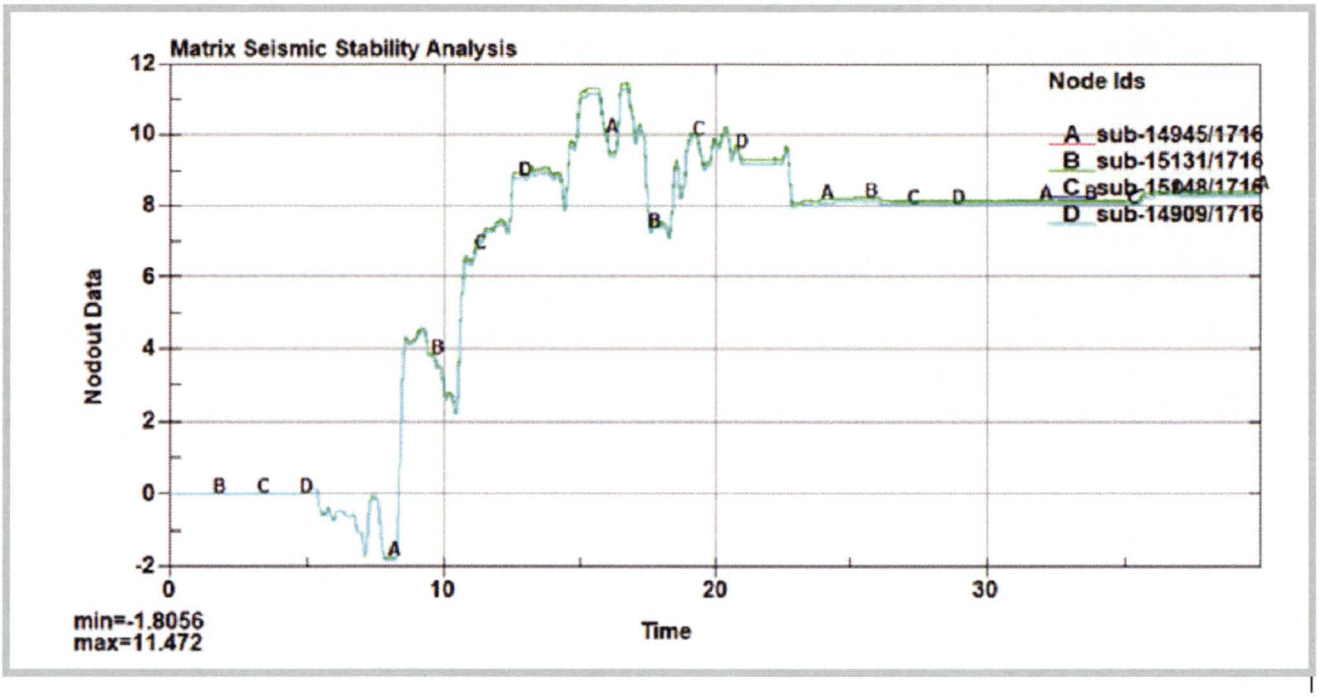

Figure A.3.9.7-8
***HSM-MX* Maximum Z-Direction Sliding MIAN, μ=0.4**

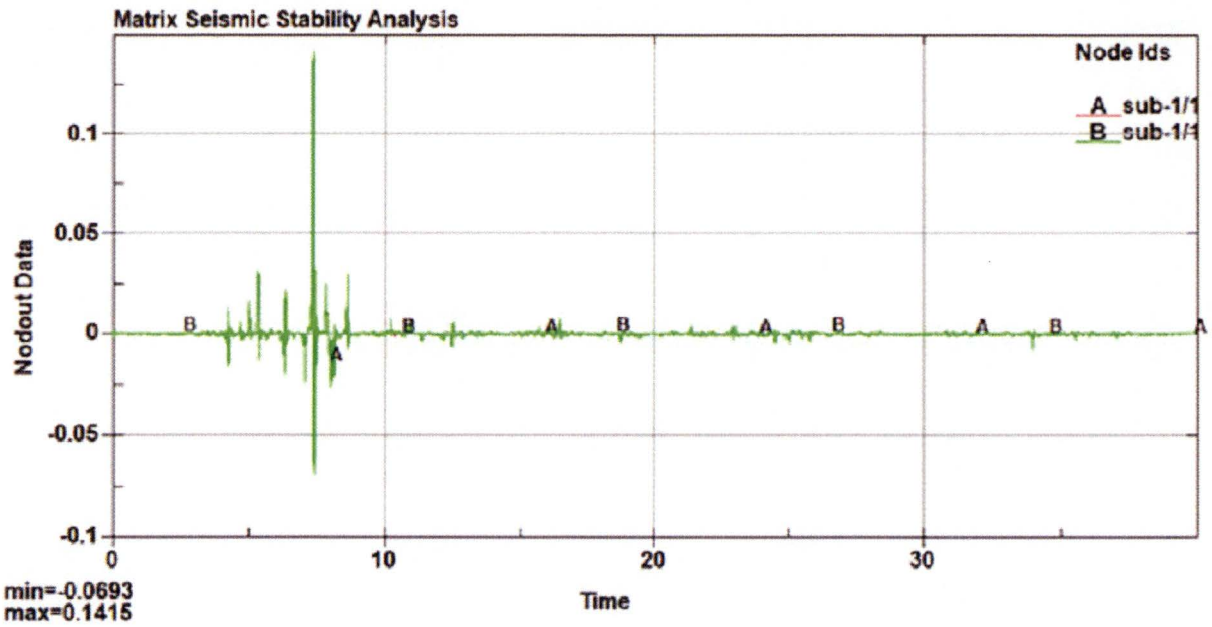

Figure A.3.9.7-9
***HSM-MX* Maximum Rocking *PS10*, μ=0.8**

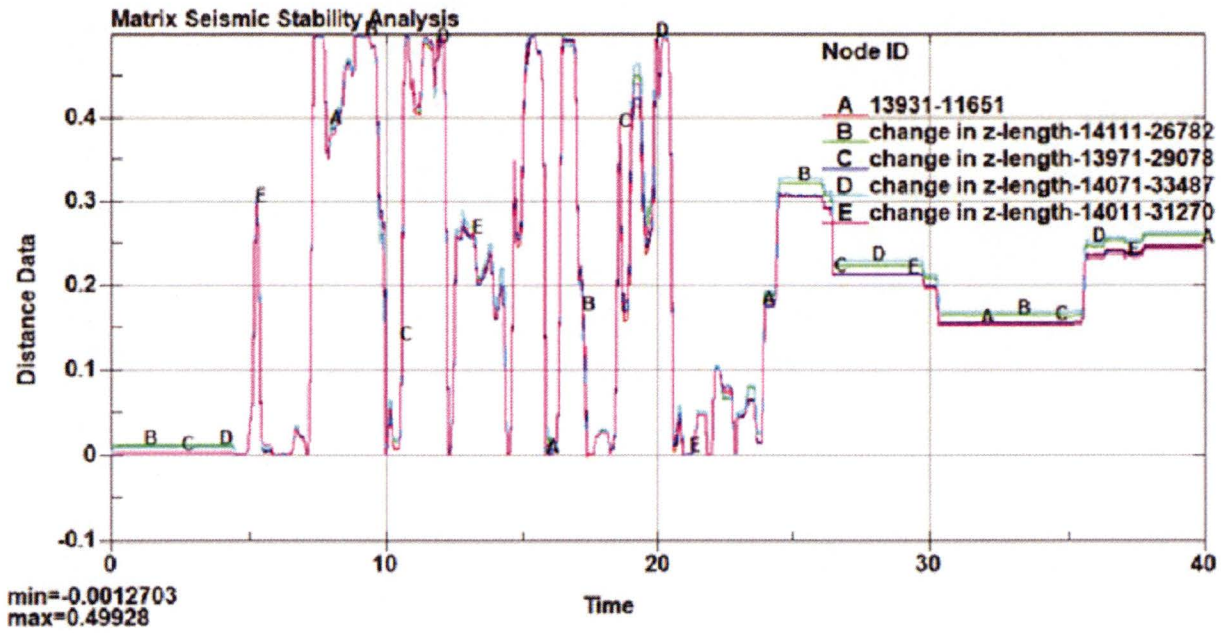

Figure A.3.9.7-10
DSC Sliding *on Supports during Max. HSM-MX Z-direction Sliding Case:* MIAN, μ=0.4

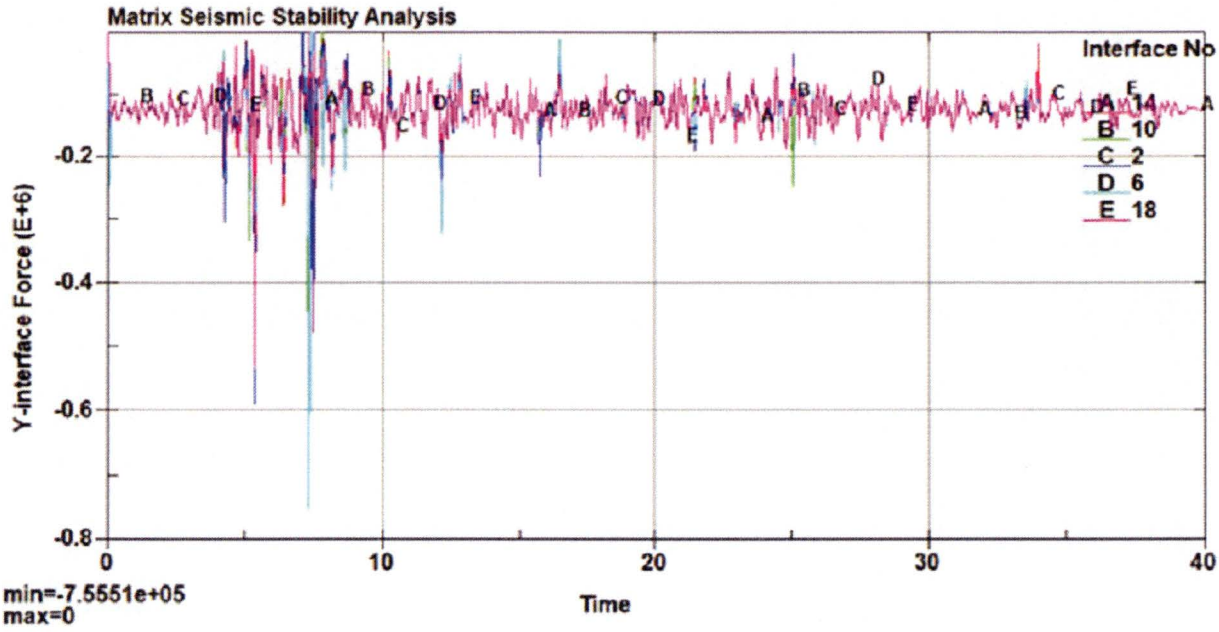

Figure A.3.9.7-11
DSC Load on Supports during Max. HSM-MX Z-Direction *Rocking* Case: *PS10*, μ=*0.8*

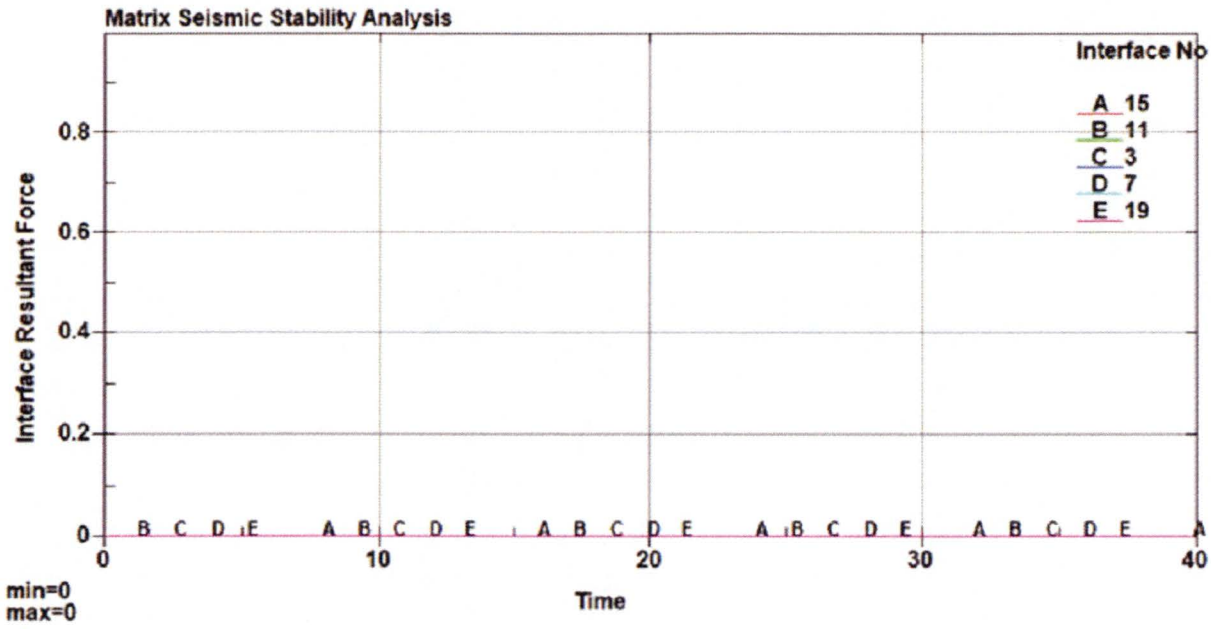

Figure A.3.9.7-12
DSC Load on Door Opening During Max. HSM-MX Z-Direction *Rocking*
Case: *PS10*, μ=*0.8*

A.4 THERMAL EVALUATION

The thermal evaluation described in this chapter is applicable to the NUHOMS® EOS System that includes EOS-37PTH or EOS-89BTH dry shielded canisters (DSCs) loaded inside the NUHOMS® MATRIX (HSM-MX).

A summary of the EOS-37PTH and EOS-89BTH DSC configurations analyzed in this chapter for storage operations in HSM-MX is shown in the Table in Chapter 4 and also below:

DSC Type	Basket Assembly Type	HLZC	Max. Heat Load (kW)	Transfer Cask	Storage Module
EOS-37PTH	4H	7	50.00	EOS-TC125/ EOS-TC135	HSM-MX
	4L/5	8(1)	46.40(2)		
	4L/5	9	37.80		
EOS-89BTH	3	3	34.44	EOS-TC125/ EOS-TC108	

Note:

(1) Basket Type 5 can only accommodate Intact FAs. Therefore, damaged or Failed FAs allowed per HLZC 8 shall only be loaded in Basket Type 4L.

(2) The maximum decay heat per DSC is limited to 41.8 kW when a damaged or failed FA is loaded

The various basket types within the EOS-37PTH DSC and EOS-89BTH DSC are described in Chapter 1, Section 1.1 and Appendix 4.9.6, Section 4.9.6.1.1.

Descriptions of the detailed analyses performed for normal, off-normal, and hypothetical accident conditions are provided in Section A.4.4 for storage operations. Transfer operations for the EOS-37PTH DSC with HLZCs 7 through 9 are presented in Section 4.9.6.2. Transfer operations for the EOS-89BTH DSC with HLZC 3 are presented in Section 4.5.6.

In order to accommodate lessons learned from the mockup development, the original HSM-MX design has been slightly revised for improved fabricability. Section A.4.5 evaluates the thermal performance of the updated HSM-MX with the EOS-37PTH and EOS-89BTH DSCs under the bounding normal, off-normal, and accident storage conditions.

A.4.4.3.4 Internal Pressure

Chapter 4, Section 4.7.1 calculates the maximum internal pressure of the EOS-37PTH DSC during storage in the EOS-HSM and transfer in EOS-TC125/135/108. For the EOS-37PTH DSC during storage in HSM-MX, the average gas temperature in the DSC cavity is computed using the same approach presented in Chapter 4, Section 4.7.1.2 and listed in Table A.4-7. As shown in Table A.4-7, the average helium temperatures determined for the EOS-37PTH DSC in HSM-MX with HLZC 7 are lower than the temperatures determined for HLZCs 1 through 3. Therefore, the maximum internal pressures in Chapter 4, Table 4-45 remain bounding for HLZC 7 under normal, off-normal, and accident storage conditions, respectively.

A.4.4.3.5 Impact of Design Changes

The original HSM-MX design has been slightly revised for improved fabricability as described in Section A.4.5.1. Detailed thermal evaluations for the storage in the updated HSM-MX are presented in Section A.4.5. This section evaluates the discrepancy of the original HSM-MX and the thermal model in Section A.4.4.2.2. The evaluation in this section is obsolete and no longer applicable.

Proprietary Information on This Page
Withheld Pursuant to 10 CFR 2.390

Proprietary Information on Pages A.4-27 through A.4-28
Withheld Pursuant to 10 CFR 2.390.

A.4.5.4 EOS-37PTH DSC with Basket Type 4H – Storage in Updated HSM-MX

A.4.5.4.1 Convergence of the CFD Model

A.4.5.4.2 Temperature Calculations

The maximum temperatures of fuel cladding and concrete of the updated HSM-MX loaded with the EOS-37PTH DSC for the bounding normal, off-normal, and accident storage conditions are summarized in Table A.4-16.

The maximum temperatures of various components of the HSM-MX loaded with the EOS-37PTH DSC for the bounding normal, off-normal, and accident storage conditions are summarized in Table A.4-17. The average temperatures of key components of the HSM-MX loaded with the EOS-37PTH DSC for the bounding normal, off-normal, and accident storage conditions are summarized in Table A.4-18.

Typical temperature plots for the key components in the HSM-MX loaded with the EOS-37PTH DSC are shown inFigure A.4-21, Figure A.4-22, andFigure A.4-23, respectively, for the bounding normal hot, off-normal hot, and accident conditions.

A.4.5.4.3 Airflow Calculations

The streamlines for the airflow inside the updated HSM-MX loaded with the EOS-37PTH DSC under normal hot storage condition are shown in Figure A.4-24. Cool air enters into the HSM-MX from the inlet, absorbs the heat from the EOS-37PTH DSC, and leaves the HSM-MX through the outlet with higher temperatures. Table A.4-20 summarizes the air temperatures and mass flow rates at the inlet and outlet for the normal and off-normal hot conditions of storage.

A.4.5.4.4 GCI Calculation

[

]

A.4.5.4.5 Internal Pressure

Chapter 4, Section 4.7.1 calculates the maximum internal pressure of the EOS-37PTH DSC during storage in the EOS-HSM and transfer in EOS-TC125/135/108. For the EOS-37PTH DSC during storage in the updated HSM-MX, the average gas temperature in the DSC cavity is computed using the same approach presented in Chapter 4, Section 4.7.1.2 and listed in Table A.4-21. As shown in Table A.4-21, the average helium temperatures determined for the EOS-37PTH DSC in the updated HSM-MX with HLZC 7 are lower than the temperatures determined for HLZCs 1 through 3. Therefore, the maximum internal pressures in Chapter 4, Table 4-45 remain bounding for HLZC 7 under normal, off-normal, and accident storage conditions, respectively.

See Encl. 4

A.4.5.5 EOS-37PTH DSC with Basket Type 4L/5 – Storage in Updated HSM-MX

This section presents the thermal evaluation of the EOS-37PTH DSC with Basket Type 4L/5 during storage operations in the updated HSM-MX. This section follows the same methodology as discussed in Section A.4.4.4. The only difference is the design changes that made to HSM-MX as discussed in Section A.4.5.1.

Same as Section A.4.4.4, this evaluation considers HLZC 8 with a maximum heat load of 46.4 kW and HLZC 9 with a maximum heat load of 37.8 kW. HLZCs 8 and 9 are discussed in Section A.4.4.4.

A.4.5.5.1 EOS-37PTH DSC and Basket Type 4L - Description of Load Cases for Storage

[

]

A.4.5.5.2 EOS-37PTH DSC with Basket Type 4L/5 - Thermal Model for Storage in HSM-MX

To evaluate the thermal performance of the EOS-37PTH DSC with Basket Type 4L/5 based on HLZCs 8 and 9 during storage operations in the updated HSM-MX, the thermal model from Section A.4.5.3 is modified to simulate LCs described in Section A.4.5.5.1. The modifications in the LCs described in Section A.4.5.5.1 are limited to the changes in material properties of the basket components as described in Appendix 4.9.6, Section 4.9.6.1.1, and heat generation rates based on the new HLZCs, but no changes are considered to the mesh.

A.4.5.5.3 EOS-37PTH DSC with Basket Type 4L/5 for HLZCs 8 and 9 –Storage Evaluation

Figure A.4-23and Figure A.4-24 present the maximum temperatures of fuel cladding and key components of the EOS-37PTH DSC with Basket Type 4L/5 loaded in the updated HSM-MX based on HLZCs 8 and 9 during storage operations.

Figure A.4-25 presents the average temperatures of fuel cladding and key components of the EOS-37PTH DSC with Basket Type 4L/5 loaded in the updated HSM-MX based on HLZCs 8 and 9 during storage operations.

Figure A.4-25 and Figure A.4-26 present the temperature profiles of key components in the HSM-MX loaded with the EOS-37PTH DSC for HLZCs 8 and 9, respectively.

Comparison with HLZC 7

Table A.4-26 presents a comparison of the maximum temperatures for HLZCs 8 and 9 with the bounding design basis values from HLZC 7. As shown in the comparison, the majority of the maximum component temperatures determined for HLZC 7 with 50 kW remain bounding for HLZCs 8 and 9. The maximum temperature of the heat shield in the upper compartment for HLZC 8 is slightly higher (2 °F) than that for HLZC 7.

Similar to the normal condition, the maximum temperatures during off-normal and accident storage conditions for HLZCs 8 or 9 will also remain bounded by HLZC 7. Therefore, no further evaluation is required for off-normal and accident storage condition with HLZCs 8 and 9.

Based on this discussion, all design criteria are satisfied for storage of the EOS-37PTH DSC with HLZCs 8 or 9 in the updated HSM-MX.

A.4.5.6 EOS-89BTH DSC with Basket Type 3 - Storage in Updated HSM-MX

[

]

Proprietary Information on Pages A.4-33 through A.4-36
Withheld Pursuant to 10 CFR 2.390.

A.4.6 References

A.4-1 NUREG-1536, "Standard Review Plan for Spent Fuel Dry Cask Storage Systems at a General License Facility," Revision 1, U.S. Nuclear Regulatory Commission, July 2010.

A.4-2 NUREG-2174, "Impact of Variation in Environmental Conditions on the Thermal Performance of Dry Storage Casks - Final Report," U.S. Nuclear Regulatory Commission, March 2016.

A.4-3 J.M. Cuta, U.P. Jenquin, and M.A. McKinnon, "Evaluation of Effect of Fuel Assembly Loading Patterns on Thermal and Shielding Performance of a Spent Fuel Storage/Transportation Cask," , PNNL-13583, Pacific Northwest National Laboratory, November 2001.

A.4-4 ACI 349-06, "Code Requirements for Nuclear Safety Related Concrete Structures" American Concrete Institute.

A.4-5 ANSYS FLUENT, ANSYS FLUENT Users Guide, Version 17.1, ANSYS, Inc.

A.4-6 ANSYS ICEM CFD, Version 17.1, ANSYS, Inc.

A.4-7 NUREG-2152, "Computational Fluid Dynamics Best Practice Guidelines for Dry Cask Applications," U.S. Nuclear Regulatory Commission, March 2013.

A.4-8 American Society of Mechanical Engineers, "Standard for Verification and Validation in Computational Fluid Dynamics and Heat Transfer," ASME V&V 20-2009, November 30th, 2009.

A.4-9 I. E. Idelchik, "Handbook of Hydraulic Resistance," 3rd Edition, Begell House, Inc., 1996.

A.4-10 A Zigh, J Solis, "Computational Fluid Dynamics Best Practice Guidelines in Analysis of Dry Storage Cask," WM2008 Conference, Phoenix, AZ, February 24-28, 2008.

A.4-11 ASHRAE Handbook, Fundamentals, SI Edition, American Society of Heating, Refrigerating and Air-Conditioning Engineers, Inc., 1997.

A.4-12 P. J. Roache, "Quantification of Uncertainty in Computational Fluid Dynamics," Annual Review of Fluid Mechanics, Vol. 29, 123-160, 1997.

A.4-13 CoC 1042 Appendix A, NUHOMS® EOS System Generic Technical Specifications, Amendment 1.

Table A.4-14
EOS-37PTH DSC in Updated HSM-MX, Design Load Cases for Storage Conditions with HLZC 7

Load Case	*Operating Condition*	*Description*	*Mesh*	*Ambient Temperature (°F)*
1e-S	*Normal*	[ ]	*Base*	*100 (1)*
1f-S			*Fine*	
2-S	*Off-Normal*		*Base*	*117 (1)*
3-S (2)	*Accident*		*Base*	*117 (1)*

Notes:

(1) Daily average temperatures are used as noted in Section A.4.3.

(2) Initial temperatures are taken from steady-state results of Load Case 2-S.

Proprietary Information on This Page
Withheld Pursuant to 10 CFR 2.390

Table A.4-16
Maximum Fuel Cladding and Concrete Temperatures for Storage Conditions of EOS-37PTH DSC in Updated HSM-MX with HLZC 7

Load Case *(1)*	*Description*	*Max Fuel Cladding Temperature (°F)*			*Concrete Temperature (°F)*	
		Upper Compartment	*Lower Compartment*	*Limit*	*Maximum*[4]	*Limit*
1e		*676*	*708*	*752*[2]	*264*	*300*[2]
1e-S		*680*	*704*		*261*	
		4	*-4*		*-3*	
2		*653*	*696*	*1058*[2]	*254*	
2-S		*648*	*685*		*245*	
		-5	*-11*		*-9*	
3		*724*	*777*		*362*	
3-S		*699*	*770*		*355*	*500*[3]
		-25	*-7*		*-7*	

Notes:

(1) See Table A.4-1 and Table A.4-14 for the description of the LCs.

(2) The temperature limits are from NUREG-1536 [A.4-1].

(3) The temperature limit for concrete at accident condition is 500 °F. The maximum concrete temperature for accident conditions is above the 350 °F limit given in ACI 349-06 [A.4-4]. Testing will be performed, as described in Chapter A.8, Section A.8.2.1.3.

Proprietary Information on Pages A.4-54 through A.4-58
Withheld Pursuant to 10 CFR 2.390.

Table A.4-23
Maximum Fuel Cladding and Concrete Temperatures for Storage Conditions of EOS-37PTH DSC in Updated HSM-MX with HLZCs 8 and 9

Load Case [1]	Max Fuel Cladding Temperature (°F)			Concrete Temperature (°F)	
	Upper Compartment	Lower Compartment	Limit	Maximum	Limit
LC 1e-S for HLZC 8	682	694	752[2]	256	300[2]
LC 1e-S for HLZC 9[3]	677	694		252	

Notes:

(1) See Table A.4-22 for the description of the LCs.

(2) The temperature limits are from NUREG-1536 [A.4-1].

(3) DSC in the upper compartment is modeled per HLZC 9, whereas DSC in the lower compartment is modeled per HLZC 8 as discussed in Section A.4.4.4.1.

Proprietary Information on Pages A.4-60 through A.4-66
Withheld Pursuant to 10 CFR 2.390.

Proprietary Information on Pages A.4-94 through A.4-114
Withheld Pursuant to 10 CFR 2.390.

The Monte Carlo transport code, MCNP5 [A.6-1], is used to compute dose fields around the HSM-MX using detailed 3D models. [

] A summary of the limiting HSM-MX dose rates is provided in Table A.6-2. The dose rate excluding the contribution from the inlet and outlet vents is small, as the dose rates are due primarily to streaming from the vents. The maximum dose rates at the inlet and outlet vents are *1,470* mrem/hr and *993* mrem/hr, respectively. The average dose rate on the front face of the module is *47.0* mrem/hr, and the average dose rate on the roof above the vent covers is *141* mrem/hr. The dose rate at the door centerline is *1.97* mrem/hr. The fluxes and dose rates on the surface of the HSM-MX are used as input to a generic site dose evaluation documented in Chapter A.11.

The shielding effectiveness of the HSM-MX is not affected by any off-normal events. *The following geometry changes may occur in an accident:*

- Loss of outlet vent covers
- Loss of dose reduction hardware
- *Damage to interior walls due to missile impact when the HSM-MX is in the construction joint expansion configuration with the removable end shield wall absent*

10 CFR 72.106 limits the dose to an individual at the site boundary to be less than 5 rem due to an accident. Monte Carlo N-Particle (MCNP) cases are developed for the HSM-MX, in which all vent covers and dose reduction hardware are absent, which is not credible. *An MCNP case is also developed for a missile impact when the HSM-MX is in the construction joint expansion configuration with the removable end shield wall absent. In this configuration, it is conservatively assumed that two interior walls are penetrated. The HSM-MX accident increases the average dose rate on the front, roof, and end of the module to 92.9 mrem/hr, 4,730 mrem/hr, and 425 mrem/hr, respectively.* The fluxes and dose rates on the surface of the HSM-MX in an accident condition are used as input to an accident site dose evaluation documented in Chapter A.11.

The minimum thickness of the roof is *4 feet 2 inches*. The minimum thickness of the integral end shield wall is 3 feet 8 inches. The minimum thickness of the optional removable end shield wall is 3 feet. In the single-row design, the thickness of the integral rear shield wall is 3 feet 8 inches. In the back-to-back design, the wall thickness between rows is 2 feet 6 inches.

Air inlet vents are located on the front and air outlet vents are located on the roof. Because little radiation directly penetrates the thick concrete shielding, essentially all of the dose rate is due to gamma radiation streaming from the vents. Radiation streaming through the outlet vents is mitigated by the use of vent covers, see Figure A.6-1. Under normal and off-normal conditions the vent covers are always in place.

The baseline MCNP configuration features an HSM-MX with a rear shield wall. On the left side (-x direction) an end shield wall is modeled, while on the right side (+x direction) a mirror boundary is modeled at the centerline of the DSC in the upper compartment, see Figure A.6-1 through Figure A.6-4. The length of the DSC is in the z-direction. This configuration is used to compute dose rates and fluxes on the end shield wall.

A second MCNP configuration features mirror boundaries on both the left and right sides of the model through the centerline of the DSCs in the lower compartments, although the rear shield wall is modeled explicitly, see Figure A.6-5. This configuration is used to simulate the interior region of a single row and is used to compute dose rates and fluxes on the rear shield wall.

A third MCNP configuration features mirror boundaries on the left, right, and rear of the model, see Figure A.6-6. This configuration is used to simulate the interior region of a double row (i.e., back-to-back arrangement) and is used to compute front and roof vent dose rates, as well as average front and roof dose rates and fluxes.

[

]

When an HSM-MX is to be expanded in the future, construction may be terminated at a construction joint and a 3 feet thick removable end shield wall is attached. The two complete compartments (one upper and one lower) nearest the end must remain empty when the HSM-MX is loaded, as indicated in Figure A.6-8. This configuration is explicitly modeled to determine the end dose rate when the removable end shield wall is absent. If an array to be expanded terminates at an expansion joint rather than a construction joint, the two compartments (one upper and one lower) nearest the end wall must remain empty. End dose rates for this configuration are bounded by the construction joint option with the end shield wall removed.

ADVANTG [A.6-3] is used to develop weight windows to accelerate problem convergence *for all* models.

The average fluxes on the faces of the HSM-MX are used as input to a generic site dose evaluation that is documented in Chapter A.11. These average fluxes are computed on the surface of a box that envelops the HSM-MX model, including the vent covers and door.

[

]

A.6.4 Shielding Analysis

A.6.4.1 Computer Codes

MCNP5 v1.40 is used in the shielding analysis [A.6-1]. MCNP5 is a Monte Carlo transport program that allows full 3D modeling of the HSM-MX. Therefore, no geometrical approximations are necessary when developing the shielding models.

A.6.4.2 Flux-to-Dose Rate Conversion

No change to Section 6.4.2.

A.6.4.3 EOS-TC Dose Rates

No change to Section 6.4.3.

A.6.4.4 HSM-MX Dose Rates

The maximum dose rate at the roof outlet vent is 993 mrem/hr. The maximum dose rate at the lower compartment inlet vent is 1,470 mrem/hr, while the maximum dose rate at the upper compartment inlet vent is 1,350 mrem/hr.

The total dose rate is dominated by primary gammas, while the dose rate from neutrons and secondary gammas is negligible. The bulk shielding of the HSM-MX is very effective in the absence of streaming. The average dose rate on the rear and end (side) shield walls is 0.484 mrem/hr and 0.632 mrem/hr, respectively. The dose rate at the door centerline is 1.97 mrem/hr. These surfaces do not contain streaming paths, although the average rear and end dose rates are computed to the top of the vent covers and include contribution from the roof vents. The average dose rate on the front face of the module is 47.0 mrem/hr, and the average dose rate on the roof above the vent covers is 141 mrem/hr.

Input for Site Dose Evaluation

The average dose rate and flux on the surface of the HSM-MX is of interest for use in the generic site dose evaluations. The site dose evaluations are documented in Chapter A.11, although the inputs to the site dose evaluation are obtained from the HSM-MX evaluations described in the current chapter.

[

]

Average fluxes and dose rates on the end, rear, front, and roof of the HSM-MX with the EOS-89BTH DSC are reported in Table A.6-3, Table A.6-4, and Table A.6-5, for primary gamma, secondary gamma, and neutron radiation, respectively. These dose rates and fluxes are applicable to normal and off-normal conditions.

[

]

Expansion Considerations

As shown in Figure A.6-8, when an array is in the construction joint expansion configuration, the two complete compartments (one upper and one lower) at the end of the module must remain empty. A removable end shield wall is attached. These empty compartments are required to maintain low dose rates when the removable end shield wall is absent during subsequent construction activities. If an array to be expanded terminates at an expansion joint rather than a construction joint, the two compartments (one upper and one lower) nearest the end wall must remain empty. End dose rates for this configuration are bounded by the construction joint option with the end shield wall removed.

Use of Low-Density Grout for HSM-MX Repair

[

]

Proprietary Information on Pages A.6-12 through A.6-33
Withheld Pursuant to 10 CFR 2.390.

A.8.2 Materials Selection

This section discusses the materials used in the HSM-MX components. Table A.8-1 summarizes the materials selected for HSM-MX. Materials utilized in the HSM-MX are largely the same as those used in the EOS-HSM, and the materials for the EOS-DSCs and EOS-TCs have not changed. Therefore, the tables described in Section 8.2 also applicable to HSM-MX. Temperature-dependent mechanical and thermal properties for the materials listed in Table A.8-1 are presented in Table A.8-2 through Table A.8-4.

A.8.2.1 Applicable Codes and Standards and Alternatives

A.8.2.1.1 EOS-37PTH and EOS-89BTH DSC

No change from Section 8.2.1.1.

A.8.2.1.2 EOS-TC Transfer Cask

No change from Section 8.2.1.2.

A.8.2.1.3 HSM-MX Horizontal Storage Module

The applicable codes for the HSM-MX are:

- Concrete construction per ACI-318-08 [A.8-4].
- Concrete Design per ACI-349-06 [A.8-5].
- DSC Support design per AISC Manual of Steel Construction [A.8-7].

Cement, aggregate, reinforcing steel, and steel *structures* conform to ASTM specifications.

The HSM-MX concrete subcomponents are designed and constructed using a specified 28-day compressive strength of 5,000 psi, normal weight concrete. The cement is Type II or Type III Portland cement meeting the requirements of ASTM C150. The concrete aggregate meets the specifications of ASTM C33. The reinforcing steel is ASTM A615 or A706 Gr. 60 deformed bars placed vertically and horizontally at each face of the walls, roof and slabs.

The concrete surface temperature limits criteria are based on the provisions in Section 3.5.1.2 of NUREG-1536, as follows:

- If concrete temperatures in general or local areas are at or below 200 °F for normal/off-normal conditions/occurrences, no tests to prove capability at elevated temperatures or reduction of concrete strength are required.
- If concrete temperatures, in general, or local areas exceed 200 °F, but do not exceed 300 °F, no tests to prove capability at elevated temperatures or reduction of concrete strength are required if the aggregates have a coefficient of thermal expansion (CTE) no greater than $6x10^{-6}$ in/in/°F, or are one of the following materials: limestone, dolomite, marble, basalt, granite, gabbro, or rhyolite.

The above criteria in lieu of the ACI 349-06 requirements do not extend above 300 °F for normal/off-normal conditions and do not modify the ACI 349-06 requirements for accident conditions. Per E.4.2 of ACI 349-06 [A.8-5], the accident conditions or short-term period (i.e., blocked vent accident transient) concrete temperatures are limited to 350 °F. Higher temperatures are allowed per E.4.3 if tests are provided to evaluate the reduction in strength and this reduction is applied to design allowables. HSM-MX concrete compressive tests are performed on specimens heated to or above that maximum accident temperature for no less than 40 hours. HSM-MX concrete temperature testing is performed whenever there is a significant change in the cement, aggregate, or water-cement ratio of the concrete mix design. See Section 5.3 of the Technical Specifications [A.8-17].

Alternatively, per the ACI 349-13 [A.8-10] commentary Section RE.4, the specified 28-day compressive strength can be increased to 7,000 psi for HSM fabrication, in lieu of the above aggregate types or coefficient of thermal expansion requirements, so that any losses in properties (e.g., compressive strength, modulus of elasticity) resulting from long-term thermal exposure will not affect the safety margins based on the specified 5,000 psi compressive strength used in the design evaluations. Additionally, also as indicated in Section RE.4, short, randomly oriented steel fibers may be used to provide increased ductility, dynamic strength, toughness, tensile strength, and improved resistance to spalling. See Section 4.4.4 of the Technical Specifications [A.8-17].

Encl. 4, Fabricability

The rear DSC supports consists of a W6 x 25 structural beam of ASTM A992 Gr.50 material *or equivalent built-up I-Beam of ASTM A572 Gr. 50 material* coated with an inorganic zinc-rich primer and a high-build epoxy enamel finish. The DSC rests on an ASTM A240 Type 304 support plate welded to the beam. A corrosion allowance of 1/16 inch is used in the design calculations. Welding procedures are in accordance with ASME Code Section IX or AWS D1.1 [A.8-11].

At coastal sites with operational experience of corrosion due to atmospheric chlorides, the front and rear DSC supports steel and weld filler metal have a minimum of 0.20% copper content or are stainless steel. For carbon steels, weld material with 1% or more nickel is acceptable in lieu of 0.20% copper content. The copper content is equivalent to weathering steel [A.8-12], and nickel-bearing weld materials show equivalent corrosion resistance [A.8-13].

A.8.2.2 Material Properties

Encl. 4, Item B.5

The material properties used in the HSM-MX design analyses are listed in Table 8-4 through Table 8-6, Table 8-13, Table 8-23, and Table 8-24. Additionally, new materials used in the HSM-MX are provided in Table A.8-2 through Table A.8-4. Each table cites the source for the properties. Table A.8-1 ties these materials to the individual components.

A.8.2.2.1 EOS-37PTH and EOS-89BTH DSC

No change from Section 8.2.2.1.

A.8.2.2.2 EOS TC Transfer Cask

No change from Section 8.2.2.2.

A.8.2.2.3 HSM-MX Horizontal Storage Module

In accordance with ACI 349-06, Section E.4.3, the strength properties of the concrete and reinforcing steel used in the HSM-MX structural analysis are taken at the maximum calculated temperature. Temperature-dependent mechanical properties of concrete and reinforcing steel are taken from [A.8-3] and presented in Table 8-23, and Table 8-24.

The material properties of the ASTM A992 Gr 50 steel used for the rear DSC support are listed in Table A.8-3, and the material properties for the ASTM A572 Gr. 50 front and rear stop plate *and optional built-up I-beam* are listed in Table A.8-2. The material properties used for the Type 304 stainless steel used for the front DSC supports and heat shields are provided in Table 8-5. The material properties used for the Type 316 stainless steel used as an option for the front DSC supports and heat shields are listed in Table 8-5.

The properties ASTM A588 for the axial retainer is provided in Table A.8-4.

A.8.2.2.4 NUHOMS® EOS System Materials Employed in the Shielding Analysis

Shielding properties of steel and concrete are obtained from [A.8-6] and are summarized in Table 8-30. Concrete used in the HSM-MX is modeled without steel rebar at a density of 138 pcf (2.211 g/cm^3).

A.8.2.2.5 NUHOMS® EOS System Materials Employed in the Criticality Analysis

No change to Section 8.2.2.5.

A.8.2.3 Materials for ISFSI Sites with Experience of Atmospheric Chloride Corrosion

Front and rear DSC supports at sites with operational experience of corrosion caused by atmospheric chlorides are fabricated from steels equivalent to weathering steel or stainless steel.

A.8.2.4 Weld Design and Inspection

There are no changes to the weld design and inspection for the DSC and TC described in Section 8.2.4.

A.8.7 References

A.8-1 NUREG-1536, "Standard Review Plan for Spent Fuel Dry Storage Systems at a General license Facility," Revision 1, U.S. Nuclear Regulatory Commission, July 2010.

A.8-2 American Society of Mechanical Engineers, ASME Boiler and Pressure Vessel Code, 2010 Edition with 2011 Addenda.

A.8-3 Mark Fintel, "Handbook of Concrete Engineering," September 1974.

A.8-4 ACI-318-08, "Building Code Requirement for Structural Concrete and Commentary," American Concrete Institute.

A.8-5 American Concrete Institute, "Code Requirements for Nuclear Safety Related Concrete Structures", ACI-349-06.

A.8-6 PNNL-15870, Re. 1, "Compendium of Material Composition Data for Radiation Transport Modeling," Pacific Northwest National Laboratory, March 2011.

A.8-7 American Institute of Steel Construction, Manual of Steel Construction, 13th Edition or 14th Edition.

A.8-8 Mark Fintel, "Handbook of Concrete Engineering, Second Edition," September 1985.

A.8-9 ASTM A572/A572M, "Standard Specification for High-Strength Low-Alloy Columbium-Vanadium Structural Steel," Latest Edition.

A.8-10 ACI-349-13, "Code Requirements for Nuclear Safety Related Concrete Structures and Commentary," American Concrete Institute.

A.8-11 American Welding Society, AWS D1.1, March 2010, Structural Welding Code-Steel.

A.8-12 [

]

A.8-13 C. P. Larrabee, S. K. Coburn, "The Atmospheric Corrosion of Steels as Influenced by Changes in Chemical Composition," First International Congress on Metallic Corrosion, 1962

A.8-14 ASTM A992, "Standard Specification for Structural Steel Shapes."

A.8-15 Duke Energy Carolinas, LLC, Oconee Nuclear Station, Docket No. 72-4, License No. SNM-2503, License Renewal Application for the Site-Specific Independent Spent Fuel Storage Installation (ISFSI) - Response to Requests for Additional Information, License Amendment Request No. 2007-06, ADAMS ML090370066, January 30, 2009 (Response to Question A-4).

A.8-16 Calvert Cliffs Nuclear Power Plant, Independent Spent Fuel Storage Installation, Material License No. SNM-2505, Docket No. 72-8, Response to Request for Supplemental Information, RE: Calvert Cliffs Independent Spent Fuel Storage Installation License Renewal Application (TAC No. L24475), ADAMS ML12212A216, July 27, 2012.

A.8-17 CoC 1042 Appendix A, NUHOMS® EOS System Generic Technical Specifications, Amendment 1.

All Indicated Changes are in response to RAI 8-5

Table A.8-1
HSM-MX Materials

HSM Subcomponents	Material
HSM-MX walls, roof, floor, end shield walls	Reinforced concrete with ASTM A615 or A706 Gr 60 reinforcing steel
DSC Support Pedestal	ASTM A992 Gr. 50 *or ASTM A572 Gr. 50*
DSC Support Pedestal Stop Plate	ASTM A572 Gr. 50
DSC Support Pedestal Support Plate	ASTM A240 Type 304 or 316
HSM-MX Door	Reinforced concrete
Door Steel Liner Assembly	Steel
Threaded Inserts	Steel
Inspection Penetration Sleeve Door	Steel
Axial Retainer Rod	ASTM A588
Axial Retainer miscellaneous plate (fastener plate, spacer plate)	Steel
HSM-MX Heat Shields	Stainless steel ASTM A240 Type 304 or 316
HSM-MX Outlet Vent Cover	Reinforced concrete
HSM-MX Outlet Vent Liners	Carbon Steel
HSM Inlet Vent Screen Assembly	Carbon Steel
Bird Screens and Dose Reduction Hardware	Stainless steel or Carbon Steel
Fasteners:	
Bolts	ASTM A193 Gr B7/ A325/A563/A490/A108
Washers	ASTM A36/F436/F844/ Stainless Steel
Nuts	ASTM A194/A563/A194/ Carbon Steel
Threaded Embedments:	
Stud Bolt	ASTM A193-Gr. B7, ASTM A193-B8 CL 2 or ASTM A193-B8M CL 2
Sleeve Nut	ASTM A194 Gr 2H or A563 Gr A
Nut	ASTM A194 Gr 8M or A563 Gr A

CAUTION: The insides of empty compartments have the potential for high dose rates due to adjacent loaded compartments. Proper ALARA practices should be followed for operations inside these compartments and in the areas outside these compartments whenever the MX-RRT operations are being performed.

6. Remove the MX-RRT *cover plates and* shield *plugs*.
7. Insert and install MX-RRT into HSM-MX. Extend the MX-RRT rollers, secure and verify that the rollers are extended.
8. Transport the TC from the plant's fuel/reactor building to the ISFSI along the designated transfer route.
9. Once at the ISFSI, move the transfer trailer inside the MX-LC at "home" position between the skid and the MX-LC grappling mechanism.
10. Use the MX-LC grappling mechanism to capture the skid along with TC, disengage the skid positioning system, move the skid up in the vertical direction to clear it from the transfer trailer, and then the transfer trailer is moved from MX-LC.
11. Remove the FC system, and install the ram cylinder assembly.
12. Remove the HSM-MX door.
13. Unbolt and remove the TC top cover plate.
14. Move MX-LC along the rail in front of HSM-MX until the TC is completely against the face of HSM-MX.
15. The skid is moved until the target compartment is reached. If necessary, adjust the MX-LC position until the MX-LC is properly aligned with the targeted compartment.
16. Secure the MX-LC/skid/cask to the front wall embedments of the HSM-MX using the restraints.
17. The hydraulic power unit is connected to the ram cylinder. The grapple is moved until it engages with grapple ring of the canister. Using the ram cylinder, fully insert the DSC into the HSM-MX compartment.
18. Disengage the ram grapple mechanism so that the grapple is retracted away from the DSC grapple ring.
19. Retract the MX-RRT rollers; the DSC is lowered onto the HSM-MX front and rear DSC supports.

Note: The time limit for transfer operations, if any, starts with the initiation of the TC/DSC annulus water draining described in Step 9 of Section 9.1.4 and ends when the DSC is fully seated onto the front and rear DSC supports.

CAUTION: Verify that the applicable time limits for transfer operations of Section 3.1.3 of the Technical Specifications [A.9-5] are met.

20. Remove the wall embedments from the HSM-MX.

21. Retract the skid with TC from docking position and lower it.

22. Place the HSM-MX door. Verify that the HSM dose rates are compliant with the limits specified in Section 5.1.2 of the Technical Specifications [A.9-5].

23. Move MX-LC to its "home" position, and the transfer trailer is moved into accepting position.

24. Lower the Skid along with TC onto the transfer trailer. Reconnect the skid positioning system. Remove the ram cylinder assembly.

25. Bolt the TC cover plate into place, tightening the bolts to the required torque in a star pattern.

CAUTION: The insides of empty compartments have the potential for high dose rates due to adjacent loaded compartments. Proper ALARA practices should be followed for operations inside these compartments and in the areas outside these compartments whenever the MX-RRT operations are being performed.

26. Remove the MX-RRT from the HSM-MX.

27. Place *MX-RRT shield plugs and cover plates* for the MX-RRT accesses.

28. Move the transfer trailer from MX-LC to the designated equipment storage area. Return the remaining transfer equipment to the storage area.

29. Close and lock the ISFSI access gate and activate the ISFSI security measures.

A.9.1.7 Monitoring Operations

1. Perform routine security surveillance in accordance with the licensee's ISFSI security plan.

2. Perform a daily visual surveillance of the HSM-MX air inlets and outlets (bird screens) to verify that no debris is obstructing the HSM-MX vents in accordance with Section 5.1.3.2(a) of the Technical Specification [A.9-5] requirements, or, perform a temperature measurement for each EOS-HSM in accordance with Section 5.1.3.2(b) of the Technical Specification [A.9-5] requirements.

A.9.2 Procedures for Unloading the DSC

The following section outlines the procedures for retrieving the DSC from the HSM-MX. The procedures for removing the FAs from the DSC are the same as described in Section 9.2.

A.9.2.1 DSC Retrieval from the HSM-MX

1. Ready the TC, transfer trailer, loading crane, and skid for service. Fill the TC liquid neutron shield and remove the top cover plate from the TC. Transport the trailer into the ISFSI.

   Note: Verify that a TC spacer of appropriate height is placed inside the TC to provide the correct airflow and interface at the top of the TC during cutting and unloading operations for DSCs that are shorter than the TC cavity length.

2. MATRIX MX-LC rails are installed, aligned and verified on the pad for the unloading campaign. Alignment is verified to the specifically designated features on the face of HSM-MX.

3. Move the transfer trailer inside the MX-LC "home" position between the skid and the MX-LC grappling mechanism.

4. Use the MX-LC grappling mechanism to capture the skid along with TC, disengage the skid positioning system, move the skid up vertically to clear it from the transfer trailer, then move the transfer trailer from the MX-LC.

5. Install the ram cylinder assembly.

CAUTION: The insides of empty compartments have the potential for high dose rates due to adjacent loaded compartments. Proper ALARA practices should be followed for operations inside these compartments and in the areas outside these compartments whenever the MX-RRT operations are being performed.

6. Remove the MX-RRT shield blocks *plugs and cover plates*.

7. Insert and install MX-RRT into HSM-MX. Extend the MX-RRT rollers, secure and verify that the rollers are extended.

CAUTION: The insides of empty compartments have the potential for high dose rates due to adjacent loaded compartments. Proper ALARA practices should be followed for operations inside these compartments and in the areas outside these compartments whenever the door from the empty compartment has been removed.

8. Remove the HSM-MX door.

24. Disconnect MX-RRT operating mechanism and retract MX-RRT to MX-RRT handling device.
25. Place *MX-RRT shield plugs and cover plates* for the MX-RRT accesses.
26. Move the transfer trailer from MX-LC and ready the trailer for transfer.
27. Replace the HSM-MX door.

A.9.2.2 Removal of Fuel from the DSC

No change, see Section 9.2.2.

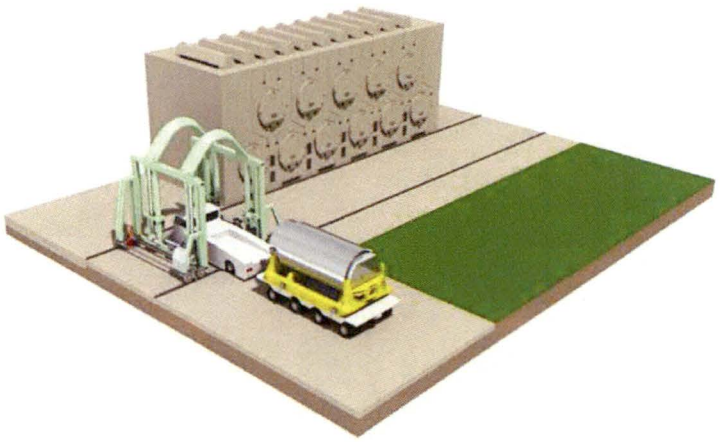

5) Tow Trailer to Loading Crane at ISFSI

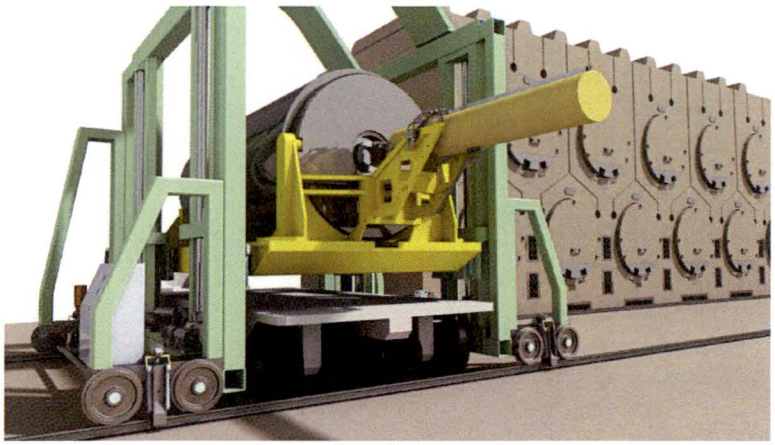

6) Transfer TC from Trailer to Loading Crane

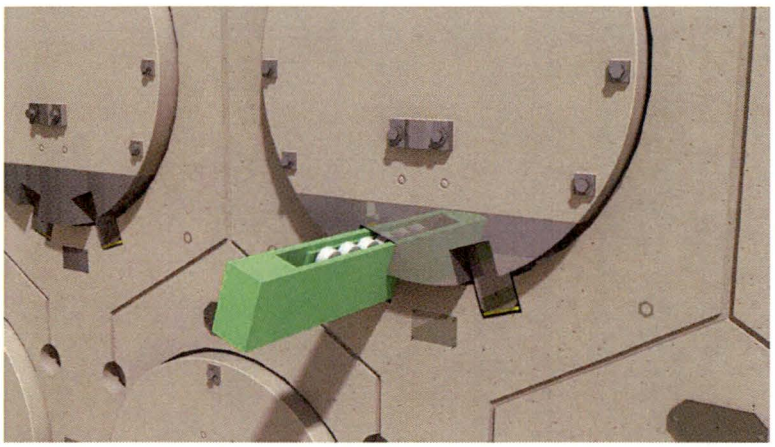

7) Insert and Install Retrievable Roller Tray (MX-RRT)

Figure A.9-1
NUHOMS® MATRIX Loading Operations
4 Pages

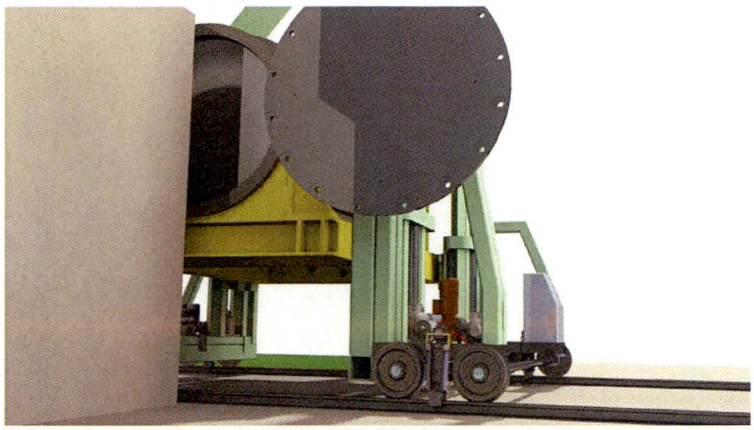

8) Remove the Transfer Cask Cover.

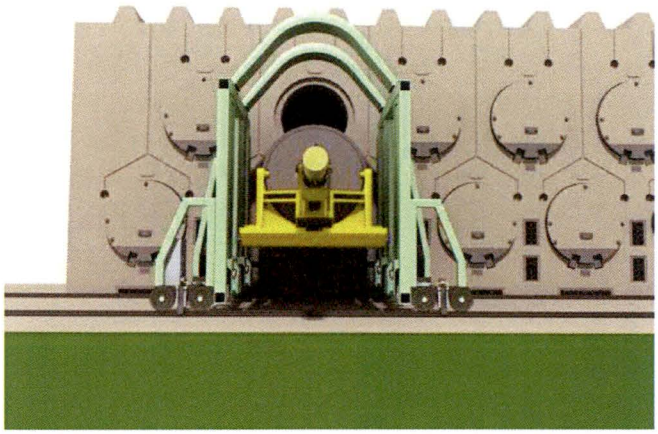

9) Align Transfer Cask at X-Plane Direction, Engage Ram Grapple with Canister, HSM Door Is Removed.

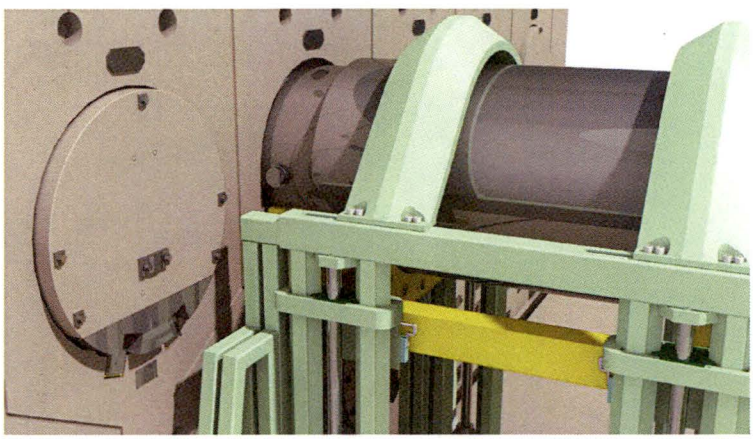

10) Align Transfer Cask at Z-Direction.

Figure A.9-1
NUHOMS® MATRIX Loading Operations
4 Pages

A.11.2 Occupational Dose Assessment

This section provides estimates of occupational dose for typical EOS transfer cask (EOS-TC) and ISFSI loading operations. Assumed annual occupancy times, including the anticipated maximum total hours per year for any individual, and total person-hours per year for all personnel for each radiation area during normal operation and anticipated operational occurrences, will be evaluated by the licensee in a 10 CFR 72.212 evaluation to address the site-specific ISFSI layout, inspection, and maintenance requirements. In addition, the estimated annual collective doses associated with loading operations will be addressed by the licensee in a 10 CFR 72.212 evaluation.

A.11.2.1 EOS-DSC Loading, Transfer, and Storage Operations

The dose rates used in the occupational dose assessment are summarized in Table A.11-1. The EOS-TC loading and transfer dose rates are unchanged from the values presented in Chapter 11. The HSM-MX dose rate reported in Table A.11-1 is the average dose rate on the front surface of an HSM-MX and is obtained from Chapter A.6.

The estimated occupational exposures to ISFSI personnel during loading, transfer, and storage operations using the EOS-TC108 (time and number of workers may vary depending on individual ISFSI practices) are provided in Table A.11-2 for the EOS-89BTH DSC. Similar operations for the EOS-TC125/135 are provided in Table A.11-3 and Table A.11-4. Transfer of the EOS-37PTH DSC to the HSM-MX using the EOS-TC108 is not currently authorized. The task times, number of personnel required, and total doses are listed in these tables. The total exposure results are as follows:

- EOS-TC108 with EOS-89BTH DSC: *4,535* person-mrem (~4.5 person-rem)
- EOS-TC125/135 with EOS-37PTH DSC: *3,200* person-mrem (*~3.2* person-rem)
- EOS-TC125 with EOS-89BTH DSC: *2,523* person-mrem (~2.5 person-rem)

The exposures provided above are bounding estimates. Measured exposures from typical NUHOMS® System loading campaigns have been 600 mrem or lower per canister for normal operations, and exposures for the HSM-MX are expected to be similar.

Regulatory Guide 8.34 [A.11-4] is to be used to define the onsite occupational dose and monitoring requirements.

A.11.2.2 EOS-DSC Retrieval Operations

Occupational exposures to ISFSI personnel during EOS-DSC retrieval are similar to those exposures calculated for EOS-DSC insertion. Dose rates for retrieval operations will be lower than those for insertion operations due to radioactive decay of the spent fuel inside the HSM-MX. Therefore, the dose rates for EOS-DSC retrieval are bounded by the dose rates calculated for insertion.

A.11.2.3 Fuel Unloading Operations

No change to Section 11.2.3.

A.11.2.4 Maintenance Operations

The dose rates for surveillance activities are shown in Table A.11-7 and Table A.11-8 for doses rates 6.1 m from the front of an HSM-MX. The 6.1-meter dose rate is a conservative estimate for surveillance activities. The HSM-MX surface dose rates provided in Chapter A.6 can be used for temperature sensor maintenance activities, including calibration and repair.

The general licensee will evaluate the additional dose to personnel from ISFSI operations, based on the particular storage configuration and site personnel requirements.

A.11.2.5 Doses during ISFSI Expansion

During the ISFSI expansion using the construction joint option, the removable end shield wall is absent, and the two complete compartments (one upper and one lower) at the end of the module are empty. The maximum dose rate at the end of the module for the array expansion configuration is 3.64 mrem/hr, which is low (see Section A.6.4.4). If the array terminates at an expansion joint, two empty compartments (one upper and one lower) are also required at the end of the array, and dose rates are bounded by the construction joint option. The maximum dose rate on the surface of the integral shield wall is 4.20 mrem/hr (see Table A.6-2). Therefore, the end dose rate during array expansion activities is approximately the same as the end dose rate with an integral end shield wall, and elevated dose rates during array expansion activities are not anticipated.

The total annual exposure for each ISFSI layout as a function of distance from each face is given in Table A.11-5 and plotted in Figure A.11-1. The total annual exposure estimates are based on 100% occupancy for 365 days. At large distances, the annual exposure from the 2x11 back-to-back configuration is similar to the two 1x11 front-to-front configuration. Per 10 CFR 72.104, the annual whole-body dose to an individual at the site boundary is limited to 25 mrem. Based on the data shown in Table A.11-5, the offsite dose rate drops below 25 mrem at a distance of approximately (349) m from the ISFSI. Therefore, (349) m is the minimum distance with design basis fuel to the site boundary for the HSM-MX system with 22-DSCs; however, a shorter distance can be demonstrated in a site-specific calculation.

The methodology, inputs, and assumptions for the MCNP analyses are summarized in the following paragraphs.

- The 2x11 back-to-back configuration is modeled as a box enveloping the HSM-MX, including the 44 inch thick shield walls on the two ends. Source particles are started on the surfaces of the box. A sketch of this geometry is shown in Figure A.11-2. The interiors of the HSM-MX and shield walls are modeled as air. Most particles that enter the interiors of the HSM-MX and shield walls will, therefore, pass through unhindered.
- The HSM-MXs in the two 1x11 front-to-front configuration are modeled as two boxes that envelop each 1x11 row, including the 44-inch thick shield walls on the two ends and 44 inch thick rear shield wall in each row. Source particles are started on the surfaces of one of the modules, which is modeled as air. The opposite module is modeled as solid concrete. A sketch of this geometry is shown in Figure A.11-3. The dose field is then created for a source in both modules by accounting for model symmetry, as indicated in Figure A.11-3.
- The ISFSI approach slab is modeled as concrete. Because the ground composition has, at best, only a secondary impact on the dose rates at the detectors, any differences between this assumed layout and the actual layout would not have a significant effect on the site dose rates.
- The "universe" is a sphere surrounding the ISFSI. To account for skyshine, the radius of this sphere (r=500,000 cm) is more than 10 mean free paths for neutrons and 50 mean free paths for gammas in air, thus ensuring that the model is of a sufficient size to include all interactions, including skyshine, affecting the dose rate at the detectors.
- The 2x11 and two 1x11 surface sources are input to reproduce the average dose rate and spectrum on the surface of the HSM-MX, as computed in Chapter A.6. The surface average fluxes on the front, roof, side, and rear of the HSM-MXs are explicitly computed and are provided in Tables A.6-3 through A.6-5. The primary and secondary gamma fluxes are simply summed in the gamma input file. These surface spectra are directly input to MCNP for each face.
- Source particles on the ISFSI surface are specified with a cosine distribution. For a cosine distribution, the outward particle current is equal to half of the flux. The MCNP source description requires the number of source particles per second emitted on each face (particle current). Because the current is half of the flux for a cosine distribution, and the flux at each face is known, the input current for each

face (particles/s) is computed as A*F/2, where A is the area of the face (cm^2) and F is the total flux on each face (particles/cm^2-s). The surface source evaluations are summarized in Table A.11-6.

- ANSI/ANS 6.1.1-1977 flux-to-dose rate factors are utilized [A.11-6]. These factors are provided in Table 6-51.
- For the 2x11 back-to-back configuration with end shield walls, the "box" dimensions are 1260 cm wide, 2096 cm long, and 903 cm high. For the two 1x11 front-to-front configuration with end and back shield walls, the "box" dimensions are 704 cm wide, 2096 cm long, and 903 cm high. The two 1x11 rows are 975 cm (32 ft) apart.
- Dose rates are calculated for distances of 6.1 m (20 ft) to 600 m from the edges of the two ISFSI configurations. Point detectors are placed at the following locations, as measured from each face of the "box": 6.095 m (20 ft), 10 m, 20 m, 30 m, 40 m, 50 m, 60 m, 70 m, 80 m, 90 m, 100 m, 200 m, 300 m, 400 m, 500 m, and 600 m. Each point detector is placed 91 cm (~3 ft) above the ground.

The MCNP results for the 2x11 back-to-back and two 1x11 front-to-front configurations are summarized in Table A.11-7 and Table A.11-8, respectively. At near distances, the 2x11 configuration results in larger front dose rates than the outward rear of the two 1x11 configuration. For example, the 6.1 m front dose rate is 16.5 mrem/hr for the 2x11 configuration compared to 1.15 mrem/hr for the two 1x11 configuration. However, at near distances, the two 1x11 configuration results in nominally larger side dose rates than the 2x11 configuration.

At large distances, the dose rates are approximately the same, regardless of configuration or direction from the ISFSI, as the dose rate at large distances is dominated by skyshine from the radiation streaming from the roof outlet vents. Also, note that the neutron dose rate is negligible compared to the gamma dose rate at all dose rate locations.

The total Monte Carlo uncertainty is < 5% for all dose rate locations. The annual exposures reported in Table A.11-5 are simply the computed dose rates multiplied by 8760 hours (1 year).

The preceding analyses and results are intended to provide high estimates of dose rates for generic ISFSI layouts. The written evaluations performed by a general licensee for the actual ISFSI must consider the type and number of storage units, layout, characteristics of the irradiated fuel to be stored, site characteristics (e.g., berms, distance to the controlled area boundary, etc.), and reactor operations at the site in order to demonstrate compliance with 10 CFR 72.104.

A.11.3.2 Accident Conditions (10 CFR 72.106)

Per 10 CFR 72.106, the exposure to an individual at the site boundary due to an accident is limited to 5 rem. In an accident, the HSM-MX outlet vent covers and all dose reduction hardware may be lost. *In addition, it is assumed that the HSM-MX is in an expansion configuration with the removable end shield wall absent and that a missile strike has damaged two interior walls. This accident scenario results in elevated dose rates on the front, roof, and side of the ISFSI. The average HSM-MX roof, front, and side dose rates and fluxes in an accident are provided in Chapter A.6, Tables A.6-6 through A.6-8.*

Table A.11-9 shows the bounding dose rate as a function of distance from a 2x11 back-to-back configuration of HSM-MXs for the accident configuration described above. These dose rates are calculated assuming *damage to every module in the array*. This is a highly conservative scenario that is not credible, as an accident is not expected to damage every module.

MCNP inputs for a 2x11 ISFSI accident configuration are prepared using the same method as described for the normal condition models. At a distance of 200 m and *349* m from the ISFSI, the accident dose rate is approximately *0.436* mrem/hr and *0.061* mrem/hr, respectively. It is assumed that the recovery time for this accident is five days (120 hours). Therefore, the total exposure to an individual at a distance of 200 m and *349* m is approximately *52* mrem and *7.3* mrem, respectively. This is significantly less than the 10 CFR 72.106 limit of 5 rem.

The EOS-TC may also be damaged in an accident during transfer operations, which would result in an offsite dose, see the discussion in Section 11.3.2.

Table A.11-1
Occupational Dose Rates

			Dose Rate (mrem/hr)		
			EOS-TC108	EOS-TC125/135	
Dose Rate Location	**Averaged Segments**	**Config.**	**EOS-89BTH DSC**	**EOS-37PTH DSC**	**EOS-89BTH DSC**
DRL1 through DRL10	(1)	(1)	(1)	(1)	(1)
HSM-MX (HMX)	Front face surface average	-	50	50	50

Note 1: Information pertaining to dose rate locations DRL1 through DRL10 is provided in Table 11-1.

Table A.11-2
Occupational Exposure, EOS-TC108 with EOS-89BTH DSC
(2 Pages)

No. [2]	Operation	Configuration	Dose Rate Location	No. of People	Duration (hr)	Dose Rate (mrem/hr)	Dose (person -mrem)	% of Total Dose
1	Place an empty EOS-DSC into an EOS-TC and prepare the EOS-TC for placement into the spent fuel pool.	N/A	N/A	6	4.00	0	0	0%
2	Move the EOS-TC containing an EOS-DSC without fuel into the spent fuel pool.	N/A	N/A	6	1.50	0	0	0%
3	Remove the loaded EOS-TC from the fuel pool and place in the decontamination area.	Decon.	DRL1	2	0.25	194	97	2.1%
4	Install neutron shield. Fill neutron shield with water.	Decon.	DRL4	3	0.33	1050	1040	22.9%
5	Prep and weld inner top cover plate.	Welding	DRL3	2	0.75	198	297	6.5%
6	Vacuum dry and backfill with helium.	Welding	DRL3	2	0.50	198	198	4.4%
7	Weld outer top cover plate and port covers, perform non-destructive examination.	Welding	DRL3	2	0.50	198	198	4.4%
8	Drain annulus. Install EOS-TC aluminum top cover. Ready the support skid and transfer trailer.	Transfer	DRL5	1	0.50	586	293	6.5%
9	Place the EOS-TC onto the skid and trailer. Secure the EOS-TC to the skid.	Transfer	DRL2	2	0.33	747	498	11.0%
10	Install retractable roller tray (RRT).	Transfer	HMX	2	2.00	50	200	4.4%
11	Remove aluminum top cover and replace with steel top cover.	Transfer	DRL3	2	0.33	199	133	2.9%
12	Transfer the EOS-TC to ISFSI.	N/A	N/A	6	1.83	0	0	0%

Table A.11-2
Occupational Exposure, EOS-TC108 with EOS-89BTH DSC
(2 Pages)

No. [2]	Operation	Configuration	Dose Rate Location	No. of People	Duration (hr)	Dose Rate (mrem/hr)	Dose (person -mrem)	% of Total Dose
13	Position the EOS-TC inside the loading crane (MX-LC).	Transfer	HMX+DRL2	2	0.50	797	797	17.6%
14	Remove forced cooling system (if used) and install the ram cylinder assembly.	Transfer	DRL9	2	0.50	137	137	3.0%
15	Remove HSM-MX door.	Transfer	HMX	2	0.50	50	50	1.1%
16	Remove the EOS-TC top cover.	Transfer	HMX+DRL6	2	0.67	150	200	4.4%
17	Align and dock the EOS-TC with the HSM-MX. Secure the EOS-TC to the HSM-MX.	Transfer	HMX+DRL7	2	0.25	239	120	2.6%
18	Transfer the EOS-DSC from the EOS-TC to the HSM-MX using the ram cylinder.	N/A	N/A	3	0.50	0	0	0%
19	Disengage the ram and un-dock the EOS-TC from the HSM-MX.	Transfer	HMX+DRL10	2	0.08	171	29	0.6%
20	Install HSM-MX access door. Move EOS-TC to the transfer skid for removal.	Transfer	HMX	2	0.50	50	50	1.1%
21	Uninstall RRT.	Transfer	HMX	2	2.00	50	200	4.4%
						Total[1]	4535	

Note:

(1) A building crane hang-up off-normal event adds 776 person-mrem (DRL1/decon * 4 workers * 1 hour).

(2) Occupational exposures for steps 1 through 9 are consistent with Chapter 11, Table 11-3.

Table A.11-3
Occupational Exposure, EOS-TC125/135 with EOS-37PTH DSC
(2 Pages)

No. [2]	Operation	Configuration	Dose Rate Location	No. of People	Duration (hr)	Dose Rate (mrem/hr)	Dose (person -mrem)	% of Total Dose
1	Drain neutron shield if necessary. Place an empty EOS-DSC into an EOS-TC and prepare the EOS-TC for placement into the spent fuel pool.	N/A	N/A	6	4.00	0	0	0%
2	Move the EOS-TC containing an EOS-DSC without fuel into the spent fuel pool.	N/A	N/A	6	1.50	0	0	0%
3	Remove a loaded EOS-TC from the fuel pool and place in the decontamination area. Refill neutron shield tank if necessary.	Decon.	DRL1	2	0.25	101	50	1.6%
4	Decontaminate the EOS-TC and prepare welds.	Decon.	DRL2	2	1.75	315	1104	34.5%
		Decon.	DRL3	2	0.50	232	232	7.2%
5	Weld inner top cover plate.	Welding	DRL3	2	0.75	127	191	6.0%
6	Vacuum dry and backfill with helium.	Welding	DRL3	2	0.50	127	127	4.0%
7	Weld outer top cover plate and port covers, perform non-destructive examination.	Welding	DRL3	2	0.50	127	127	4.0%
8	Drain annulus. Install EOS-TC top cover. Ready the support skid and transfer trailer.	Transfer	DRL5	1	0.50	196	98	3.1%
9	Place the EOS-TC onto the skid and trailer. Secure the EOS-TC to the skid.	Transfer	DRL2	2	0.33	248	164	5.1%
10	Install RRT.	Transfer	HMX	2	2.00	50	200	6.2%

Table A.11-3
Occupational Exposure, EOS-TC125/135 with EOS-37PTH DSC
(2 Pages)

No. [2]	Operation	Configuration	Dose Rate Location	No. of People	Duration (hr)	Dose Rate (mrem/hr)	Dose (person -mrem)	% of Total Dose
11	Transfer the EOS-TC to ISFSI.	N/A	N/A	6	1.83	0	0	0%
12	Position the EOS-TC inside the loading crane (MX-LC).	Transfer	HMX+DRL2	2	0.50	298	298	9.3%
13	Remove forced cooling system (if used) and install the ram cylinder assembly.	Transfer	DRL9	2	0.50	76	76	2.4%
14	Remove HSM-MX door.	Transfer	HMX	2	0.50	50	50	1.6%
15	Remove the EOS-TC top cover.	Transfer	HMX+DRL6	2	0.67	108	145	4.5%
16	Align and dock the EOS-TC with the HSM-MX. Secure the EOS-TC to the HSM-MX.	Transfer	HMX+DRL7	2	0.25	147	74	2.3%
17	Transfer the EOS-DSC from the EOS-TC to the HSM-MX using the ram cylinder.	N/A	N/A	3	0.50	0	0	0%
18	Disengage the ram and un-dock the EOS-TC from the HSM-MX.	Transfer	HMX+DRL10	2	0.08	88	14	0.4%
19	Install HSM-MX access door. Move EOS-TC to the transfer skid for removal.	Transfer	HMX	2	0.50	50	50	1.6%
20	Uninstall RRT.	Transfer	HMX	2	2.00	50	200	6.2%
						Total	3200[1]	

Note:

(1) Use of aluminum cask lid increases total occupational dose by approximately ~95 person-mrem.

(2) Occupational exposures for steps 1 through 9 are consistent with Chapter 11, Table 11-4.

Table A.11-4
Occupational Exposure, EOS-TC125 with EOS-89BTH DSC
(2 Pages)

No.(1)	Operation	Configuration	Dose Rate Location	No. of People	Duration (hr)	Dose Rate (mrem/hr)	Dose (person -mrem)	% of Total Dose
1	Drain neutron shield if necessary. Place an empty EOS-DSC into an EOS-TC and prepare the EOS-TC for placement into the spent fuel pool.	N/A	N/A	6	4.00	0	0	0%
2	Move the EOS-TC containing an EOS-DSC without fuel into the spent fuel pool.	N/A	N/A	6	1.50	0	0	0%
3	Remove a loaded EOS-TC from the fuel pool and place in the decontamination area. Refill neutron shield tank if necessary.	Decon.	DRL1	2	0.25	62	31	1.2%
4	Decontaminate the EOS-TC and prepare welds.	Decon.	DRL2	2	1.75	181	634	25.1%
		Decon.	DRL3	2	0.50	98	98	3.9%
5	Weld inner top cover plate.	Welding	DRL3	2	0.75	113	170	6.7%
6	Vacuum dry and backfill with helium.	Welding	DRL3	2	0.50	113	113	4.5%
7	Weld outer top cover plate and port covers, perform non-destructive examination.	Welding	DRL3	2	0.50	113	113	4.5%
8	Drain annulus. Install EOS-TC top cover. Ready the support skid and transfer trailer.	Transfer	DRL5	1	0.50	191	96	3.8%
9	Place the EOS-TC onto the skid and trailer. Secure the EOS-TC to the skid.	Transfer	DRL2	2	0.33	239	158	6.3%
10	Install RRT.	Transfer	HMX	2	2.00	50	200	7.9%
11	Transfer the EOS-TC to ISFSI.	N/A	N/A	6	1.83	0	0	0%

Table A.11-4
Occupational Exposure, EOS-TC125 with EOS-89BTH DSC
(2 Pages)

No.[1]	Operation	Configuration	Dose Rate Location	No. of People	Duration (hr)	Dose Rate (mrem/hr)	Dose (person -mrem)	% of Total Dose
12	Position the EOS-TC inside the loading crane (MX-LC).	Transfer	HMX+DRL2	2	0.50	289	289	11.5%
13	Remove forced cooling system (if used) and install the ram cylinder assembly.	Transfer	DRL9	2	0.50	114	114	4.5%
14	Remove HSM-MX door.	Transfer	HMX	2	0.50	50	50	2.0%
15	Remove the EOS-TC top cover.	Transfer	HMX+DRL6	2	0.67	93	125	4.9%
16	Align and dock the EOS-TC with the HSM-MX. Secure the EOS-TC to the HSM-MX.	Transfer	HMX+DRL7	2	0.25	141	71	2.8%
17	Transfer the EOS-DSC from the EOS-TC to the HSM-MX using the ram cylinder.	N/A	N/A	3	0.50	0	0	0%
18	Disengage the ram and un-dock the EOS-TC from the HSM-MX.	Transfer	HMX+DRL10	2	0.08	88	14	0.6%
19	Install HSM-MX access door. Move EOS-TC to the transfer skid for removal.	Transfer	HMX	2	0.50	50	50	2.0%
20	Uninstall RRT.	Transfer	HMX	2	2.00	50	200	7.9%
						Total[2]	2523	

Note:

(1) Occupational exposures for steps 1 through 9 are consistent with Chapter 11, Table 11-5.

(2) Use of an aluminum cask lid increases the total occupational exposure by approximately 70 person-mrem.

Table A.11-5
Total Annual Exposure from ISFSI

Distance (m)	2x11		Two 1x11	
	Front Total Dose (mrem)	Side Total Dose (mrem)	Back Total Dose (mrem)	Side Total Dose (mrem)
6.1	144687	12069	10042	58090
10	88673	9504	8176	30971
20	32767	5876	5366	11061
30	16063	4035	3807	5937
40	9324	2925	2826	3815
50	6007	2205	2157	2689
60	4137	1703	1679	1992
70	2979	1338	1331	1520
80	2221	1087	1071	1197
90	1698	867	869	961
100	1323	706	714	776
200	191	126	131	135
300	43	31	32	32
400	12	8	9	9
500	4	3	3	3
600	1	1	1	1

Table A.11-6
ISFSI Surface Sources

2x11 Back-to-Back Configuration			
Source	**Area (cm^2)**	**Neutron Source (n/s)**	**Gamma Source (γ/s)**
Roof	2.640E+06	2.157E+08	2.414E+11
Front 1	1.892E+06	1.145E+08	9.324E+10
Front 2	1.892E+06	1.145E+08	9.324E+10
Side 1	1.137E+06	8.005E+05	3.898E+08
Side 2	1.137E+06	8.005E+05	3.898E+08
Total	8.697E+06	4.464E+08	4.287E+11
Two 1x11 Front-to-Front *Arrays* (source for one of the two rows)			
Source	**Area (cm^2)**	**Neutron Source (n/s)**	**Gamma Source (γ/s)**
Roof	1.474E+06	1.205E+08	1.348E+11
Front	1.892E+06	1.145E+08	9.324E+10
Back	1.892E+06	1.195E+06	8.996E+08
Side 1	6.351E+05	4.470E+05	2.177E+08
Side 2	6.351E+05	4.470E+05	2.177E+08
Total	6.528E+06	2.371E+08	2.294E+11

Table A.11-7
2x11 Back-to-Back Dose Rates
(2 Pages)

In Front of ISFSI				
Distance (m)	**Gamma Dose Rate (mrem/hr)**	**Neutron Dose Rate (mrem/hr)**	**Total Dose Rate (mrem/hr)**	**σ**
6.1	1.62E+01	3.58E-01	1.65E+01	0.02%
10	9.90E+00	2.21E-01	1.01E+01	0.03%
20	3.66E+00	8.23E-02	3.74E+00	0.05%
30	1.79E+00	4.05E-02	1.83E+00	0.1%
40	1.04E+00	2.32E-02	1.06E+00	0.1%
50	6.71E-01	1.46E-02	6.86E-01	0.1%
60	4.62E-01	9.84E-03	4.72E-01	0.2%
70	3.33E-01	6.88E-03	3.40E-01	0.1%
80	2.49E-01	4.97E-03	2.54E-01	0.2%
90	1.90E-01	3.74E-03	1.94E-01	0.2%
100	1.48E-01	2.87E-03	1.51E-01	0.2%
200	2.14E-02	4.23E-04	2.18E-02	0.3%
300	4.78E-03	1.18E-04	4.90E-03	0.7%
400	1.28E-03	4.74E-05	1.33E-03	1.2%
500	4.18E-04	1.87E-05	4.37E-04	4.9%
600	1.33E-04	6.57E-06	1.40E-04	1.6%

Table A.11-7
2x11 Back-to-Back Dose Rates
(2 Pages)

At Side of ISFSI				
Distance (m)	**Gamma Dose Rate (mrem/hr)**	**Neutron Dose Rate (mrem/hr)**	**Total Dose Rate (mrem/hr)**	**σ**
6.1	1.31E+00	6.67E-02	1.38E+00	0.1%
10	1.03E+00	5.15E-02	1.08E+00	0.1%
20	6.42E-01	2.93E-02	6.71E-01	0.1%
30	4.43E-01	1.81E-02	4.61E-01	0.2%
40	3.22E-01	1.19E-02	3.34E-01	0.1%
50	2.43E-01	8.20E-03	2.52E-01	0.2%
60	1.89E-01	5.89E-03	1.94E-01	0.2%
70	1.48E-01	4.34E-03	1.53E-01	0.2%
80	1.21E-01	3.29E-03	1.24E-01	1.6%
90	9.65E-02	2.53E-03	9.90E-02	0.3%
100	7.85E-02	2.00E-03	8.05E-02	0.2%
200	1.40E-02	3.66E-04	1.44E-02	0.4%
300	3.40E-03	9.85E-05	3.50E-03	1.2%
400	9.26E-04	3.66E-05	9.62E-04	0.9%
500	2.92E-04	1.41E-05	3.06E-04	1.9%
600	9.88E-05	6.59E-06	1.05E-04	1.9%

Table A.11-8
Two 1x11 Front-to-Front Dose Rates
(2 Pages)

In Back of ISFSI				
Distance (m)	**Gamma Dose Rate (mrem/hr)**	**Neutron Dose Rate (mrem/hr)**	**Total Dose Rate (mrem/hr)**	**σ**
6.1	1.09E+00	5.54E-02	1.15E+00	0.3%
10	8.89E-01	4.43E-02	9.33E-01	0.1%
20	5.86E-01	2.63E-02	6.13E-01	0.1%
30	4.18E-01	1.66E-02	4.35E-01	0.1%
40	3.11E-01	1.12E-02	3.23E-01	0.1%
50	2.39E-01	7.72E-03	2.46E-01	0.1%
60	1.86E-01	5.54E-03	1.92E-01	0.2%
70	1.48E-01	4.08E-03	1.52E-01	0.2%
80	1.19E-01	3.08E-03	1.22E-01	0.3%
90	9.68E-02	2.44E-03	9.92E-02	0.2%
100	7.96E-02	1.87E-03	8.15E-02	0.3%
200	1.46E-02	3.34E-04	1.50E-02	0.5%
300	3.53E-03	1.09E-04	3.63E-03	0.8%
400	1.01E-03	3.61E-05	1.05E-03	1.4%
500	3.17E-04	1.40E-05	3.31E-04	1.9%
600	1.11E-04	5.94E-06	1.17E-04	3.8%

Table A.11-8
Two 1x11 Front-to-Front Dose Rates
(2 Pages)

At Side of ISFSI				
Distance (m)	**Gamma Dose Rate (mrem/hr)**	**Neutron Dose Rate (mrem/hr)**	**Total Dose Rate (mrem/hr)**	**σ**
6.1	6.46E+00	1.70E-01	6.63E+00	0.02%
10	3.44E+00	9.81E-02	3.54E+00	0.03%
20	1.22E+00	3.94E-02	1.26E+00	0.1%
30	6.56E-01	2.13E-02	6.78E-01	0.1%
40	4.22E-01	1.32E-02	4.36E-01	0.1%
50	2.98E-01	8.82E-03	3.07E-01	0.1%
60	2.21E-01	6.19E-03	2.27E-01	0.1%
70	1.69E-01	4.54E-03	1.74E-01	0.1%
80	1.33E-01	3.30E-03	1.37E-01	0.1%
90	1.07E-01	2.57E-03	1.10E-01	0.2%
100	8.66E-02	2.00E-03	8.86E-02	0.2%
200	1.50E-02	3.62E-04	1.54E-02	0.3%
300	3.55E-03	1.02E-04	3.65E-03	0.6%
400	9.99E-04	3.21E-05	1.03E-03	0.7%
500	3.21E-04	1.46E-05	3.36E-04	1.4%
600	1.06E-04	5.52E-06	1.12E-04	1.3%

Table A.11-9
2x11 Back-to-Back Accident Dose Rates
(2 Pages)

In Front of ISFSI				
Distance (m)	**Gamma Dose Rate (mrem/hr)**	**Neutron Dose Rate (mrem/hr)**	**Total Dose Rate (mrem/hr)**	**σ**
6.1	5.74E+01	7.25E-01	5.81E+01	0.05%
10	4.11E+01	5.01E-01	4.16E+01	0.1%
20	2.18E+01	2.39E-01	2.20E+01	0.1%
30	1.40E+01	1.39E-01	1.41E+01	0.1%
40	9.80E+00	9.00E-02	9.89E+00	0.1%
50	7.25E+00	6.09E-02	7.32E+00	0.1%
60	5.56E+00	4.39E-02	5.60E+00	0.2%
70	4.36E+00	3.24E-02	4.39E+00	0.2%
80	3.48E+00	2.50E-02	3.51E+00	0.2%
90	2.82E+00	1.94E-02	2.84E+00	0.2%
100	2.30E+00	1.56E-02	2.32E+00	0.3%
200	4.19E-01	2.94E-03	4.22E-01	0.4%
300	1.03E-01	8.40E-04	1.04E-01	0.8%
400	2.91E-02	3.28E-04	2.94E-02	0.9%
500	8.83E-03	1.41E-04	8.97E-03	1.3%
600	2.92E-03	5.79E-05	2.98E-03	2.0%

Table A.11-9
2x11 Back-to-Back Accident Dose Rates
(2 Pages)

At Side of ISFSI				
Distance (m)	**Gamma Dose Rate (mrem/hr)**	**Neutron Dose Rate (mrem/hr)**	**Total Dose Rate (mrem/hr)**	**σ**
6.1	*1.33E+02*	*7.31E-01*	*1.34E+02*	*0.04%*
10	*7.96E+01*	*4.72E-01*	*8.01E+01*	*0.1%*
20	*3.21E+01*	*2.16E-01*	*3.23E+01*	*0.1%*
30	*1.81E+01*	*1.25E-01*	*1.82E+01*	*0.4%*
40	*1.17E+01*	*8.07E-02*	*1.18E+01*	*0.1%*
50	*8.34E+00*	*5.60E-02*	*8.39E+00*	*0.1%*
60	*6.19E+00*	*4.04E-02*	*6.23E+00*	*0.1%*
70	*4.76E+00*	*3.04E-02*	*4.79E+00*	*0.2%*
80	*3.76E+00*	*2.34E-02*	*3.78E+00*	*0.2%*
90	*3.00E+00*	*1.84E-02*	*3.01E+00*	*0.2%*
100	*2.42E+00*	*1.46E-02*	*2.44E+00*	*0.2%*
200	*4.33E-01*	*2.95E-03*	*4.36E-01*	*0.4%*
300	*1.05E-01*	*8.18E-04*	*1.06E-01*	*0.7%*
400	*3.00E-02*	*3.02E-04*	*3.03E-02*	*1.1%*
500	*9.36E-03*	*1.36E-04*	*9.49E-03*	*2.1%*
600	*3.09E-03*	*5.60E-05*	*3.15E-03*	*1.6%*

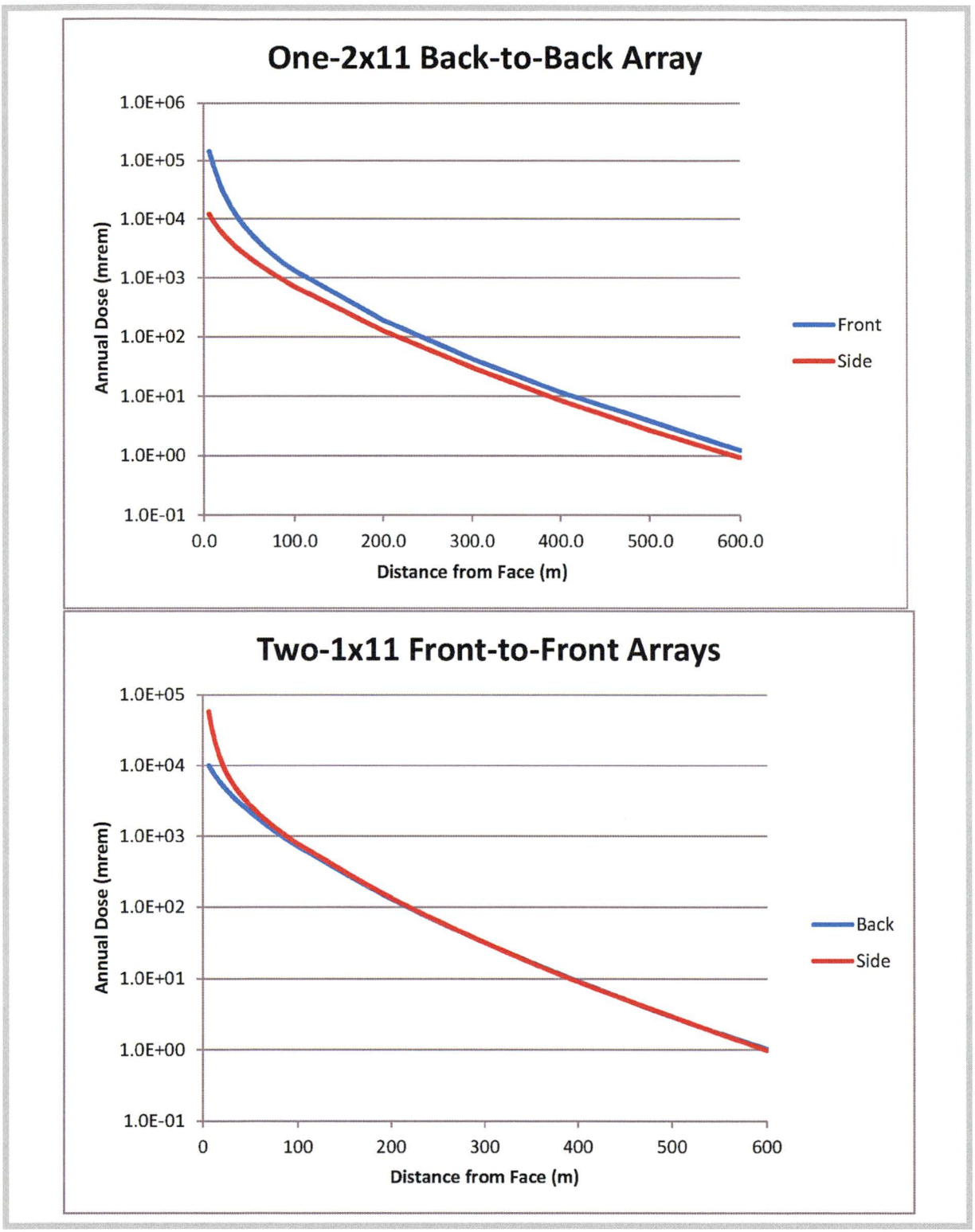

Figure A.11-1
Total Annual Exposure from the ISFSI

A.12.3.2 Earthquake

Cause of Accident

The explicitly evaluated seismic response spectra for the NUHOMS® HSM-MX consist of the U.S. Nuclear Regulatory Commission (NRC) Regulatory Guide 1.60 (Reg. Guide 1.60) [A.12-6] *with enhanced spectral accelerations above 9 Hz, and* anchored to a maximum ground acceleration of 0.85g horizontal and 0.80g for the vertical peak accelerations. The results of the frequency analysis of the HSM-MX structure (which includes a simplified model of the DSC) yield a lowest frequency of *23.94* Hz in the transverse direction and *24.08* Hz in the longitudinal direction. The lowest vertical frequency is *49.02* Hz. Thus, based on the Reg. Guide 1.60 response spectra amplifications, the corresponding seismic accelerations used for the design of the HSM-MX are *1.33*g and *1.33*g in the transverse and longitudinal directions, respectively, and 0.80g in the vertical direction. The corresponding accelerations applicable to the DSC are *1.62*g and *1.61*g in the transverse and longitudinal directions, respectively, and 0.80g in the vertical direction.

Accident Analysis

The seismic analyses of the components that are important to safety are analyzed as follow:

Components	**UFSAR Sections**
EOS-37PTH DSC and EOS-89BTH DSC Shell	Appendix 3.9.1 and A.3.9.1
EOS-37PTH Basket and EOS-89BTH Basket	Appendix 3.9.2
HSM-MX	Appendices A.3.9.4 & A.3.9.7
EOS-TC	Appendix 3.9.5

The results of these analyses show that seismic stresses are well below the applicable stress limits.

Accident Dose Calculations

The dose rate increase is bounded by Section A.12.3.3.

Corrective Actions

No change to corrective actions described in Section 12.3.2.

A.12.3.3 Tornado Wind and Tornado Missiles Effect on HSM-MX

Cause of Accident

No change to the cause of accident described in Section 12.3.3.

Accident Analysis

Stability and stress analyses are performed to determine the response of the HSM-MX to flood, massive missile impact and tornado wind pressure loads.

The stress analyses are performed using the ANSYS [A.12-7]. HSM-MX storage modules arranged in a back-to-back row array provides a conservative estimate of the response of the HSM-MX under postulated static and dynamic loads for any HSM-MX array configurations. These analyses are described in Appendix A.3.9.4.

The sliding and overturning stability analyses due to wind, flood and massive impact loads are performed using closed-form calculation methods to determine the sliding and overturning response of the HSM-MX. A non-linear seismic stability analysis is performed using LS-DYNA [A.12-8]. These analyses are described in Appendix A.3.9.7, Section A.3.9.7.1.

Thus, the requirements of 10 CFR 72.122 are met.

Accident Dose Calculation

As discussed in the evaluations, the tornado wind and tornado missiles do not breach the HSM-MX to the extent that the DSC confinement boundary is compromised. Localized scabbing of the end shield wall of a HSM-MX array may be possible. *When the array is in the expansion configuration with the removable end shield wall absent, two inner walls may be damaged as a result of a missile impact.*

The HSM-MX outlet vent covers and all dose reduction hardware (DRH) may be lost due to a tornado or tornado missile event. *The assumed accident damage increases the dose rates on the front, roof, and end (side) of the HSM-MX. The effect on the average rear dose rate is negligible because the rear surface does not contain vents and sustains little damage in an accident. The HSM-MX accident increases the average dose rate on the front, roof, and end of the module to 92.9 mrem/hr, 4,730 mrem/hr, and 425 mrem/hr, respectively (see Section A.6.1).*

The evaluation for the impact on public exposure, a 2x11 ISFSI configuration and a distance to the site boundary of *349* m is used. As documented in Chapter A.11, Section A.11.3.2, for a 2x11 ISFSI configuration, the accident dose rate is approximately *0.436* mrem/hour and *0.061* mrem/hr at a distance of 200 m and *349* m, respectively, from the ISFSI. It is assumed that the recovery time for this accident is five days (120 hours). Therefore, the total exposure to an individual at a distance of 200 m and *349* m is *52* mrem and *7.3* mrem, respectively. This is significantly less than the 10 CFR 72.106 limit of 5 rem. Note that the dose is bounded by the EOS-HSM accident dose documented in Section 12.3.3.

Corrective Action

No change to corrective actions described in Section 12.3.3.

Cause of Accident

Since the HSM-MX is located outdoors, there is a remote probability that the air inlet or outlet openings could become blocked by debris from such unlikely events as floods and tornadoes. There are no credible scenarios that could block both the inlet and outlet vents at the same time due to the significant height difference between the inlet and out vent locations. Therefore, only blockage of the inlet vents is considered in the UFSAR. The HSM-MX design features, such as the perimeter security fence and the redundant protected location of the air inlet and outlet openings, reduce the probability of occurrence of such an accident. Nevertheless, for this conservative generic analysis, such an accident is postulated to occur and is analyzed.

Accident Analysis

The thermal evaluation of this event is presented in Chapter A.4, Section A.4.5 for the EOS-37PTH DSC stored inside an HSM-MX. The analysis performed for the EOS-37PTH DSC bounds the values for the EOS-89BTH DSC. Therefore, the temperatures determined for Load Case #3-S in Section A.4.5 are used in the HSM-MX structural evaluation of this event. The HSM-MX structural analysis, presented in Appendix A.3.9.4, demonstrates that the HSM-MX component stresses remain below allowable values.

Accident Dose Calculation

There are no offsite dose consequences as a result of this accident.

Corrective Actions

No change to corrective actions described in Section 12.3.6.

A.12.3.7 Lightning

Cause of Accident

No change to cause of accident described in Section 12.3.7.

Accident Analysis

No change to accident analysis described in Section 12.3.7.

Corrective Actions

No change to corrective actions described in Section 12.3.7.

A.12.3.8 Fire/Explosion

Cause of Accident

No change to cause of accident described in Section 12.3.8.